

Oxidation of Fuels in the Cool Flame Regime for Combustion and Reforming for Fuel Cells

Manuscript submitted to: Progress in Energy and Combustion Science

A. Naidja, C.R. Krishna, T. Butcher and D. Mahajan

August 2002

**Energy Sciences and Technology Department
Energy Resources Division
Brookhaven National Laboratory
Brookhaven Science Associates
Upton, New York 11973-5000**

**Under Contract No. DE-AC02-98CH10886 with the
United States Department of Energy**

DISCLAIMER

This report was prepared as an account of work sponsored by an agency of the United States Government. Neither the United States Government nor any agency thereof, nor any employees, nor any of their contractors, subcontractors or their employees, makes any warranty, express or implied, or assumes any legal liability or responsibility for the accuracy, completeness, or any third party's use or the results of such use of any information, apparatus, product, or process disclosed, or represents that its use would not infringe privately owned rights. Reference herein to any specific commercial product, process, or service by trade name, trademark, manufacturer, or otherwise, does not necessarily constitute or imply its endorsement, recommendation, or favoring by the United States Government or any agency thereof or its contractors or subcontractors. The views and opinions of authors expressed herein do not necessarily state or reflect those of the United States Government or any agency thereof.

Available electronically at-

<http://www.doe.gov/bridge>

Available to U.S. Department of Energy and its contractors in paper from-

U.S. Department of Energy
Office of Scientific and Technical Information
P.O. Box 62
Oak Ridge, TN 37831
(423) 576-8401

Available to the public from-

U.S. Department of Commerce
National Technical Information Service
5285 Port Royal Road
Springfield, VA 22131
(703) 487-4650



Printed on recycled paper

Manuscript submitted to: *Progress in Energy and Combustion Science*

**Oxidation of Fuels in the Cool Flame Regime for Combustion
and Reforming for Fuel Cells**

A. Naidja, C. R. Krishna, T. Butcher and D. Mahajan*

*Energy Sciences and Technology Department, Brookhaven National Laboratory,
Upton, NY 11973 USA*

*Corresponding author: Dr. Devinder Mahajan

*Brookhaven National Laboratory
Energy Sciences and Technology Department
Blg. 815, Upton, NY 11973 USA
Tel: (631) 344-4985
Fax: (631) 344-7905
E-mail: mahajan@bnl.gov*

Abstract

The purpose of this review was to integrate the most recent and relevant investigations on the auto-oxidation of fuel oils and their reforming into hydrogen-rich gas that could serve as a feed for fuel cells and combustion systems. We consider the incorporation of partial oxidation under cool flame conditions to be a significant step in the reforming process for generation of hydrogen-rich gas. Therefore, we have paid particular attention to the partial oxidation of fuels at low temperature in the cool flame region. This is still not a well-understood feature in the oxidation of fuels and can potentially serve as a precursor to low NO_x emissions and low soot formation. Pretreatment, including atomization, vaporization and burner technology are also briefly reviewed. The oxidation of reference fuels (*n*-heptane C₇H₁₆, *iso*-octane C₈H₁₈ and to a lesser extent cetane C₁₆H₃₄) in the intermediate and high temperature ranges have been studied extensively and it is examined here to show the significant progress made in modeling the kinetics and mechanisms, and in the evaluation of ignition delay times. However, due to the complex nature of real fuels such as petroleum distillates (diesel and jet fuel) and biofuels, much less is known on the kinetics and mechanisms of their oxidation, as well as on the resulting reaction products formed during partial oxidation. The rich literature on the oxidation of fuels is, hence, limited to the cited main reference fuels. We have also covered recent developments in the catalytic reforming of fuels. In the presence of catalysts, the fuels can be reformed through partial oxidation, steam reforming and autothermal reforming to generate hydrogen. But optimum routes to produce cost effective hydrogen fuel from conventional or derivative fuels are still debatable. It is suggested that the use of products emanating from partial oxidation of fuels under cool

1 flame conditions could be attractive in such reforming processes, but this is as yet
2 untested. The exploitation of developments in oxidation, combustion and reforming
3 processes is always impacted by the resulting emission of pollutants, including NO_x , SO_x ,
4 CO and soot, which have an impact on the health of the fragile ecosystem. Attention is
5 paid to the progress made in innovative techniques developed to reduce the level of
6 pollutants resulting from oxidation and reforming processes. In the last part, we
7 summarize the present status of the topics covered and present prospects for future
8 research. This information forms the basis for recommended themes that are vital in
9 developing the next generation energy-efficient combustion and fuel-cell technologies.

10
11 [Keywords: Cool flame, Oxidation, Combustion, Fuel oils, Kinetics, Fuel cell, Fuel
12 reforming]

Contents

Abstract

1. Introduction

2. Preparation of the fuels for oxidation: atomization and vaporization, burner and reactor concepts

3. Oxidation and combustion of liquid fuels

3.1. Oxidation of fuels at low temperature and cool flame regime

3.2. Role of oxidation reactions in the ignition of fuels

3.3. Kinetics and mechanisms of the oxidation and combustion of reference fuels

3.4. Oxidation of commercial fuels and biofuels

4. Reforming of fuels for fuel cell technology

4.1. Reforming of methane, natural gas and methanol

4.1.1. Reforming of methane

4.1.2. Reforming of natural gas

4.1.3. Reforming of methanol

4.2. Reforming of gasoline, diesels and biodiesels

5. Impact of NO_x emissions and soot formation on the oxidation and reforming of fuels and the evolution of burner technology

5.1. Impact of NO_x emissions on burner technology

5.2. Impact of soot formation on burner technology

6. Conclusions and prospects for future research

Acknowledgements

Appendix

References

1) Introduction

As a source of energy, fossil fuels have a tremendous impact on the planet in different ways, including human welfare and the environment. In order to deal with the problem of petroleum derived fuels as a source of energy, and also, as a source of pollution, scientists are investigating the means to improve the yield of energy conversion with a minimum level of toxic effluents. This is possible by making engines and burners more efficient, removing impurities such as sulfur and nitrogen from fuels, lowering soot and coking, which are precursors to carcinogenic polyaromatic hydrocarbons (PAH). SO_x , NO_x , CO_2 and particulate emissions all contribute variously to acid rain, photochemical smog, greenhouse effects and destruction of ozone in the stratosphere [1-3] and may lead to global warming and severe damages to the ecosystem health.

In the dawn of this twenty-first century, fossil fuels remain the main source of energy for the planet and by far exceed geothermal, wind and solar energy. Nuclear energy was considered very promising in the 1970s until mid 1980s till incidents such as that at Chernobyl disaster made this path questionable. Hydrogen is an environmentally friendly and "clean" fuel. Despite its abundance in the hydrosphere, generating hydrogen by electrolysis from water is still not economical. However, the oxidation of conventional gaseous and liquid fuels, including natural gas, petroleum distillates (gasoline, diesel and Jet-fuels) and biodiesels to light hydrocarbons and oxygen-containing substances, may form a major step in the preparation of the fuel for reforming and production of hydrogen for use in fuel cells. The fuel cell, an attractive but challenging technology, transforms chemical energy directly to electrical energy, with less pollution when compared to burning fossil fuels [4]. It is well known that hydrogen is the best-suited fuel for fuel cell

1 systems; unfortunately hydrogen infrastructure costs are currently unacceptably high
2 compared to the existing natural gas or petroleum distillate facilities [5]. Although
3 methanol can yield an appreciable proportion of hydrogen through its transformation into
4 synthesis gas ($\text{H}_2 + \text{CO}$) [6], still it is a secondary derivative fuel and requires new
5 infrastructure. Therefore, on station or onboard processing of natural gas and petroleum
6 distillates remains a viable alternative for the generation of hydrogen and will be
7 discussed in detail in the third part of this paper. But prior to that and to shed more light
8 on the partial oxidation of complex fuels like diesel and jet propulsion (JP) oils, we focus
9 on the oxidation of reference fuels and their mixtures, especially at low temperatures in
10 the cool flame region. This phenomenon is still not well understood and may play a
11 significant role in the formation of the reaction products prior to reforming, as well as in
12 subsequent low NO_x emission systems [7-8].

13
14 During the last decade, progress has been made in the experimental and theoretical
15 modeling of the kinetics and formation of reaction products during the oxidation
16 reactions of reference fuels [9-13]. Indeed, numerous studies have been carried out on the
17 oxidation and conversion of major (single component) reference fuels, such as *n*-heptane
18 [10,14], *iso*-octane [10] and *n*-hexadecane (cetane) [15]. There is some study of mixtures
19 of two single components, for example *n*-heptane and *iso*-octane [11] as surrogate to the
20 multi-component and complex fuels used in internal combustion engines. However, little
21 is known on the details of conversion of complex fuels like diesel and JP oils, which are
22 mixtures of a broad range of hydrocarbons, mainly composed of paraffins (saturated
23 alkanes), naphthenes (unsaturated cyclics) and aromatics [16,17].

To the best of our knowledge, a literature review of the most recent relevant data integrating the research on the partial oxidation and combustion of hydrocarbons including commercial fuels, as well as the reforming processes of various potential fuels to generate hydrogen-rich gases as feed stock for fuel-cell powered vehicles, is still lacking. Integrating the data of the oxidation at the cool flame regime and reforming of fuels will shed more light on the effort done in both areas that is intertwined. The knowledge gained in the oxidation mechanisms of reference fuels are needed to better understand the oxidative transformation of petroleum distillates such as gasoline and diesel, and also, biofuels. Here, we will discuss the most recent investigations related to the oxidation and reforming of fuels for fuel cell technology as well as for burners, with regard to fuel preparation processes and experimental designs. The developments in the oxidation and reforming processes have always been impacted by the resulting emission of pollutants, namely NO_x and soot. The numerous investigations on the oxidation of the major reference fuels reviewed here, have constituted a basis for developing our project on both experimental and theoretical aspects related to the oxidation and reforming of complex fuels. The mechanisms of the fuel pyrolysis under oxygen-deficient conditions leading to the cracking of the hydrocarbons, is out of the scope of this paper and have been reviewed elsewhere [14].

The aim of this study is to integrate the recent relevant investigations on the auto-oxidation, combustion and reforming of fuels in addressing the following issues: (i) the fuel preparation prior to the oxidation, including atomization, vaporization and the role of novel burners in the oxidation processes (ii) the fundamental aspects of the oxidation and

combustion of fuels with emphasis on the low temperature processes in the cool flame regime as a significant step prior to reforming of the fuel, (iii) The reforming processes of fuels into hydrogen-rich gas from methane, natural gas, methanol, gasoline, diesel and biofuels; (iv) future prospects and the insights from the existing data that will help to develop new processes integrating the oxidation of fuel oils at cool flame regime and their reforming into hydrogen-rich gas for fuel cell technology and (v) the impact of NO_x and soot pollutants, on the oxidation and reforming processes and the evolution of technology.

2) Preparation of fuels for oxidation: atomization and vaporization of fuels, burner and reactor concepts

The chemical composition and structure are inherent to the fuel, but the physical properties, including droplet size and distribution can be controlled by atomization prior to oxidation and reforming, and thus, an adequate preparation should result in a maximum conversion of the liquid fuel with minimum soot and NO_x formation. Fig. 1 depicts the major themes illustrated in this review that will be used in our experimental design: a) the preparation of the fuel consists in the atomization and vaporization, b) the fuel is partially oxidized in the reactor in the presence of preheated air at low temperature under cool flame conditions and c) the reaction products obtained at cool flame can be either catalytically reformed into hydrogen-rich gas for fuel cell systems or burned for combustion, heating purposes or other applications.

Mixture preparation of liquid fuels in many technical applications remains an important problem; uncontrolled atomization of liquid fuel leads to inhomogeneities in

the mixture and thus to the formation of pollutants [7]. Indeed, it is worthwhile to briefly delineate some theoretical aspects of fuel droplet vaporization, which plays an important role in determining air/fuel mixing with a significant impact on the evolution of oxidation and combustion. Detailed information is given by Glassman [18], Sirignano [19] and Warnatz et al. [20].

In the original Spalding evaporation model, the droplet surface conditions are calculated from mass and energy balance [21]:

$$d(4\pi r^3 \rho_l / 3) / dt = - dm / dt \quad (1)$$

$$4\pi^2 h_\infty (T_\infty - T) = mc_l T + (dm/dt) L_v \quad (2)$$

where r is the droplet radius, T the droplet temperature, c_l and ρ_l are the specific heat and density of the liquid, L_v the latent heat of vaporization, T_∞ the ambient temperature, h_∞ the convection coefficient and dm/dt the mass transfer rate. For the model, the internal temperature distribution described by 1D Fourier equation must be solved:

$$\partial T / \partial t = (k_l / \rho_l c_l) (1/r^2) [\partial(r^2 \partial T / \partial r) / \partial r] \quad (3)$$

Details of the theoretical considerations are out of the scope of this study. We only present the derived parameters, namely, the diameter of droplets as influenced by heating, vaporization, residence time and theoretical vaporization rate. The combustion of the dense cloud emerging from the fuel spray is modeled as an ensemble of single droplet combustion using several assumptions [20]. Therefore the rate of evaporating mass $\partial m / \partial t$

$$\text{is:} \quad \partial m / \partial t = (2\pi \lambda_g d / c_{p,g}) \text{Ln}(1 + B) \quad (4)$$

where B is the Spalding transfer number:

$$B = [\Delta h_{\text{com}} / v + c_{p,g} (T_\infty - T_s)] / h_{t,g}, \quad (5)$$

1 λ_g , the thermal conductivity of the gas phase; d , the droplet diameter; $c_{p,g}$, the heat
 2 capacity of the gas phase, Δh_{comb} , the specific enthalpy of combustion; v , the stoichiometric
 3 mass ratio of the oxidizer to the fuel; $(T_\infty - T_s)$, the difference between the temperature of
 4 the gas phase far away from the droplet and that at the droplet surface and $h_{f,g}$, the
 5 enthalpy of formation of the gas phase.

6 In the limit of pure evaporation with no reaction, $\Delta h_{\text{comb}} = 0$, and thus:

$$7 \quad B = c_{p,g}(T_\infty - T_s)/h_{f,g} \quad (5a)$$

$$8 \quad \text{Also,} \quad \partial m / \partial t = -(\rho_l \mu d^2 / 2) \partial d / \partial t = -(\rho_l \mu d / 4) \partial d^2 / \partial t. \quad (6)$$

$$9 \quad \text{From equation (6) one has:} \quad \partial d^2 / \partial t = -(8 \lambda_g / \rho_l c_{p,g}) \text{Ln}(1 + B) \quad (7)$$

10 Integration of equation 7 leads to the well-known d^2 -law for the droplet lifetime:

$$11 \quad d^2(t) = d_0^2 - Kt \quad (8)$$

12 with $K = (8 \lambda_g / \rho_l c_{p,g}) \text{Ln}(1 + B)$. It has been shown that the d^2 -law (equation 8) holds for
 13 mass and heat transfer with chemical reaction [18]. Three phases of droplet combustion
 14 can be identified: heating, fuel evaporation and combustion. Based on equation 9, the
 15 theoretical heating time t_h of droplet can be estimated [22]:

$$16 \quad t_h = c_{pi} \rho_l c_{pg} d_h^2 (T_s - T_{s0}) / 12 \lambda_g \text{Ln}(1 + B_{Mh}) L_v [(B_{Th} / B_{Mh}) - 1] \quad (9)$$

17 where $T_s - T_{s0}$, the difference between free stream and droplet surface temperatures; L_v ,
 18 latent heat of vaporization; B_{Th} and B_{Mh} , thermal and mass transfer numbers, which will
 19 be equal at quasi-steady conditions. In practice, equation 8 is used to estimate the
 20 diameter of the fuel droplets at any given temperature. At a residence time $t = \tau$
 21 (complete evaporation of the droplet), $d^2(\tau) = 0$, and thus, $d_0^2 = K\tau$, or $d_0 = (K\tau)^{0.5}$

Hence, for single component droplet vaporization, the distribution of fuel droplet size in a reactor can be estimated to characterize the type of burners. Theoretical approach to multicomponent droplet vaporization is out of the scope of this paper and has been presented by a number of investigators [23-27].

The impact of drop size and initial momentum on the residence time and distance required for complete combustion of fuel with air atomized burners was studied using a model incorporating diffusion-limited combustion at different excess air levels [28]. By measuring the drop size distributions in sprays from different atomizers, these authors [28] showed that the spray from pressure nozzles has mean diameters that vary with the flow and the design. They also observed that soot production is critically dependent on drop size. Active research is being carried out for the development of burner concepts based on low-pressure, air atomization with substantial advances, including low firing rates, low excess air/high efficiency, modulation or two-stage firing rates, low NO_x emissions and low electric power consumption [29-30]. Also, an oil burner and a high temperature burner for thermophotovoltaic (TPV) applications have been developed using the low-pressure air atomizer [29]. This air atomizer will be used in our project for the spray and gasification of droplets from petroleum based fuels and biofuels. Fig. 2 illustrates a high-flow fan atomization burner (HFAB) head developed in this laboratory [31]. In this prototype system, the air tube and the flame tube are arranged in such way that most of the combustion air passes through the atomizer and forms the spray. A small fraction of the air (secondary air) passes outward through radial holes in the center tube into the air tube. This secondary air serves two purposes: a) supplies more air to the combustion zone to allow higher firing rates without increasing the nozzle diameter and

b) provides a small air flow through the annular space between the nozzle and the air tube to keep the electrodes cool and prevent backflow of combustion products. High recirculation rates lead to low NO_x emissions and transparent blue flames. The level of NO_x emission is about 40 % lower than in the conventional retention head burner [31]. Further, there is ongoing research on other burner concepts, including blue flame [32], radiant and catalytic burners [33,34]. More details on burners and their applications are given elsewhere [35,36].

To separate the vaporization from the flame zone in an oil-fired burner for stirling engines, Steinbach et al. [37] used the ignition delay time. The evaporation and mixing are carried out during the autoignition delay time. Tests in a continuous flow apparatus were conducted under atmospheric pressure in order to get a better understanding of ignition delay times and to avoid flashback into the vaporization and mixing zones, especially, when combustion air is preheated up to 873 K. A flow reactor test rig of high-grade steel 1 m long and 10 cm in diameter was used. The fuel is injected into an electrically heated mixture of combustion air and exhaust gas from an oil burner via a simplex nozzle. The autoignition delay time τ_i in a flow reactor is calculated by:

$$\tau_i = L/V \quad (10)$$

where L is the length of the flow reactor and V the average mixture velocity (flow rate)

The tests showed that the autoignition delay times could be prolonged by a factor of 4 when the recirculation ratio (mass flow of recirculated exhaust gas/mass flow of combustion air) is increased from 0 to 1.3. Thus, error free operation of a burner, which separates the vaporization from the flame zone, could be realized.

Premixing of fuel oil and air for the purpose of lean-premixed combustion in gas turbine combustors was studied experimentally with laser-induced fluorescence (LIF) and numerically using a modified KIVA-3 code [27]. Three improved sub-models were used: 1) a droplet-vaporization model including multiple components and real-gas effects, 2) an improved droplet dispersion model (so-called linear-filter model), and 3) a swirl correction to the k- ϵ turbulence model. Considerable differences were found in fuel-vapor distribution when using different models. The simulation results were found to be sensitive to the initial Sauter mean diameter (SMD), in particular in the presence of air-swirl. Remaining discrepancies are supposed to originate either from a turbulence-modeling error and the occurrence of secondary droplet breakup, which was not modeled, or on the other hand, the assumption of proportionality between LIF intensity and fuel oil concentration. From the studies reported above, one can see that an adequate atomization and vaporization of the fuel are paramount for an optimum oxidation reaction where the undesirable NO_x and soot pollutants could be minimized.

3. Oxidation and combustion of fuel oils

During the previous decades, among potential hydrocarbons investigated as fuel surrogates for oxidation and combustion studies, *n*-heptane has gained a major attention because it is found in relatively large amounts in commercial fuels like gasoline and kerosene [38] and it is used as a reference fuel for the definition of octane number (RON = 0). However, much less is known on the details of oxidation of petroleum distillate fuels and biofuels. Here, we have attempted to focus on the nature of the reaction products formed during the oxidation of such fuels at low and high temperature, as well

as on the proposed mechanisms of their formation in the cool flame regime. Furthermore, we have paid attention to the conditions where the cool flame could be stabilized. In some studies, there are limitations that could be improved with new techniques and instrumentation. In addition to being a preparatory step to the reforming process, the cool flame regime has an important role in combustion systems and could be a possible regulator for the autoignition delay time of fuels as will be discussed below. As depicted in Fig. 1, the reaction products stemming from the cool flame can be either reformed into hydrogen-rich gas for fuel cells or can be combusted for heat.

3.1. Oxidation of fuels at low temperature and in the cool flame regime

At temperatures as low as 393 K, some fuel-air mixtures react chemically and produce very weak flames called cool flames that generate very little heat. The reaction has not gone to complete combustion; rather the molecules break down and recombine to produce a variety of stable chemical compounds including alcohols, acids, peroxides, aldehydes and carbon monoxide [39]. The weak temperature rise is due to the heat produced by breaking and reforming of the fuel chemical bonds. Cool flame is an important and complex ignition phenomenon associated with multistage ignition. It is a faint pale blue luminescence, due to chemiluminescence of electronically excited formaldehyde, and occurs preferentially under fuel rich conditions during degenerate branching reactions in early combustion [40]. Cool flames have been studied since 1930s and their oscillatory nature has been recognized a few decades ago [41]. Thus, the majority of workers consider the cool-flame to be a key part of reaction during which the bulk of the fuel is incompletely oxidized [42]. On the other hand, Shtern [43] considers

1 the cool flame to be a minor process, which plays little part in the overall reaction, since
2 the cool flame oxidation and the slow combustion are very similar in their chemical
3 nature. During 1970s, although not plentiful, there were investigations including some
4 theoretical hypotheses on low temperature oxidation in the cool flame regime [40,44-48].
5

6 More than three decades ago, Burgess et al. [49] shed more light on the controversy
7 about aldehydes (RHO) and hydroperoxide (ROOH) candidate species causing cool
8 flames in the gaseous oxidation of hydrocarbons. By measuring the concentration of
9 hydroperoxide, they suggested that the chain-branching intermediates in the cool-flame
10 oxidation of *n*-heptane, are hydroperoxides (ROOH). On the other hand, Barat et al. [50]
11 showed that the highest total conversion of 3-ethylheptane (C_7H_{16}) to O-heterocycles (up
12 to 42 %) takes place in the low-temperature slow-combustion region, whereas typical
13 conversion in the cool-flame region is about 18 %. However, the conversion to olefins
14 reached up to 60 % (Table 1). Also, they observed a decrease in the O-heterocycles yields
15 and an increase in beta-scission products with increasing octane number of the fuel,
16 which has an important implication with regard to atmospheric pollution from vehicle
17 exhausts. It is likely that hydrocarbons beta-scission often results in alkenes that may
18 react photochemically to form smog.
19

20 Luck et al. [45] found remarkable similarities in the products formed and in their
21 distribution in the different systems: single-cylinder experimental engine during fired and
22 motored operation, low-pressure “static” apparatus and a stabilized cool-flame flow
23 reactor. It was concluded that the nature of the chemical steps involved in cool-flame

oxidation play an important role in the processes leading to both; autoignition in motored engine and “knock” in a fired engine. In their study, it is asserted that these processes are essentially independent of pressure, reactant ratio and surface. Beside CO, CO₂ and unburned fuel, a large number of products were identified and quantified in the low temperature oxidation of *n*-heptane and *iso*-octane. Fig. 3 outlines the reaction scheme of *n*-heptane oxidation showing the main possible reaction products. The major reaction products were about 50 % Olefins (C₄-C₇) and about 40 % oxygenates, mainly cyclic ethers (Table 2). The distribution of the intermediate products from the oxidation of low-molecular-weight hydrocarbons, *iso*-butane, *n*-butane and *n*-pentane was studied by Atherton et al. [51] in the temperature range of 523-673 K and pressures from 9.3 to 26.3 kPa. The data show that the variation of pressure has only a little effect on the amount and distribution of the reaction products, which is largely dominated by oxygenates (Table 3).

In order to fully explain the oxidation and combustion of fuels in the entire range of temperatures and for practical reasons as well, low temperature and cool flame regime phenomena have gained interest in the last few years [7,52-54]. The low temperature regime (523-673 K) can be divided into three regions: slow combustion, cool flame and the negative temperature coefficient (NTC). In the cool flame region, periodic behavior has been observed occasionally [55]. The NTC is a unique phenomenon in hydrocarbons oxidation, in which the overall reaction rate decreases with increasing temperature and it represents a barrier for autoignition to occur. Also, these phenomena must be taken into account in any proposed mechanism for multistage ignition and for the modes of product formation [42]. In the low-temperature region, the oxidation of hydrocarbons is a very

1 complex process involving different propagation and chain branching reactions, which
2 can lead to the phenomena cited above. Slow combustion and the NTC dependence of
3 reaction rate are wholly kinetic in origin, but oscillatory cool flame, single-, two- and
4 multi-stage ignitions are consequences of the interactions of kinetics and heat release
5 [52]. Ignition can occur in adiabatic conditions, while cool flames require heat losses.
6 The model proposed by Gaffuri et al. [52], apparently, reproduced quite well
7 thermochemical oscillations and the NTC region of the reaction rate for low-temperature
8 oxidation of *n*-heptane and *iso*-octane in a jet-stirred flow-reactor (JSFR), in terms of
9 experimental frequencies and intensities of cool flames. Also, very good agreement was
10 observed for fuel conversion and intermediate species formation.

11
12 Using an appropriate technique, Mantashyan [56] was able to detect free radicals in a
13 stabilized cool flame. For this, a small part of the gas flow was sampled from each
14 section of a two-section flow reactor and continuously directed at low pressure to a
15 freezing pin at liquid nitrogen temperature inside the cavity of an electron paramagnetic
16 resonance (EPR) spectrometer. The behavior of free radicals in propane and butane
17 oxidation shows that the cool flame appears as a result of self-acceleration of the chain
18 reaction of hydrocarbon oxidation. The temperature increase due to self-heating or
19 increased heating of a stabilized cool flame, leads to the decrease of radical
20 concentrations in the temperature interval from 623-673 K followed by the cool flame
21 disappearance. In addition, it was shown that there is a relationship between the cool
22 flames and oscillations. Thus, small variations of the process parameters lead the
23 stabilized cool flame into oscillatory regime. Low-temperature processes (initiation,

branching, propagation) are strongly dependent upon the size and structure of the fuel molecule [57]. In order to understand the kinetic steps that control the low-temperature oxidation of linear and branched alkanes and their auto-ignition properties, Dagaut et al., [58] measured the reactants, intermediates, and final products formed from *n*-heptane in three different oxidation regimes; cool flame, negative temperature coefficient and normal combustion. In addition, concentration profiles of the major cyclic ethers formed at low temperature were measured. The evolution of the transition from low to high temperature oxidation regime as a function of pressure was observed, showing the quasi-disappearance of the negative temperature coefficient at 40 atm. This was interpreted in terms of formation and isomerization of the further reactions of hydroperoxyalkyl radicals. The stabilization of the excited intermediate QOOH* is favored when the total pressure is increased, which explains the disappearance of the NTC.

The temperature and chemical composition changes [59] were also investigated during the low-temperature oxidation of stoichiometric *n*-heptane and *iso*-octane. The experiments were carried out in a stainless steel JSFR (volume = 100 cm³), which operates at a pressure as high as 10 bar. The reactor was conditioned before the experiments by burning rich hydrocarbon/air mixture for several hours to reduce the occurrence of heterogeneous reactions on the reactor walls. The significant presence of aldehydes in the products of *n*-heptane was attributed to a degenerate chain-branching path involving the addition of molecular oxygen to hydroperoxide radicals and isomerization by internal H-atom abstraction. The latter step is particularly favored in linear alkanes where easy-to-abtract H-atoms are available. On the other hand, cyclic

ethers and fuel-conjugate olefins were the dominant products of the low-temperature oxidation of *iso*-octane. Also, as a function of temperature, the conversion of *n*-heptane is higher than that of *iso*-octane. There is a significant difference between low and high temperature oxidation mechanisms. The impact of temperature on the changes in the reaction path is clearly shown in Fig. 4 where the estimated selectivity of each reaction step is indicated from the lumped mechanism [14]. At high temperature, beta-decomposition reactions of alkyl radicals prevail over the oxygen addition reactions. Thus, the high temperature mechanism mainly involves interactions of oxygen and small radicals and olefins. At 820 K, the proportion of beta-decomposition products, conjugate olefins and heterocycles (cyclic ethers) is predominant (up to 80 %), whereas the selectivity for ketohydroperoxide does not exceed 3 %. The low temperature mechanism is a complex process involving propagation and chain branching. At 620 K, a temperature in the cool flame region, the addition of oxygen to the peroxide radical is favored and the selectivity in ketohydroperoxide is prevalent (up to 80 %) (Fig. 4). It is suggested that the transition between low and high temperature mechanisms gives rise to a variety of typical behaviors: such as damped and oscillatory cool flames or single and multi-stage ignitions [14].

Chen et al. [55] investigated the lean oxidation of *iso*-octane in the low temperature regime. Approximately 50 % of the fuel was consumed in 0.1 s at an equivalence ratio of 0.05 (0.8 mmoles fuel) and 0.9 MPa. GC analyses of the reaction products at different temperatures from 600 to 700 K showed 42 intermediate species. However, only 16 of them were identified, which included two C₈ conjugate olefins, three C₇ olefins, three C₈

cyclic ethers, *iso*-butene, propene, acetone, acetaldehyde, *iso*-butyraldehyde, and 2,2-dimethyl-propanal, methacrolein, and *iso*-butene oxide. The reaction mechanism followed the general one (Fig. 3), starting with *iso*-heptyl radicals $x\text{C}_8\text{H}_{17}$, which go through beta-scission to form smaller olefins and a radical. With addition of O_2 , there is formation of hydroperoxy radicals, which are significant in low-temperature regime as mentioned above. Battin-Leclerc et al. [60] used the software system EXGAS of automatic generation of detailed mechanism to reproduce the oxidation of *n*-heptane, *iso*-octane, *n*-decane and some binary mixtures. In addition to the experimental data, giving some of the reaction products at low and high temperatures, the influence of temperature on the conversion of *n*-heptane and *iso*-octane was studied. The conversion of *n*-heptane reached a maximum level of 74 % at 650 K, then decreased through the NTC region to 40 % at 750 K before rising again with increasing temperature (Table 4). On the other hand, the conversion of *iso*-octane was much lower and only reached 8 % in the same range of temperature. In the low temperature region and around the NTC, the fitting of the experimental data by the proposed theoretical model is still unsatisfactory. The difference between the experimental data and the fitting model reached up to 30 % in this range of low to intermediate temperatures (Fig 5). Even the most recent and upgraded chemical kinetic models [60,61] seem unsatisfactory and need to be improved. Ranzi et al. [14] anticipate that low and high temperature mechanisms of the oxidation process can be organized into a comprehensive kinetic scheme able to simulate the oxidation of natural gas, commercial gasoline and jet-fuels.

1 In view of the cited promising applications of the cool flame, the German group at
2 Aachen [7,53,62] conducted a detailed experimental procedure at the cool flame regime
3 to partially oxidize numerous fuels with initial boiling temperature range of 231-830 K.
4 They took into account the air-fuel mixture and the inhomogeneities in the fuel-oxidizer
5 distribution in the reactor to assess the impact on pollutants and soot formation.
6 Homogeneous fuel-oxidizer mixture was achieved by an atomization of the liquid
7 leading to a partial or complete evaporation in a mixture of air and recirculated product
8 gas. Due to the well-known problems with the formation of deposits on the reactor wall
9 during evaporation of liquid fuels, contact of unburned fuel with hot walls should be
10 avoided [53]. With an appropriate set up of the parameters (temperature, equivalence
11 ratio, flue gas) a partial chemical conversion of the fuel was obtained.

12
13 The direct addition of the fuel to the preheated air can lead to an exothermic reaction
14 and the resulting rise in temperature may lead to ignition. The technical problem is solved
15 for a fuel with a boiling temperature range (231-830 K), under the following
16 characteristics: a) $p \geq 1$ bar and temperature of at least 520 to 880 K, C/O between 1:0.14
17 to 1:25 and b) adjusting the residence time t of the mixture produced in the reaction
18 chamber in step a) $t > 25$ ms at $p \leq 1$ bar and limited removal of heat from the reaction
19 zone via an inert gas flow. For a particular liquid fuel, rise of the gas temperature after
20 addition of the fuel may reach 453 K (Fig. 6). Some endothermic reactions may occur, if
21 overall, the reaction is isothermal. Once the operating temperature of the cool flame is
22 defined, the cool flame regime can be stabilized. The rise in temperature for the oil
23 studied at atmospheric pressure begins at 583 K for an air/fuel ratio of 0.7 to 2.0. For

fuel like diesel # 2, *n*-heptane or *iso*-octane, the initial temperature of the system to create cool flame conditions should be over 583 K. The data show that the final temperatures of cool flames reach similar values independently of the type of fuel (Fig. 7). By controlling the temperature within the range of cool flame with adjustment of heat loss from the reactor external wall, the ignition of a sub-stoichiometric mixture can be avoided and the cool flames could be manipulated safely. It was observed that up to 813 K, no ignitions occurred, whereas around 873 K, the mixtures ignite. Below 823 K, the ignition delay time was estimated to be over 1 s (Fig. 6), and thus, ignition can certainly be excluded. It is suggested [7,53] that under the above conditions and despite the small dependence of the cool flame on the boiling point of the fuel, it is possible to prepare the cool-flame products in a mixing chamber.

Experimentally, the reactor used consists in a thin-walled high-grade steel pipe with a diameter of 10 cm and a length of 100 cm. Prior to premixing and to initiate the cool flame, the air flow must be preheated accordingly. The wall heat losses are limited by insulation, resulting in an initial temperature from 583 to 723 K. The cool flame can be initiated by variation of the oil mass flow to obtain an equivalence ratio $\lambda = (\text{O}_2/\text{F})/(\text{O}_2/\text{F})_{\text{stoich}}$ of 0.3 to 2.0. Exothermic reaction of the cool flame results in a spontaneous temperature rise enabling a partial conversion of the fuel. Due to the reaction-kinetic inhibition characteristic of the cool flame, the temperature rise of the mixture is limited, so that ignition of the cool flame product (exhaust) is avoided. A maximum mixture temperature of approximately 753 K results for the fuel oil at atmospheric pressure and is to large extent independent of the adjusted air-fuel ratio λ

[62] (Fig. 7). After cooling to ambient temperature, the products can be gaseous, liquid or aerosol. The resulting short molecular chain (smaller molecular weight) entities have a boiling temperature range under that of kerosene.

The initial operating cool flame temperature can be lowered by recirculation of the reaction products. This process can maintain the cool flame for a longer time; thereby at sub-stoichiometric modes of operation, the compression ignition is inhibited. On the other hand, reduction in the pressure will lower the initiating temperature. Also, the addition of a catalyst will help to decrease the activation energy necessary for the initiation of the cool flame, and thus, lower the initiating temperature. For the production of synthesis gas ($H_2 + CO$), it is necessary to vaporize the fuel. From this group's experience, the final temperature of the cool flame tends toward a constant value independently of the initial temperature.

The condensed reaction products resulting from the cool flame procedure have a lower boiling temperature range than the original fuel. With additional steps, this technology becomes possible in new range of applications: Thus, the gaseous product can be stored and possibly transported to the consumer. Also, development of the cool flame procedure may even lead to selectively produce petrochemical synthesis components with high yield from the gas reaction products, namely, olefin and formaldehyde [7]. The cool flame procedure makes the conversion of liquid fuels to the gas and vapor phase possible in a strongly sub-stoichiometric condition without noticeable soot deposits. In fact, the extent of soot formation during cool flame regime is still unknown. However, aiming to

1 reduce the total NO_x emission, especially the NO_x caused by conversion of fuel nitrogen,
2 Schrag et al. [8] described the concept of an oil burner using cool flames. In the first step,
3 the preheated fuel-air mixture is subjected to cool flame regime before being burned in a
4 second step. The level of the inhibition of NO_x formation through the utilization of cool
5 flame process is still unknown. The cool flame method can be applicable for diesel
6 engines and/or fuel cells. Indeed, the recent investigations on cool flame regime and the
7 suggestions made by the RTWH group in Germany [7,53,62] pave the way for thorough
8 studies of this process and can lead to its use beneficially in industrial applications
9 including fuel cell technology.

11 Due to their complex nature, cool flames were also studied in microgravity to
12 minimize natural convection using *n*-butane as fuel [39]. It seems that cool flames
13 generally occur at lower temperatures and pressures in reduced-gravity environments
14 [39]. The tests were conducted onboard NASA's KC-135 microgravity aircraft where the
15 *g*-levels are effectively reduced to $10^{-2} g_{\text{earth}}$ [54]. The irreproducibility resulting from
16 radical-wall interactions were minimized either by baking or chemically deactivating the
17 stainless steel vessel by using a deactivating agent (Sylon). In the untreated vessel about
18 42 % more of fuel was consumed at 1 *g* than at micro-*g* at 22 kPa and 583 K. The
19 difference in fuel consumption cannot be attributed to a purely thermal effect since no
20 difference in fuel consumption was measured when the walls were inactive. The author
21 hypothesized that possibly the symmetric distribution of species at micro-*g* may have led
22 to enhanced termination at the vessel walls, which moderates the reaction rate. It was not

clear whether the additional amount of fuel consumed at 1 g had reacted or the fuel molecules were adsorbed on the vessel wall surfaces.

3. 2. Role of oxidation reactions in the ignition of fuels

Autoignition is defined as the ignition of a combustible material, commonly with air, as a result of heat generation from exothermic oxidation reactions without the aid of external energy source such as spark or flame [40]. It is influenced by several parameters, including vessel size and geometry, fuel/oxygen ratio, diluents gas, pressure, ignition zone (cool flame), ignition delay τ_i , chemical structure, additives, surface effect (catalysis) and physical state of the fuel. Ignition delay time τ_i (equation 11) is an important factor in the autoignition process. It is composed of physical (time for the droplet to evaporate, diffuse and mix with air and heat up to chamber temperature) and chemical delay (contact of fuel and oxygen involving kinetics of chemical reaction that form the critical concentration of free radicals and other intermediates necessary for ignition). This delay time may take a fraction of a second or as long as many minutes, depending on the temperature, composition and chemical structure of the fuel.

$$\tau_i = \tau_{\text{phys}} + \tau_{\text{chem.}} \quad (11)$$

There is abundant literature on the modeling of ignition [63]. In this section, we briefly illustrate the dependence of the ignition on the kinetics of the oxidation reaction and evidently the boundary between cool flame and ignition [40]. Measurements of ignition delay have been correlated [64] as follows:

$$\text{Log}_{10}\{\tau_i [\text{fuel}]^a [\text{O}_2]^b [\text{Ar}]^c\} = A/T + B \quad (12)$$

where τ_i is the induction period (delay time), A and B are constants, a, b and c correlation parameters. The apparent activation energy is given by $2.303 AR$, with R the universal gas constant. In accord with classical chemical kinetics, the ignition delay time of several fuels (Jet-A, JP-4, Diesel # 2, cetane) correlate with the inverse of the pressure and the exponent of the inverse temperature [65]:

$$\tau_i = Ap^{-n}\exp(E/RT) \quad (13)$$

where A and n are constants, and E the global apparent activation energy. For an inlet temperature of 1000 K, an equivalent ratio of 0.3 to 1.0 and a pressure of 1 to 3 MPa; ignition delay times were in the range of 1-50 ms, at free stream flow velocities varying from 20 to 100 m/s. Computational techniques using chemical kinetic reaction mechanisms as those used by Dagaut et al., [9,10], Ranzi et al. [13] and Gaffuri et al. [52] have been applied to the calculation of knock tendencies in internal combustion engines [57,66,67]. In addition, knocking properties of the fuel mixtures have been examined for *n*-heptane and cetane [68].

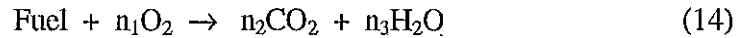
The kinetic mechanisms were used to simulate the end gas reactions during compression and flame propagation periods in an engine. This end gas is heated and compressed by piston motion and by the moving flame and would eventually ignite spontaneously and produce knock, given sufficient time. Under normal engine operations, the flame consumes the end gas before this ignition occurs and knock is avoided. It was shown that the ignition delay time increases with the research octane number (RON) [67]. Some additives have a little effect or no change on the computed time of ignition, including acetone, methanol, acetaldehyde and the olefin species [57].

All alkylhydroperoxides produced strong pro-knock effect resulting from the decomposition of the hydroxyperoxide (ROOH) at the O-O bond to produce a large amount of OH and alkoxy (RO) radicals when T exceeds 900 K, and thus, ignition delay times are reduced for all the fuels examined [57]. The self-ignition behavior of *n*-decane and dimethyl ether in the temperature range of 650-1300 K are very similar to that of *n*-heptane, with a two-step self-ignition: The first step, a cool flame process at lower temperatures and a very short deflagration phase followed by a secondary explosion [69]. The time difference between the first pressure rise caused by the cool flame process and the detonation, decreases with decreasing temperature, whereas the intensity of the cool flame process increases. The ignition delay times of both *n*-decane and dimethyl ether showed a negative temperature coefficient (NTC) in the Arrhenius plot.

3.3. Reaction Kinetics and mechanisms of the oxidation and combustion of reference fuels

The oxidation of hydrocarbon fuels is an important element in modeling autoignition, flame propagation and pollutant emissions in automobile engines. The continued interest in the modeling of *n*-heptane and *iso*-octane (2,2,4-trimethylpentane) may help for a better understanding of knocking behavior in internal combustion engines. A reliable kinetic model of these two reference fuel molecules is the starting point for comparing the knocking tendency of commercial fuels and additives of interest to automotive combustion [13,14]. The great progress in computing systems enables the use of thousands of complex chemical reactions, especially of large hydrocarbon molecules in chemical kinetic modeling. To validate kinetic models, different parameters including

temperature, air/fuel equivalence ratio, residence time, pressure, fuel composition and physico-chemical properties have to be experimentally studied. For this, several experimental techniques have been used: flame supported by burners, static reactors, plug flow reactors, single-pulse shock tubes and continuous-flow stirred tank reactors [9,10,58,70]. Westbrook et al. [71] reviewed the chemical kinetic modeling of high temperature hydrocarbon oxidation and combustion ($T = 1000$ K) for simple hydrocarbons (up to C_4) and proposed a simplified mechanism for larger alkanes (up to C_7), such as *n*-heptane. The simplest overall reaction representing the oxidation of a typical hydrocarbon fuel is:



where the stoichiometric coefficients (n_i) are determined by the choice of fuel. This global reaction is often a convenient way of approximating the effects of the many individual reactions, which actually occur. The rate must therefore represent an appropriate average of all the individual reaction rates involved. The single rate expression is usually expressed as:

$$\text{Rate} = AT^n \exp(-E_a/RT) [\text{fuel}]^a [\text{oxygen}]^b \quad (15)$$

The general reaction rate constant, which depends on the temperature, is given by the modified Arrhenius form as: $k = AT^n \exp(-E_a/RT)$, where A is the preexponential collision factor and E_a , the activation energy. In a great majority of cases, it is assumed that the overall reaction is first order with respect to both fuel and oxidizer, so that $a = b = 1$. However, this choice of reaction order may lead to serious errors [71]. Based on a quasi-global mechanism, the kinetic parameters for the oxidation of *n*-heptane at high

temperatures calculated by Westbrook and Dryer [71], were as follows: $a = 0.25$, $b = 1.5$,
 $A = 4.3 \times 10^{11}$ and $E_a = 30$ kcal.

Analysis of combustion in laminar flames, shock tubes, flow systems and in internal combustion engines using detailed kinetic modeling has frequently provided more knowledge about the system than was available from the experimental results alone [72]. However, much of this research has been limited to rather small fuel molecules, such as hydrogen, methane, ethane and propane (H_2 , CH_4 , C_2H_6 and C_3H_8), which are not characteristic of those found in conventional liquid hydrocarbon fuels [71,73]. Still, the kinetic models of larger hydrocarbon molecules were developed on the basis of the reaction mechanisms and the kinetic parameters of the different steps involved in the oxidation of the cited small molecules and are summarized in a valuable table by Baulch et al. [74]. The effect of the molecular structure on the engine knock characteristics has led to the developments of detailed chemical kinetic models for larger molecules, such as *n*-heptane and *iso*-octane [9,10,68,75].

In the mid 1990s, a valuable study on the oxidation of *n*-heptane, *iso*-octane and their mixture was conducted [9,10,11]. Oxidation experiments were carried out using a continuous-flow stirred tank reactor (CFSTR) in fused silica to prevent wall catalytic reactions under operating pressures up to 10 atm (~ 1 MPa). The quartz reactor is located inside a stainless-steel pressure resistant jacket. The mean residence time was well defined from 0.01 to 3 s by regulating the flow of the pre-heated air mixture within temperature ranges from 550 to 1150 K and from 900 to 1200 K under a pressure of 1

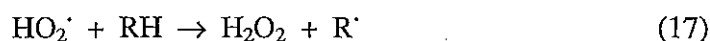
MPa and an equivalence ratio λ from varying from 0.3 to 1.5. In order to reduce temperature gradient, heat release and avoid ignition, a high degree of dilution was used to get an initial fuel mole fraction of 0.001 (0.1 %). The liquid fuel was delivered by HPLC pump, diluted with nitrogen and sent to the vaporizer. This homogeneous nitrogen-fuel mixture was introduced through a capillary to prevent reactions before entry into the reactor. A nitrogen flow of 100 l/h was used to dilute the fuel. The gases were preheated before injection in order to reduce the temperature gradient, which was within 10 K inside the fused silica reactor. Several gas chromatographs with different columns were used to identify the reaction products, including CO, CO₂, C₁ to C₈ hydrocarbons and oxygenates (aldehydes, ketones, alcohols and ethers). Identification and quantification of species was accomplished using standard gas mixtures and GC/MS analyses. Identification of unknown components was confirmed by GC/FTIR.

The reaction scheme of *n*-heptane oxidation (Fig. 3) shows the main possible reaction products (89 compounds, with 25 products determined) and had been suggested three decades ago [45]. With the evolution of analytical techniques, namely gas chromatography coupled with mass spectrometry; the experimental mole fraction profiles as a function of temperature were obtained for over 30 of the reaction products from *n*-heptane [9]. H₂, CO, CO₂, CH₄, ethane, ethylene, acetylene, propane, propene, propadiene, propyne, 1,3-butadiene, 1-pentene, 2-pentene (*cis*- and *trans*-), 1,3-pentadiene, 1-hexene, benzene, 1-heptene, 2-heptene (*cis*- and *trans*-), 3-pentene (*cis*- and *trans*-), *n*-heptane. Oxygenates (CH₂O, CH₃OH, CH₃CHO, ethylene oxide, ethers, acetone). Cyclics (2-methyl,5-ethyl-tetrahydrofuran (*cis*- and *trans*-) and 2-

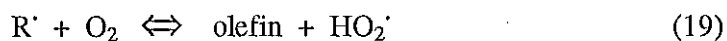
1 methyltetrahydrofuran) were also detected at 50 to 80 ppm. Below 750 K, low
2 temperature oxidation of *n*-heptane occurs with the formation of CO, CO₂ and several
3 oxygenate compounds. The data show that a large fraction of the initial fuel (up to 75 %)
4 was converted into products in this cool flame region. From 640 to 750 K, the negative
5 temperature coefficient (NTC) of reaction rate was observed. More details will be given
6 on the NTC region in the next section. At higher temperatures ($T > 750$ K), there is a
7 rapid production of CO, CO₂, CH₂O, and saturated and unsaturated hydrocarbons until
8 complete initial fuel consumption. It is worthy to note that ethylene is the major
9 hydrocarbon followed by methane, propene and 1-butene. Formaldehyde is the major
10 oxygenated intermediate after carbon monoxide in the whole range of temperature.
11 Chakir et al. [76] showed that in the range of 950-1200 K, with a mean residence time
12 varying from 0.08 to 0.3 s, an equivalence ratio varying from 0.2 to 2.0 and an initial
13 concentration of *n*-heptane of 0.15 %, the major reaction products of the lean mixture
14 oxidation were carbon monoxide and carbon dioxide, as well as ethylene, propene,
15 methane and 1-butene, 1-heptene, 1-hexene and acetylene and other olefins present as
16 minor products. Also, they stated that the mechanism presented could closely predict the
17 ignition delay time of alkanes (up to C₇).

18
19 For *iso*-octane oxidation [10], the reaction products and their profile differ from those
20 obtained from *n*-heptane. In addition to H₂, CO, CO₂, CH₄, ethane, ethylene, acetylene,
21 propene, propadiene, propyne, 1,3-butadiene, which were formed upon *n*-heptane
22 oxidation, several branched alkenes were produced [*iso*-butene, methyl-1-butene, 2-
23 methyl-2-butene, *iso*-propene (2-methyl-1-3-butadiene), 4,4-dimethyl-2-pentene (*cis*- and

1 *trans*-), 2,4-dimethyl-2-pentene, 4,4-dimethyl-1-pentene, 2,4-dimethyl-1-pentene, *iso*-
 2 octane, 2,4,4-dimethyl-2-pentene] and also traces of acetaldehyde and acetone. Below
 3 700 K, low temperature oxidation of *iso*-octane takes place with formation of CO, CO₂, a
 4 small amount of oxygenated compounds (< 1ppm) and only a very small fraction of fuel
 5 was converted into products. Above 720 K, rapid high temperature oxidation started with
 6 formation of CO, CO₂, CH₂O and saturated and unsaturated hydrocarbons until complete
 7 fuel consumption. *iso*-Butylene is the major intermediate hydrocarbon in fuel lean
 8 conditions, followed by methane, ethylene and propene. The branched alkane structure of
 9 *iso*-octane and its higher molecular weight might be reasons for the difference of
 10 behavior. Dagaut et al. [9] rationalized it in terms of structure-reactivity relationship at
 11 low temperatures and presented the major steps (reactions 16-25) of the general
 12 mechanism for alkanes, which has also been described by numerous other authors
 13 [13,14,42,71].



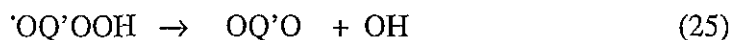
16 Since reaction 16 is quite slow, reaction 17 represents the main alkyl radical production
 17 route in the system. Either *n*-heptane or *iso*-octane can lead to the formation of four
 18 different heptyl radicals (Fig. 3), which can (a) decompose by C-C bond scission to
 19 produce an olefin and an alkyl radical, (b) isomerize to another alkyl radical and (c) react
 20 with O₂ to produce a peroxy radical (reaction 18) or an olefin and HO₂[·] (reaction 19).



The rate constant of channel (reaction 19) depends on the structure of R. The peroxy radicals can react with the fuel to produce the corresponding alkylhydroperoxy radical (reaction 20) or isomerize to another alkylhydroperoxide QOOH by internal H abstraction (reaction 21)



The alkylhydroperoxy radical goes through several reactions, namely, OH elimination (reaction 22), reaction with O_2 (reaction 23), internal H-atom abstraction and OH elimination (reaction 24) and branching (reaction 25).



It is suggested that the susceptibility of long chain hydrocarbon fuels to produce engine knock is tied to the ease of the internal isomerization of the peroxy radical to an alkylhydroperoxy [77]. Ranzi et al. [13] presented a semi detailed kinetic scheme for the oxidation of *iso*-octane at low and high temperatures. The mechanism was also reduced to a "lumped" kinetic model involving only a limited number of intermediate steps. The authors suggested that this model is flexible enough to give accurate prediction of intermediate components, heat release, and ignition delay times for a wide range of operating parameters.

1 In a complementary study, Dagaut et al. [11] investigated the reaction products
2 formed upon oxidation of mixtures of *n*-heptane and *iso*-ocatane in the same conditions
3 as before [9] and at various compositions giving different research octane numbers
4 (RON) at a stoichiometric ratio $\lambda = 1$. The data show that up to 60 % of the initial fuel in
5 low RON mixtures was converted to products. At very high RON (RON = 90), much
6 lower reactivity was observed, but still higher than for pure *iso*-octane, indicating the
7 strong activating effect of *n*-heptane on the oxidation of *iso*-octane in the low temperature
8 regime. Ethylene is the major intermediate hydrocarbon and formaldehyde is the major
9 oxygenated intermediate after carbon monoxide in all the conditions from cool flame to
10 high temperature oxidation. In the low temperature range, several cyclic ethers are
11 formed and their importance varies with RON.

12
13 Knowing the most important reaction products formed and based on the general gas
14 phase oxidation mechanism, several studies have used computer softwares, such as
15 CHEMKIN II and EXGAS, to generate detailed chemical kinetic models [78,79]. In
16 order to test the accuracy of the theoretical model, Côme et al. [78] compared their
17 kinetic model to the experimental data of Dagaut et al. [9] at low temperature (550-850
18 K) and to the experimental data of Chakir et al. [76] at high temperature (900-1200 K).
19 The model does not predict well the experimental data at low temperature and the
20 simulation of some of the reaction products, including alkenes, methane and CO still
21 remained approximate. However, at temperatures higher than 1080 K, the experimental
22 data fitted quite well in the kinetic model for CH₄, C₂H₄ and CO. At low temperature
23 (550-850 K), the kinetic model was fitted into the experimental data of the reacting fuels

(*n*-heptane and *iso*-octane) consumption versus temperature and among the reaction products; only the fitting of CO by the model was shown. Table 5 shows the concentrations of the reaction products formed in the low temperature range upon oxidation of *n*-heptane, mainly consisting of alkenes and methane. Apparently, there is a significant difference between the model and the experimental data. Therefore, whether based on the major steps of the reaction or lumped mechanisms, these kinetic models are still not satisfactory for predicting the reaction products formed at low temperature and in the cool flame regime and around the NTC region.

Curran et al., [80] developed a chemical kinetic mechanism for the oxidation of *n*-heptane in flow reactor, shock tube, and rapid compression machines over a range of pressure 0.1-4.2 MPa, a range of temperature from low to high (550-1700 K) and an equivalence ratio varying from 0.3 from 1.5. The analysis shows that the low-temperature chemistry is very sensitive to the formation of stable olefin species from hydroperoxyalkyl radicals and to the chain-branching steps involving ketohydroperoxide molecules. Experimental and modeling results agree with automotive engine experience that a fuel-rich mixture has a greater tendency to autoignite and lead to knock than stoichiometric or fuel-lean mixtures. Also, the magnitude of NTC region is very closely reproduced by the reaction mechanism, as well as the shift of the NTC to higher temperatures as the pressure increases, indicating the influence of the pressure on the equilibria of the addition reaction of molecular oxygen to the alkyl and hydroperoxy-alkyl radicals.

More recently, Glaude et al. [81] constructed a simplified model for the oxidation of alkanes based on the chemical and kinetic principles using the automatic generation of reaction mechanisms by the computer software EXGAS. The simplification was devoted to the complex primary mechanism for *n*-heptane. The mechanism includes 3662 reactions (excluding termination steps involving 470 species). However, the simplified mechanism seems to be influenced by the temperature range. The same group [61] coupled EXGAS, THERGAS and KINGAS softwares to obtain thermochemical and kinetic data, suggesting that the complete package makes EXGAS a unique and very powerful tool for the production of complete chemical models directly usable for simulation. According to the authors, this software permitted their laboratory to be the first to perform a detailed modeling of complex chemicals, namely the oxidation of *n*-octane, *n*-decane, mixture of *n*-heptane and *iso*-octane or mixtures of *n*-heptane and ethyl-ter-butyl ether.

Favored by the vertiginous progress in computing systems, there is an appreciable extension of modeling capabilities, and thus, abundant literature on chemical kinetic models has emerged [14,82,83]. Further, the major reaction products of fuel oxidation that have an impact on engine knock and ignition delay time were determined [9,13,71]. However, most of these studies are limited to the pure hydrocarbons *n*-heptane and *iso*-octane [14,81] that are used as references or surrogates to the complex fuel oils whether derived from coal or petroleum distillates. On the other hand, few kinetic studies on representative aromatic hydrocarbons present in commercial fuels, such as benzene and alkylbenzene, have seen the light [82,83]. Due to their complex chemical composition and

1 their physico-chemical properties, to date and to the best of our knowledge, studies on the
2 kinetic modeling and reaction products, including experimental data on fuel oils are still
3 scanty [38].
4

5 Axelsson et al. [72] presented a kinetic model that generally predicted the rate of
6 octane fuel disappearance and the level of the larger intermediate species in both the
7 turbulent flow reactor and in the low-pressure laminar flame. They suggested that site-
8 specific H atom abstraction reactions, internal H atom abstraction and thermal
9 decomposition of the octyl radicals were found to be important in the oxidation behavior
10 of octane. In order to understand the oxidation of petroleum based oils, which are
11 complex mixtures of hydrocarbons, where heteroatom-containing compounds that can
12 function as pro-oxidants or anti-oxidants are often present, Blaine et al. [15] developed a
13 reaction model describing under severe conditions, the auto-oxidation of cetane (*n*-
14 hexadecane) as relevant model reactant. Numerical analysis showed that hydroperoxides
15 were formed in the reaction step with the smallest rate constants, and they decomposed in
16 the step with the largest rate constants, indicating that hydroperoxides are key reaction
17 products and play a major role in the oxidation reaction network. In addition, the
18 mathematical model correlated quite well with experimental data obtained at low
19 temperature (413-453 K).
20

21 Because of its use for the estimation of cetane number in diesel engines, a detailed
22 chemical model of the hexadecane gas-phase oxidation and combustion will help to
23 enhance diesel performance and reduce the emission of pollutants. Among the few

studies on hexadecane oxidation modeling, Fournet et al. [84] presented a model based on experiments performed in a jet stirred reactor at high temperature (1000-1250 K), 1 atm, a residence time of 0.07 s, an equivalence ratio varying from 0.5 to 1.5 and high nitrogen dilution (0.03 mol % fuel). The computer software EXGAS [81] was used to generate the detailed high temperature kinetic mechanism, which includes 1787 reactions and 265 species. It seems that the long chain of cetane necessitates the use of a detailed secondary mechanism for the consumption of the alkenes formed as a result of primary parent fuel decomposition. Using the same experimental conditions at high temperature as those of Fournet et al. [84], Ristori et al. [85] obtained new experimental results for the oxidation of *n*-hexadecane. Molecular species including reactants, intermediates and final products were measured via sonic quartz probe sampling and on-line/off-line gas chromatography (GC-MS, FID, TCD). Therefore, a detailed kinetic reaction mechanism consisting of 1801 reactions and 242 species was built and validated by the experimental measurements. To further validate the proposed kinetic scheme and include it in a model for the combustion of diesel fuel, more experimental measurements are still needed, including ignition delays, flame speeds and flame structures. Also, adapting the model to lower temperatures around cool flame region deserve attention.

After the work of Gueret et al. [38] on the modeling of kerosene and the mixture of three reference fuels that may closely represent kerosene, little is yet known on the oxidation of diesel fuels. The oxidation of kerosene and a mixture of 3 pure hydrocarbons (*n*-undecane, *n*-propylcyclohexane and 1,2,4-trimethylbenzene at the ratio of 79:10:11 % was studied in a jet-stirred flow reactor, in the range of temperature 873-1033 K at

atmospheric pressure. The reaction products formed during the oxidation of kerosene and the ternary mixture, measured by gas chromatography (GC) at different mean residence times, up to 0.3 s, were identical. The main hydrocarbon intermediates found, were ethylene, propene, methane, 1-butene, 1,3-butadiene and ethane. Several other unsaturated hydrocarbons were also detected as minor products: 1-pentene, 1-hexene, 1-heptene, 1-octene, 1-nonene, 1-decene and also 1,3-pentadiene, cyclopentadiene, benzene, toluene and xylene. The concentration profiles of the reaction product molecular species in the oxidation of kerosene and the surrogate mixture were very similar, indicating that the mixture of 3 hydrocarbons from C₉ to C₁₁ belonging to 3 different chemical families (*n*-alkanes, cyclane and aromatics) is representative of the kerosene studied. On the basis of the experimental observation at low concentration level for large hydrocarbon intermediates, quasi-global chemical kinetic reaction mechanisms were developed to reproduce the experimental data. The rate expressions for the first global reaction step derived from equation 15 with $n = 0$, is:

$$\text{Rate} = A \exp(-E_a/RT) [\text{fuel}]^a [\text{oxygen}]^b \quad (26)$$

The values of a , b , A and E_a (kcal) are presented in Table 6.

Dagaut et al. [11] studied the oxidation of kerosene and Jet A-1 aviation fuel in a jet-stirred reactor (JSR) at high pressure from 10 to 40 atm in the temperature range of 750 to 1150 K. The main intermediate reaction products of kerosene oxidation were carbon monoxide, lower alkene (ethylene, propene, 1-butene), methane and lower unsaturated hydrocarbons (acetylene, propadiene, propyne). Among other products, they detected C₆ to C₉ alkenes and aromatics (benzene, toluene and xylene). Their study showed that the

use of a detailed chemical kinetic reaction mechanism written for the reference fuel *n*-decane was applicable to predict with reasonable accuracy the main combustion characteristics of kerosene under the conditions cited above.

Keeping in mind the difficulty of fitting the kinetic models to the experimental data in the cool flame region (573-773), we used the general rate equation 26 to estimate the conversion of some fuels with known kinetic parameters, such as, *n*-heptane, *n*-undecane, trimethylbenzene and kerosene (Fig. 8). For that, we made the general assumption that the reaction is of first order to both the fuel and the oxidizer, and for each mole of fuel there are b/a moles of reacting oxygen, with $a = 0.25$ and $b = 1.5$ ($b/a = 6$) according to the assumption of Westbrook and Dryer [71]. Thus, equation 26 becomes:

$$d[\text{fuel}]/dt = -k[\text{fuel}][\text{O}_2] \quad (27)$$

with $[\text{fuel}] = x$, $[\text{O}_2] = 6x$ and $k = A\exp(-E_a/RT)$, we have $dx/dt = -6kx^2$, which can be written as:

$$dx/x^2 = -6kdt \quad (28)$$

Initially at $t = 0$, the concentration of fuel is $x(0)$, thus, integration of equation 28 gives the concentration of the fuel at time t :

$$x(t) = 1/[6kt + 1/x(0)] \quad (29)$$

Since the constant rate $k = A\exp(-E_a/RT)$ depends on the temperature, the conversion of the fuel will also be function of temperature:

$$\text{Conversion (\%)} = [(x(0)_T - x(t)_T) \times 100] / x(0)_T \quad (30)$$

Given the values of A and E_a (Table 6), the conversion of *n*-heptane, *n*-undecane, trimethylbenzene and kerosene were estimated as a function of the temperature and residence time at an equivalence ratio $\lambda = 1$ corresponding to an initial fuel concentration

1 of 1.87 % and a concentration of O_2 of 20.60 % (air containing 21.0 % O_2 used as an
2 oxidant). The conversion of *n*-heptane is much higher than that of other fuels and reaches
3 more than 99 % at a residence time of 0.5 s and 773 K (Fig. 8). It is clear that to have
4 more accurate estimations, the major steps of the oxidation reactions have to be taken
5 into account in a model incorporated in computer software.

6
7 As it has been emphasized all along in this review, most investigations on the
8 oxidation modeling of fuels are limited to the alkanes (*n*-heptanes and *iso*-octane) and
9 only a few studies have targeted aromatic compounds, which constitute a significant
10 proportion (up to 20 %) of fuel oils, such as diesel. On the other hand, the kinetic
11 mechanisms of polyaromatic hydrocarbons (PAHs) generation and soot formation from
12 gas phase combustion, which remain a topic of a significant debate [14], are still obscure.
13 Although, the condensation reactions and the PAH formation mechanisms are further
14 unifying elements in pyrolysis, partial oxidation and combustion kinetics, so far little is
15 known on the modeling of these phenomena. Ranzi et al. [14] suggested that PAH growth
16 in delayed coking and liquid phase pyrolysis, fouling phenomena in steam cracker coils
17 and soot formation in combustion processes, can be at least, partially explained on the
18 basis of similar kinetic mechanisms. To date, published data on kinetics of oxidation of
19 commercial fuels, such as gasoline and diesel fuels are still scarce [9,38].

20 21 **3.4. Oxidation and combustion of commercial fuels and biofuels**

22 Because of their complex chemical composition, the behavior of commercial fuel in
23 terms of reactivity is still not elucidated. In effect, most of the investigations used

1 surrogate reference fuels, namely *n*-heptane, *iso*-octane, and to a lesser extent, cetane and
2 undecane. Despite the difficulties encountered in these complex hydrocarbons, it is
3 important to experimentally examine real fuels, whose general characteristics are given in
4 Table 7, in order to elucidate their behavior *vis-à-vis* of knocking, ignition, and also,
5 oxidation and combustion. The distillation curve of diesel # 2 (Fig. 9) illustrates very well
6 the complexity of this fuel that contains a multitude of components. The distillation curve
7 of *n*-heptane corresponds to a horizontal straight line indicting the boiling point at 371.4
8 K of a single component [86]. Whereas, the gradual increase in the recovery of the diesel
9 distillates with increasing temperature from 460 to 600 [16] indicate the change in the
10 boiling point of the fuel complex structure (Fig. 9), which results from a multitude of
11 components and fractions in the diesel. This complex behavior of the diesel fuel is often
12 approached by using single component hydrocarbon surrogates and in a few more
13 advanced studies by a mixture of 2 or 3 hydrocarbons [9,11,17,38].

14
15 Combustion modeling of real fuels like gasoline, jet fuel and diesel is hampered by
16 the complexity of these hydrocarbon distillates [17]. Characterization of these fuel and
17 also elucidation of their oxidation, may enable us to develop suitable methods for fuel
18 preparation for the applications mentioned previously, namely, pre-vaporized burning, as
19 well as reforming for fuel cell technology, using cool flames. According to Edwards [17],
20 analysis of aviation kerosene indicates that a modeling surrogate would match real
21 aviation fuel with more accuracy if (1) the fraction of aromatics was increased to about
22 18 % (v/v), (2) the aromatic was a C₁₀ alkyl benzene, and (3) the non-aromatic
23 component was an *iso*-paraffin and/or naphthene, as opposed to *n*-paraffin. Given the

scarcity of experimental data, it is certainly debatable whether these changes would improve the accuracy of the model prediction for aviation kerosene combustion. The author suggested that surrogates for specialty kerosenes like JP-7, RP-1 and RG-1 should be based primarily on C₁₁-C₁₂ naphthenes and *iso*-paraffins to match the real fuels as closely as possible.

To test the thermal and oxidative stability of Jet fuel (Jet A-1, JP-TS and Jet A), Heneghan and Shultz [87] used a surrogate fuel Jet P-8S composed of a mixture of a dozen components adding to 65 % alkanes, 20 % aromatics and 15 % naphthenes. The oxidation of these fuels in static and flowing conditions was studied by following the oxygen consumption, the appearance of peroxides, alcohols and ketones. After exposure of the fuels to a temperature of 290 K, the deposits were analyzed by FTIR, GC and HPLC techniques. The thermal stability was measured by the Jet fuel thermal oxidative tester (JFTOT). The data showed that contrary to the expectations, the rate at which the fuel oxidizes was found to be inversely related to the rate of formation of insoluble products. Some properties of Jet and diesel fuels of different boiling ranges, namely, aromatic contents, hydrogen content, smoke point, density and cetane number, can be determined from simple linear relations [88]:

$$P = a_1 C_n + a_2 C_{ar} + b_1 T_{10} + b_2 T_{90} + k \quad (31)$$

Where a_1 , a_2 , b_1 , b_2 , k , are constants and T_{10} and T_{90} , temperatures at 10 and 90 % of fuel vaporized. The predictive equation 31 correlated well with experimental data and should assist in defining broad refining requirements for fuels. The influence of fuel composition on first stage of combustion and soot formation was tested for tetradecane, *n*-heptane and

1 diesel fuel using spectral extinction and flame intensity to evaluate the effect of aromatic
2 compounds in diesel fuel on soot formation [16]. The total amount of soot formed during
3 combustion was in the order: *n*-heptane < tetradecane < diesel, indicating the contribution
4 of the aromatic components in the diesel fuel.

5
6 In the presence of heat and dissolved O₂, jet fuel degrades through a complex
7 sequence of chemical reactions forming oxidized products and fouling surfaces [89]. Jet
8 fuel oxidation and the effect of antioxidants and antioxidant additives have been studied
9 [89] using a chemical kinetic model and a computational fluid dynamics code (CFD)
10 which employs pseudo-detailed kinetic modeling of dissolved O₂ consumption and
11 antioxidant chemistry in Jet fuel. Concentration profiles of various species along a
12 stainless-steel tube were calculated for both nearly isothermal and non-isothermal
13 flowing systems. Predicted dissolved oxygen and hydroperoxide profiles agreed well
14 with the measured profiles over a range of bulk fuel temperatures and flow conditions.
15 The model was found to be able to simulate a synergistic reduction in the oxidation rate
16 in the presence of antioxidants. However to date, little is known on the gas phase
17 oxidation kinetic mechanisms of commercial fuels, including gasoline and diesel.

18 19 **4. Reforming of fuels for fuel cell technology**

20 The studies discussed above were related to the oxidation and combustion of fuels.
21 They have contributed a great deal in understanding mainly the oxidation and combustion
22 of reference fuels. These investigations have made a significant contribution in
23 developing efficient engines and oil burners, projecting optimum fuel consumption to

1 reduce the energy demand and lowering pollutant emissions that have to meet the
2 regulations. During the last 3 decades there are growing concerns about the shortage in
3 energy supply in the world, as well as about the increase of pollution including that of
4 green house gases. This has spurred the development of fuel cells that convert chemical
5 energy to electrical energy [4,90,91,92] using hydrogen as fuel with low to zero pollutant
6 emission.

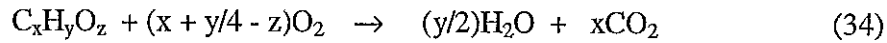
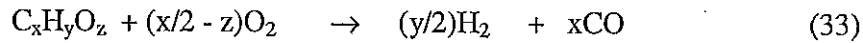
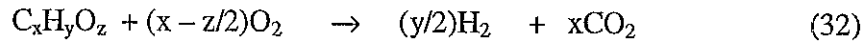
7
8 Hydrogen is an ideal fuel for fuel cells. Unfortunately, this valuable gas is not a
9 primary source of energy as fuel to be used in transportation vehicles, aerospace and
10 other industrial sectors and has to be produced through conversion of hydrogen-rich
11 energy carriers, such as natural gas, petroleum derived hydrocarbons, methanol and coal.
12 Therefore, the successful development of fuel cell-powered vehicles is dependent on the
13 development of fuel processors. The most common techniques of hydrogen production
14 for fuel cell technology are the catalytic partial oxidation and catalytic reforming of
15 primary (natural gas, gasoline, diesel) or secondary (methane, methanol) fuels into
16 synthesis gas ($H_2 + CO$). As discussed in the cool flame section, the pretreatment of the
17 fuel via partial auto-oxidation under cool flame conditions (Fig. 1) is more advantageous
18 to the reforming processes than the direct use of untreated fuels for the generation of
19 hydrogen.

20
21 As the focal point of this review remains on the oxidation and reforming of fuels, the
22 fundamentals of fuel cell as an electrochemical system and an energy conversion device
23 are out of the scope of this study and is the subject of several reviews [4,90-94].

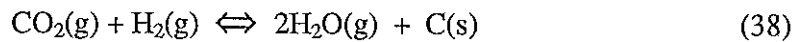
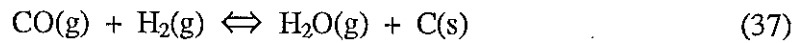
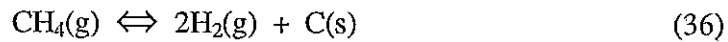
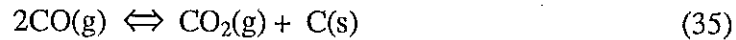
Nevertheless, it is relevant here to briefly discuss the different types of fuel cells that will be referred to in the fuel reforming section. Fuel cells are named by the kind of electrolyte, which plays a paramount role in the transport of the electrons upon oxidation of hydrogen at the anode and reduction of oxygen at the cathode, and thereby generating current. The main investigated fuel cells include phosphoric acid fuel cells (PAFCs) [4], molten carbonate fuel cells (MCFCs) [95-98], and solid oxide fuel cells (SOFCs) [99-101] that demonstrate high efficiency (45 %) [6] and operates at intermediate to high temperatures [4,99,102]. Given the state of technology, the polymer electrolyte fuel cell (PEFC) has the potential to replace the internal combustion engine for propulsion power [103], if it could operate on hydrogen [6]. Proton exchange membrane fuel cell (PEMFC) also called solid polymer fuel cell (SPFC) [4,104] have gained interest in the recent years and superseded alkaline electrolyte fuel cells (AEFC) that were developed in 1960s and 1970s [4]. Detailed description of the different fuel cell systems and the advancement in this technology are presented by Kordesch and Simader [94] and Larmini and Dicks [4]. As mentioned above, the alternative to the lack of hydrogen refueling infrastructure and the low density of hydrogen storage is to carry liquid fuels that have high energy density and convert them to H_2 -rich gas (reformat) via onboard fuel processor using the different techniques described below.

Before discussing the most recent studies on the partial oxidation and reforming of methane and natural gas as major sources of hydrogen, we briefly highlight the theoretical aspects and mechanisms of these processes [6,105]. The process of partial oxidation (PO) is based on extreme rich combustion (low air/fuel ratio). The fuel is

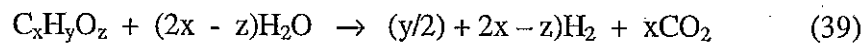
oxidized to give CO, CO₂, H₂ and H₂O according to the following reactions, both catalytically and non-catalytically [105]:



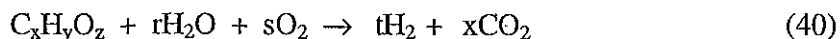
A catalytic system will reduce the operating temperature if the heat can be supplied directly to the catalytic bed. An advantage of this process is the insensitivity to contaminants and also indifference to the fuel type. The drawback is the risk of carbon precipitation and deactivation of the catalyst [105]. In addition to Boudouard reaction 35, methane decomposition (reaction 36) as well as CO and CO₂ hydrogenation (reactions 37 and 38) must be controlled:



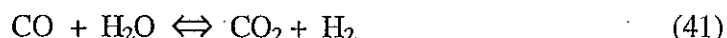
Methane cracking is an endothermic reaction ($\Delta H_r > 0$), while the others are exothermic ($\Delta H_r < 0$). Partial oxidation (PO) can be followed by steam reforming (SR), and thus, the heat generated by the partial oxidation will be used to supply the energy necessary for the steam reforming (reaction 39). The main role of steam in the reforming reactions is to push the equilibrium toward H₂ and CO formation (reactions 37 and 38) [93].



Usually, reforming processes including both steam and oxygen are often designed as autothermal reforming (ATR); with ($\Delta H_r \sim 0$) in the reaction 39, but in reality a certain excess of air is added to compensate for heat losses (reaction 40).



Lower temperatures favor the water-gas shift reaction (reaction 41), which results in a higher selectivity for carbon dioxide and hydrogen.



Based on an idealized calculation using the packaged software HSC-Chemistry, Ahmed and Krumpelt [6] stated that PO and ATR processes are more attractive for practical applications and capable of higher reforming efficiencies than SR. Whatever the type of the fuel reforming process, the fact that petroleum derivatives contain sulfur, which is a notorious catalyst poison, a preliminary desulphurisation step is required. Careful design of a desulphurization system is required to ensure that the fuel gas passing through the reformer catalyst to the fuel cell stacks contains only very low levels of sulphur (< 0.1 ppm) [4]. However, it is worth mentioning that biofuels are free of sulfur and should be considered for reforming. The other additional step is to clean up through water gas shift reaction (preferential oxidation) to lower the level of CO [105]. Fig. 10 depicts the different steps undertaken in the reforming process of fuels into hydrogen-rich gas followed by a preferential oxidation prior to supply the fuel cell system with hydrogen. To the original scheme presented by Thomas et al. [5], we have incorporated a new category of potential fuel (biofuel) and a new step delineating the pretreatment of fuel oils in cool flame prior to the reforming. However, there is no data available on the

yield of H_2 to be expected from the reforming of either biofuel (Fig. 10, path b) or cool flame treatment of liquid fuels, including biofuels (Fig. 10, path c).

4.1. Reforming of methane, natural gas and methanol

Methane is the major component (up to 90%) of natural gas. Also, methanol can be produced from different sources, including a large amount from steam reforming of natural gas via syngas [106].

4.1.1. Reforming of methane

In view of the high ratio H/C in methane ($H/C = 4$) and natural gas, these hydrocarbons seem best suited for hydrogen production. It is well known that the most common process for H_2 generation for fuel cells is based upon the steam reforming (endothermic reaction) of methane and natural gas [107-109]. However, partial oxidation is a commonly used process because of its mild exothermicity. Antonucci et al. [110] examined a 150 W tubular solid oxide fuel cell (SOFC) stack prototype, directly fuelled by methane. The fuel was partially oxidized to synthesis gas (reaction 42) an alternative route to the strongly endothermic steam reforming (reaction 43) [111].

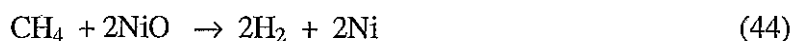


Further, they suggested that development of a cost effective catalyst (without noble metal) able to withstand low O_2/CH_4 ratios in order to maintain electrochemical efficiencies, as well as controlling the uniformity in temperature distribution along the

1 fuel cell units, likely represent most critical issues for the development of solid oxide fuel
2 cells.

3 Cavallaro and Freni [111] studied the feasibility of overall process economy of an
4 integrated system of molten carbonate fuel Cell (MCFC) and autothermal reformer
5 (ATR). They presented a theoretical approach and evaluated the ATR-MCFC
6 performance in terms of pressure, inlet rates of oxygen and steam, current density and
7 cell configuration (indirect or direct) at $T = 923$ K. Also, different types of catalysts
8 ($\text{Ln}_2\text{Ru}_2\text{O}_7$, transition metals $\text{Me}_1/\text{Al}_2\text{O}_3$, $\text{Me}_2/\text{Al}_2\text{O}_3$, CoO/MgO , $\text{NiO}/\text{Ln}_2\text{O}_3$, (Cr,
9 La)Ni/MgO; Ln = lanthanide and $\text{Me}_2 = \text{Pt}$, Pd, Rh, Ir, 1% w/w) and microreactors
10 (Labcon, quartz, silica) were studied. Up to 94 % of methane was converted. The
11 selectivity toward hydrogen on $\text{Ln}_2\text{Ru}_2\text{O}_7$ and $\text{Me}_1/\text{Al}_2\text{O}_3$ catalysts was about 99 %.
12 However the selectivity to CO varied from 40 to 97 and from 0 to 97 %, respectively,
13 depending on the type of catalyst. Using partial oxidation process on a commercial
14 Ni/ Al_2O_3 catalyst (CRG-F), Recupero et al. [112] showed that 97 % of methane was
15 converted, oxygen conversion was close to 100 % and the selectivity toward both
16 hydrogen and CO reached 99 %. The influence of several operating parameters on the
17 mass and energy balances of a 10 kW power plant was also investigated using a
18 mathematical model [113]. The electrical efficiency obtained for the examined system is
19 lower than that from a direct methane steam reforming monocell (DIR-MCFC), but the
20 exhaust gas composition seems to be usefully adoptable for the production of organic
21 compounds, such as methanol.

The mechanism of the partial oxidation of methane to synthesis gas was studied over a reduced NiO/SiO₂ catalyst using isotopic GC-MS technique with CD₄ [114]. It was suggested that CH₄ was activated via dissociation before its oxidation, but dissociation was not rate determining. Besides the general expressions of the methane oxidation mechanism (reactions 44 and 45), the authors gave the different steps of the reaction on the catalyst surfaces.

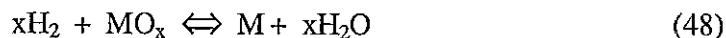
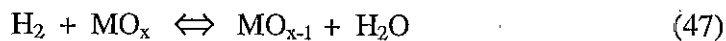


The kinetics of internal steam reforming of methane were examined on Ni-ZrO₂(Y₂O₃)-cermet electrodes under open circuit conditions at T = 1073-1173 K and partial pressures of methane and steam up to 60 and 5 kPa, respectively [109]. A kinetic expression was derived describing quantitatively the basic surface reactions on the Ni-YSZ-Cermet surface. The reaction exhibits the Langmuir-Hinshelwood kinetic behavior and consists in two-rate limiting steps, which are represented by the activated adsorption of CH₄ for the production of active species (most probably in the form of active adsorbed carbon C_{ads}) and the surface reaction of adsorbed Carbon with adsorbed oxygen (originating from water dissociative adsorption) for the production of CO. The H₂/CO₂ ratio is finally influenced by the water-gas shift reaction (reaction 41). Also, due to the methane pyrolysis, deposition of coke can occur in the second stage. This coke cannot be removed in a fixed-bed reactor and may cause catalyst deactivation. Marschall and Mleczko [115] used an internally circulated fluidized-bed (ICFB) reactor to investigate the partial oxidation of methane to syngas over Ni/αAl₂O₃ catalyst (1 and 5 % Ni loading, 71-160 and 250-355 μm particle diameter) at 1073 K with a CH₄/H₂ ratio of 2. Methane

conversion achieved was up to 97 % with a selectivity of 97 % toward hydrogen. However, the conversion and selectivity were strongly influenced by the temperature distribution in the reactor. Deactivation of the catalyst due to carbon deposition occurred and a significant drop in the catalyst activity was noticed during 150 hours of operation.

Investigation of novel solid oxide fuel cell (SOFC) type catalytic reactor utilizing a partial oxidation of methane as internal reforming reaction was promising [116]. Large electric power densities (731 mW/cm²) and heat energy were obtained simultaneously by applying LaGaO₃ based Perovskite solid electrolyte, which exhibits fast oxide ion conduction especially when doped with Fe. Also, a parametric model combining both empirical and mechanistic qualities was developed [117] in order to predict the performance of proton exchange membrane fuel cell (PEMFC) for a Ballard Mark V with 5 kW and 35 cell stack. The model, that can be applicable to a variety of transportation situations, allows calculating the cell voltage output as a function of a complex relationship between current, stack temperature and inlet partial pressure of hydrogen and oxygen. More promising is the most recent study by Otsuka et al. [118], which showed the possibility to produce hydrogen from methane without CO₂ emission by decomposition of the hydrocarbon over iridium and iron oxide catalysts. Firstly, methane is completely decomposed to carbon and hydrogen (reaction 46) over a solid catalyst in the presence of a metal oxide (MO_x), which is reduced by hydrogen (reactions 47 and 48). The resulting water is condensed in a trap cooled at < 273 K and the hydrogen is stored as reduced solid metal oxide (MO_{x-1}).





The carbon produced should be carried back to the gas field or used as graphite, fibers and plastics. The reduced metal oxide (MO_{x-1} or M) is transported, stored and used for the system H_2 - O_2 fuel cells. Contact of water vapor with the reduced metal oxide recovers the pure hydrogen without carbon oxides. For this study, Ni fumed silica (Ni/Cab-O-Sil) was chosen as a catalyst for decomposition of methane (reaction 46) and In_2O_3 , Fe_2O_3 and Fe_3O_4 as metal oxide mediators for the storage and production of hydrogen (reactions 47 and 48). Indium and iron oxides seem promising mediators for the storage of H_2 from CH_4 decomposition. The reduced states of these oxides are resistant under open-air at room temperature, and economically, iron oxide may be a better mediator than indium oxide. It was also suggested that hydrogen could be generated from aqueous solution of sodium borohydride (NaBH_4) for fuel cell power systems [119]. However, the latter process may not be economical for large use.

4.1.2. Reforming of natural gas

As a potential source of hydrogen, natural gas offers many advantages. It is widely available and can be converted to hydrogen quite easily [120]. However, sulfur impurities may constitute a drawback and would have to be removed. When catalytic steam reforming is used to generate hydrogen from natural gas, it is essential that sulfur compounds are removed upstream of the reformer by various desulphurization processes. On the other hand, low temperature cells will not tolerate high concentrations of carbon

monoxide, whereas the molten carbonate fuel cell (MCFC) and solid oxide fuel cell (SOFC) anodes contain nickel on which it is possible to electrochemically oxidize carbon monoxide directly, and thus, can internally reform fuel gas [4]. Dicks [120] reviewed the principle methods of converting natural gas into hydrogen by catalytic steam and autothermal reforming, pyrolysis and partial oxidation. In addition, he examined purification techniques and the recent advances in the internal reforming and the direct use of natural gas in fuel cells. A thermodynamic analysis of natural gas fuel processing based on simultaneous partial oxidation and steam reforming was conducted to predict the yield of H_2 , CO and C (graphite) [121]. It was shown that with different combinations of the air-fuel and water-fuel molar ratios, it is possible to obtain a maximum hydrogen yield with minimum production of CO and C. The results obtained under the assumption of adiabaticity with a temperature of 1093-1144 K, show optimal hydrogen yield of 36.5 % with 2.2-4.4 % CO and 0.55-0.96 % residual methane, while the solid carbon was suppressed.

Usually, synthesis gas is produced by steam reforming of sweet natural gas (sulfur free to avoid catalyst poisoning) and thus sulfur has to be separated from sour natural gas. Abdel-Aal and Shalabi [122] carried out a study to validate the technical feasibility of a non-catalytic partial oxidation process of sour natural gas. They presented the basic reactions along with thermodynamic data and compared the existing processes of handling sour natural gas. Stressing the thermodynamics and stoichiometry of the partial oxidation reaction, this group [123] simulated the direct production of synthesis gas from sour natural gas by a non-catalytic partial oxidation (NCPO). They suggested that the

transformation of hydrogen sulfide into sulfur dioxide and hence sulfuric acid along with production of synthesis gas via NCPO offers a novel scheme that could compete with the conventional steam reforming. Moreover, there is elimination of both the expensive gas desulfurization process and the steam generation. In this respect, NCPO is described as self-sufficient steam-producer for the reaction. However, economic feasibility remains to be established.

In addition to natural gas, biogas has a high potential as fuel for fuel cell power plants. Nauman and Myrèn [124] described the development of biogas processes for a phosphoric acid fuel cell (PAFC) power plant to be located in rural India. The biomass fuel cell power plant consists of four major blocks. In the primary conversion step animal wastes and/or biomass are converted to a fuel gas by anaerobic digestion or thermal gasification. Secondly, the fuel processor removes impurities and converts the fuel gas to a hydrogen-rich gas. A PAFC generator is used for direct current (DC) production and a final block as inverter to convert the DC to alternating current (AC). Fairly high yields of hydrogen from biogas were obtained at relatively low temperatures (up to 800 °C) and steam-to-carbon ratios. Also, the large carbon dioxide content of biogas enhances hydrogen production and CO content can be kept at a tolerable level to the PAFC generator with two shift reactors. Therefore, the system seems technically feasible and it is comparable to a PAFC plant using natural gas. Biomass is another source that may have a future as co-feedstock with natural gas, or alone, for production of fuel for fuel cell vehicles. Although the unit cost of biofuels produced from biomass alone is still too high to compete with currently priced gasoline produced from petroleum, the higher

1 value of transportation fuels per unit of energy content will provide greater incentive for
2 considering this source of energy to be taken into account [125].

3
4 An alternative approach to the production of hydrogen from biomass is fast pyrolysis
5 to generate a liquid product known as bio-oil that can catalytically be steam reformed.
6 This approach has the potential to be cost competitive with the current commercial
7 processes of hydrogen production [126]. The organic compounds derived from biomass
8 pyrolysis are mainly composed of oxygenates (aldehydes, alcohols and acids derived
9 from carbohydrates and phenolics from lignin) [126]. The overall steam-reforming
10 reaction of bio-oil or any oxygenate compound ($C_xH_yO_z$) is given by the reaction (40).
11 Model compounds (methanol, acetic acid, syringol and *meta*-cresol), both separately and
12 in mixture as well as the whole oil and its aqueous fraction were studied [108]. It was
13 shown that bio-oil or its aqueous fraction could be efficiently reformed to generate
14 hydrogen by a thermodynamic process using commercial nickel based catalysts with a
15 hydrogen yield up to 85 % of the stoichiometric value. Provided that the catalyst
16 temperature is above 923 K, acetic acid was almost completely converted to hydrogen
17 and carbon oxides. Reforming the complex oxygenates seems chemically possible, using
18 nickel based catalysts, but it may require high steam to carbon ratios because oxygenates
19 rapidly dehydroxylate, which results in the formation of aromatics on the surface of the
20 catalyst [127]. This work on the reforming of oxygenates concords with our hypothesis
21 that the reaction products of cool flame treated fuels, which are predominately formed by
22 oxygenates, have potential for reforming. This view suggests that biofuels, which contain
23 a significant proportion of oxygenates, could be good candidates for reforming.

Despite the advances in basic fuel cell technology, the fueling options for fuel cell vehicles are still uncertain and the nascent fuel cell vehicle industry faces fundamental choices concerning the type of fueling infrastructure [128]. Realistic cost effective options for both onboard hydrogen storage and for economically viable hydrogen infrastructure development have been described [128]. The authors concluded that hydrogen produced by small-scale equipment would be cost effective with gasoline per mile driven with direct environmental benefits.

4.1.3. Reforming of methanol

Methanol is an alternative fuel and has been considered as a potential source of syngas production. At Argonne National Laboratory, Kumar et al. [129] have compared a partial oxidation reformer (POR) and a steam reformer (SR) for methanol. While the reformat from POR has a concentration of H_2 about 50%, the steam reformer produced a concentration of H_2 up to 70-75%, leading to a small decrease (10 mV) in cell voltage. But the POR has an advantage; it is a compact, light-weight, rapid-start and dynamically responsive device. The Argonne POR concept has also been used to reform simple hydrocarbons, such as octane and pentane, as surrogates for more complex hydrocarbon fuels. Preliminary tests with selected catalysts have yielded H_2 concentration above 40 %. Kinetic studies of methanol-steam reforming on a commercial low-temperature shift catalyst (BASF K3-110) have been reported by Peppley et al. [130]. They presented a comprehensive Langmuir-Hinshelwood kinetic model of methanol-steam reforming on $Cu/Zn/Al_2O_3$ catalyst to simulate a methanol-steam reformer operating at pressures up to 4.5 MPa. The model developed predicts both the selectivity and the activity of the

1 catalyst. The simulation showed a minimum temperature near the entrance of the catalyst
2 bed resulting from the endothermic nature of the reaction. The reformer performance will
3 decrease dramatically, if this minimum temperature is below the dew point of the
4 vaporized mixture.

5
6 Ahmed et al. [131] have developed a specific reactor, using ceramic honeycomb disks
7 coated with the copper zinc oxide catalyst, along with a mechanism for controlling the
8 oxygen/methanol molar ratio and regulating temperature to produce a commercially
9 viable system. The partial oxidation reformer is provided with a system for introducing
10 methanol and water in small droplets (0.1 mm diameter) and intimately mixing the
11 droplets with air prior to partial oxidation. In more recent investigations, Ramaswamy et
12 al. [132] and Sundaresan et al. [133] focused on the steam reformation process of
13 methanol. Their system consists in a steam reformer, a catalytic burner and the fuel
14 preparation unit (preheater-vaporizer-superheater) and the CO cleanup units. In this study
15 an integrated reformer-burner was used as a "bi-catalyst plate". One side of each plate is
16 coated with the reformer catalyst and the other side with the burner catalyst. This
17 reformer-burner configuration uses conduction across the width of the thin plate to
18 rapidly transfer heat from the burner to the reformer. The start up time can also be
19 reduced significantly. Avci et al. [134] studied quantitatively the conversion to hydrogen
20 of methane, propane and octane as surrogate for natural gas, LPG, gasoline and methanol
21 under conditions pertinent to fuel cell operation. They also examined the process by a
22 series of computer simulations. The results show that in terms of hydrogen produced per
23 weight of fuel and water carried, direct partial oxidation of propane or oxidation/steam

1 reforming of octane are the best alternatives. To minimize coke formation on the Ni
2 catalyst, particularly for gasoline, a steam/carbon ratio of 2.5 was required. Still, the
3 presence of aromatics in gasoline may produce coke, and thus, the use of precious metal
4 catalyst, such as Rh is required to partially prevent coke formation. Methanol reacts at
5 room temperature but gives lower yields.

6
7 A large-scale prototype direct methanol fuel cell (DMFC) has recently been built, as
8 well as a series of engineering models developed for predicting stack voltage, the fluid
9 distribution from the stack manifolds, the overall system pressure, the chemical
10 equilibrium in both anode and cathode flow beds and the thermal management of the
11 stack [135]. The model predicted within 5% of the measured values.

12
13 Methanol fuel cells are also the focus of research that is being carried out at
14 Brookhaven National Laboratory. Our interest consists in developing a low-cost
15 methanol synthesis process via catalytic conversion of methane-derived synthesis gas
16 (primarily a mixture of CO, H₂ and CO₂) from methane. Our approach is to develop a low
17 temperature ($T < 423$ K) catalyst to achieve a high conversion (> 90 %) per pass [136]. In
18 our overall low temperature methanol fuel cell scheme, a catalyst has been developed to
19 produce CO-free H₂ as a fuel-cell feed to enhance the fuel cell catalyst life [137, 138].

20 21 **4. 2. Reforming of gasoline, diesel, and biodiesel**

22 Several types of fuels have been considered for fuel cell systems (Fig. 10). Although
23 methane is the most abundant of alkanes, it is the least reactive and its selective

conversion to more useful compounds remains challenging [114]. Among the abundant literature on methanol conversion [129,132,133,135], some of the recent relevant investigations were highlighted above. But since methanol itself has to be produced from other sources, other conventional fuels more easily obtainable and also abundant, including gasoline, which has more than twice the energy content of methanol, diesel and hydrocarbons are being considered. Provided there is progress in new reactor designs and new class of catalysts, these fuels may be competitive [139]. Docter and Lamm [140] conducted thermodynamic equilibrium calculations to estimate the potential energy efficiency of different hydrocarbon fuel reformer concepts. The efficiency of the reformer, η_{ref} was defined as:

$$\eta_{\text{ref}} = (n_{\text{CO}} + n_{\text{H}_2})\text{LHV}_{\text{H}_2}/n_{\text{fuel}} \text{LHV}_{\text{fuel}} \quad (49)$$

where n is the number of moles of CO, H₂ and the fuel and LHV the lower heating values (LHV_{H₂} = 242 kJ/mol and LHV_{fuel} = 4050 kJ). According to the simulation results for the gasoline studied, as represented by C₇H₁₂ and the German “normalbenzin”, autothermal-reforming can yield higher energy efficiencies than partial oxidation. The reformer efficiency showed a maximum around a steam/carbon ratio of 0.7 and was coupled to the equivalence ratio. A maximum efficiency of 83 % was calculated at a minimum λ of 0.28 and a reactor temperature of 1103 K. It was also stated that from a thermodynamic point of view, the formation of solid carbon-soot or -coke depends on the ratio of carbon to hydrogen in the fuel, as well as on the air to fuel ratio, the steam to carbon ratio and the reactor temperature.

Brown [106] surveyed seven common fuels for their utility as hydrogen sources for PEM fuel cells used in automotive propulsion. Hydrogen, methanol, ethanol, natural gas, gasoline, diesel fuel, and aviation jet fuel were considered. Except for methanol, and of course pure hydrogen, the processes generating hydrogen require: a) temperatures higher than 1000 K, b) appropriate water-gas shift reactors to remove CO and c) no sulfur or low-sulfur in the fuels. The gases produced by steam reforming contain up to 70 % hydrogen, whereas those obtained by partial oxidation have lower hydrogen content (35-45 %). According to the author, since hydrogen has severe distribution and storage problems, the steam reforming of methanol is the leading candidate process for on-board generation of hydrogen. However, if methanol is unavailable or the price makes it unaffordable, reforming processes for gasoline and diesel fuel have potential and remain a challenging task. For instance, tests on the effect of fuel constituents including impurities on the durability of catalysts and carbon formation during the fuel processing were conducted at Los Alamos National Laboratory [141]. The report shows the negative effect of sulfur on the catalyst ($\text{Ni}/\text{Al}_2\text{O}_3$) as hydrogen production decreases by 3 times after 5 hours. The tendency for carbon formation as a function of the fuel studied showed the following general trend: xylene > methylcyclohexane > pentane > *iso*-octane, although this still remains to be quantified. This work should be extended to real fuels, including gasoline and diesels.

Kopasz et al. [142] tested a fuel-flexible catalyst, which appears to be effective in partial oxidation of conventional (gasoline and diesel) and alternative (ethanol, methanol, natural gas) fuels to hydrogen-rich product gases with high hydrogen selectivity.

Alcohols were reformed at lower temperature (up to 873 K), while alkanes and unsaturated hydrocarbons require slightly higher temperatures. Cyclic hydrocarbons and aromatics have also been reformed at relatively low temperature. Complex fuels like gasoline and diesel require reforming temperatures up to 973 K. This group tried to answer the question: which hydrocarbon fuel is optimal for fuel cell systems? While methanol and ethanol have the advantages of being easy to reform, water soluble and renewable, gasoline and diesel have the advantage over the alcohols because of the existing refueling infrastructures and higher energy density. However, they are blends of different kinds of hydrocarbons and are believed to be more difficult to reform. Catalytic partial oxidation reforming in micro-reactors showed high conversion and hydrogen yields from methane, methanol, ethanol, cyclohexane, *iso*-octane, hexadecane, gasoline and diesel (Table 8). Alcohols as well as cyclic hydrocarbons and aromatics have been reformed at relatively low temperatures, while alkanes and unsaturated hydrocarbons require slightly higher temperatures. Complex fuels like gasoline and diesel require temperatures higher than 973 K for maximum hydrogen production. Results from a bench scale (3-kWe) reactor [143] showed that the reforming of gasoline and natural gas generated 38 and 42 % hydrogen on a dry basis at the reformer exit, respectively.

Aware of the importance and availability of gasoline and diesel fuels as potential source of energy, the Argonne National Laboratory research group [144-146] have paid significant attention to the catalytic reforming of these fuels. Further, they developed a process incorporating partial oxidation/steam reforming catalyst that converts gasoline and diesel fuels. Tests of 3 types of diesel fuel (hexadecane, which is a saturated alkane

1 and used as a diesel surrogate, low-sulfur diesel fuel, Diesel # 1 and a regular diesel fuel,
2 diesel # 2) showed a complete conversion of the feed to the products. Hexadecane
3 yielded 60 % on a dry nitrogen-free basis at 1123 K. In turn, higher temperatures were
4 required to approach the level of hydrogen produced for the two other fuels. On the other
5 hand, some unexpected results are of interest. At 1073 K, hydrogen yield of the low
6 sulfur diesel was 32 %, while that of the regular diesel grade 2 was 52 % with residual
7 products in both cases including CO, CO₂, ethane, ethylene and methane. Diesel # 2 has
8 higher level of sulfur and a higher fraction (40 %) of aromatics (2 times) than that of
9 diesel # 1 (20 %), which tends to reduce the H/C ratio of the feed and thereby, the
10 hydrogen level in the products, but this was not the case. It is suggested that aromatics
11 might have been more easily reformed than cyclic aliphatic [145]. Therefore, more in-
12 depth studies should be carried out to elucidate this result. The diesel reformat was
13 further processed to remove sulfur and CO using a train of reactors consisting of a sulfur
14 scrubber and two water gas shift beds that reduced CO content from 20 to 2 %. To better
15 evaluate the effect of sulfur on catalyst activity, coke formation and the thermal stability
16 of the catalyst, longer-term tests with diesel fuel are intended to be conducted by this
17 group [145].

18
19 Anumakonda et al. [147] described a method of processing sulfur-containing heavy
20 hydrocarbon fuels in a substantial absence of steam through catalytic partial oxidation. It
21 consists of two steps; i) vaporizing the fuel and mixing with air at a ratio $\lambda = 1$ to 2 and
22 ii) feeding this mixture through a reactor containing a noble metal catalyst (typically
23 Rh/alumina) at contact times of no more than 0.5 s and lower hourly space velocity

(LHSV) of not less than $0.5\text{--}1.0\text{ h}^{-1}$. Despite the presence of the catalyst, the reaction occurred at no less than 1323 K, but the conversion to hydrogen and CO seems complete and the sulfur compounds present were predominantly converted into H_2S . By using *n*-octane as surrogate to gasoline with the combination of supported catalysts (Ni and Pd up to 10 %) on alumina, Yanhui and Diyong [148] obtained good hydrogen selectivity for catalytic partial oxidation and steam reforming at lower temperatures than those of Pereira et al. [145]. In addition, a significant amount of hydrogen (up to 65 % at 973 K) was obtained in the gas reformat.

Targeting the real industrial market for fuel cell technology in the near future, Amphlett et al. [149] developed a simulation of a diesel reformer system to identify potential design issues and obtain preliminary estimate of the system efficiency. A 250 kW fuel cell system that used reformed diesel as the hydrogen source has been modeled in HYSYS, a commercial process simulation package. For the simulation, a mixture of normal paraffins ($\text{C}_9\text{--C}_{20}$), alkylated benzene ($\text{C}_6\text{--C}_{12}\text{-benzene}$) and alkylated naphthalene ($\text{C}_1\text{--C}_4\text{-naphthalene}$) that have similar heats of formation, Gibbs energy and distillation curves were used. The authors suggested that to do an in-depth optimization, it would be necessary to include kinetic information for the reformer performance. Unfortunately to date, no information is available concerning the kinetics of hydrogen production from diesel or its alkane surrogates.

In addition to their significant contribution in investigating the optimum conditions for the partial oxidation of fuel oils at low temperatures under cool flame conditions

[7,53,62,150], the group of RTWH in Aachen (Germany) has focused on the implementation of the cool flame regime prior to the reforming of fuel oils to hydrogen-rich gas [150]. If this is realized, diesel fuels can be processed at low cost and with minimum formation of soot and low emission of NO_x , SO_x and CO, and thus, will be very good candidates as feedstock for fuel cell technology. The authors [150] studied the reforming of industrial gas oil (IGO) under atmospheric pressure. Their aim was to complete a compact 5 kW demonstration unit for use with a high temperature fuel cell. After preparation of the fuel in the cool flame regime where the mixture of the vaporized fuel and the preheated air were brought to 753 K, the partial oxidation is initiated in a second chamber by a spark ignition of the vapor mixture from the first chamber. After 3 to 4 min, the gas temperature reached 1523 K and the flame was stabilized in a ceramic porous solid-state matrix. The H_2 -rich gas was directed to a high temperature fuel cell. In this process, hydrogen and CO produced were each about 20 % at an equivalence ratio λ of 0.39, indicating a low conversion of the fuel and an unacceptable high amount of CO in the reformat. In a project that is being planned, we propose to combine the cool flame preparation step with the catalytic autothermal reforming of the reaction products that are rich in oxygenates and expect to produce a high yield of hydrogen.

Moon et al. [151] aimed to develop and integrate a gasoline reforming system with a PEM fuel cell using POR or ATR. In addition to naphta and gasoline, *iso*-octane was tested as a reference fuel in the absence and the presence of 100 ppm sulfur to test the catalyst's resistance. Also, high temperature water-gas shift over $\text{Fe}_3\text{O}_4\text{-Cr}_2\text{O}_3$ and low temperature shift reaction over $\text{Cu/ZnO/Al}_2\text{O}_3$ catalysts were investigated to remove CO

1 from the hydrogen-rich stream produced by the fuel-processing section. For *iso*-octane, a
2 maximum concentration of hydrogen (67.3 %) was observed at an O/C ratio of 0.5, which
3 decreased to 49.5 % at an O/C ratio of 2.0. The CO₂ concentration increased from 14.7 to
4 41.9 %, over the same range of O/C ratio. However, the concentration of the methane
5 formed remained virtually unaffected by the O/C ratio. The overall trend revealed that an
6 O/C ratio of 1.0 is ideal for the reaction at the H₂O/C ratio of 3. At these settings,
7 hydrogen concentration remained around 60 % and was little affected by the reaction
8 temperature in the range of 773-1023 K. The maximum production of H₂ was obtained at
9 a space velocity ranging from 4,000 to 17,000 h⁻¹. Reformulated naphta containing 4.5
10 ppm sulfur was tested using a commercial naphta reforming catalyst (NRC). The product
11 composition at T = 723 K and a space velocity of 4227 h⁻¹ was 49.8 % H₂, 1.77 % CO, 20
12 % CO₂ and 28.45 % air. After the high temperature shift, there was a slight increase in
13 the H₂ concentration, which remained constant during the low temperature shift, whereas
14 the concentration of CO abruptly decreased to 0.3 %. The authors suggested that in order
15 to reduce CO concentration in hydrogen-rich streams and obtain a compact size fuel
16 processor, a preferential partial oxidation (high shift temperature) reactor and a new high
17 performance catalyst with sulfur- and coke-resistance would be needed.

18
19 In their review paper, Ogden et al. [152] compared hydrogen, methanol and gasoline
20 as fuels for fuel cell vehicles. They presented modeling results comparing three leading
21 options for fuel storage onboard fuel cell vehicles: a) compressed gas hydrogen storage,
22 b) onboard steam reforming of methanol and c) onboard partial oxidation of hydrocarbon
23 fuels derived from crude oil, e.g., gasoline, diesel and middle distillates. The idea of

generating hydrogen from conventional fuels is making its way and the progress of the last years in the reforming processes [143] renders it possible to envisage onboard reforming for fuel cell vehicles. Recently, Ahmed and Krumpelt [6] assessed the theoretical conditions of the three principle pathways (steam reforming, partial oxidation, and autothermal reforming). The reforming efficiency varied from 88.2 % for benzene to 96.3 % for methanol and was correlated to the fuel properties and its heat of formation. Based on their theoretical calculation for some reference fuels including oxygenates, and contrary to the widely held beliefs, the authors stated that partial oxidation and autothermal reforming processes are capable of higher reforming efficiencies than are steam reformers. More studies are needed to confirm these results.

Besides improved dehydrodesulfurization of fuels [153,154], attention has been paid to reduce coking on the catalytic surfaces [155,156]. These efforts will help in facilitating the use of middle distillate hydrocarbons, including gasoline and diesels for reforming. Recently, Suzuki et al. [157] used a highly dispersed Rh on alumina ($\text{Ru}/\text{Al}_2\text{O}_3$) as a catalyst to explore the steam reforming of kerosene. After dehydrosulfurization of the fuel on a commercial catalyst (Cosmos-HDS catalyst, CDS-3), steam reforming was performed in a fixed bed flow reactor, where the mixture of the vaporized fuel and steam (ratio $S/F = 3.5$) passes through the fixed bed catalyst ($\text{Ru}/\text{Al}_2\text{O}_3$) at 1073 K and a rate of 10 ml h^{-1} . The product distribution was determined by GC analysis. The conversion of kerosene varied from 72 % on Ni/SiO_2 commercial catalyst to 99.5 % on $\text{Ru}/\text{Al}_2\text{O}_3$ and the selectivity toward hydrogen varied from 60 % on Ni catalyst to 70 % on $\text{Ru}/\text{Al}_2\text{O}_3$. The concentration of CO and CH_4 in the reformat was

1 slightly lower for Ru/Al₂O₃. When ceria (CeO₂) doped the catalyst system, the sulfur
2 resistance improved dramatically and the hydrogen production from hydrosulfurized
3 kerosene lasted for more than 8000 hours. Therefore, this study [157] illustrates the
4 possibility of hydrogen production using safe and easily transportable light middle
5 distillate oil, such as kerosene.

6 7 **5. Impact of NO_x emission and soot formation on the oxidation and reforming of** 8 **fuels and the evolution of burner technology**

9 During the oxidation and reforming processes, several parameters including the type
10 of burner, equivalence ratio and the quality of fuel have an influence on the pollutant
11 emissions, namely, the undesirable NO_x (NO + NO₂), as well as, soot formation, which is
12 a source of carcinogenic polyaromatic hydrocarbons (PAH). In this review, we will not
13 be concerned with sulfur oxides because sulfur can be removed by dehydrosulfurization
14 [153-154] and scrubbing [158-159].

15 16 **5.1. Impact of NO_x emissions on burner technology**

17 Outside the engine or burner exhaust, nitric oxide (NO) formed will oxidize to
18 nitrogen dioxide and react with unburned hydrocarbons in the presence of UV radiations
19 to form a photochemical smog [2]. Experimental results show that NO_x formation is
20 influenced by the equivalence ratio, fuel feed rate, the distribution of dispersion in diluted
21 air, but the fuel droplet diameter had the most significant effect on the change in NO_x
22 released [160]. In premixed or diffusion hydrocarbon flames, the main mechanisms of

NO formation are the Zeldovich “thermal NO” [1,2] and the Fenimore “prompt NO” [161] as described by Delabroy et al. [162].

NO_x can be reduced to N₂ and H₂O by selective catalytic reduction (SCR) with ammonia, which is an after-treatment technique used in stationary diesel applications [163-165] and scrubbing [158-159]. Research is still ongoing to overcome the drawbacks of the SCR technique, such as the narrow window of catalyst operation and the stability of catalysts [163]. Muzio and Quartucy [166] illustrated burner and boiler concepts resulting in a new generation of low NO_x porous surface radiant burners and the use of intelligent software systems allowing the operator to reduce NO_x emissions, while maintaining unit-operating parameters in the desired range. Furthermore, they suggested that the fuel NO_x would need to be controlled differently from thermal NO_x, since the nitrogen containing organic compounds can react at significantly lower temperatures. Low NO_x emissions were also achieved by a non-premixed, direct fuel-injection burner, equipped with a unique double swirler for gas turbine combustors [35]. The burner has circular and annular air channels to which swirlers are fitted. The inner channel converges into a throat, and gaseous (natural gas) fuel is injected into the airflow by a multihole fuel nozzle. For the double-swirler burner, the conventional small-hub swirler and the large-hub swirler burners, the NO_x emission indices were 0.5, 1.1 and 2.2 g/kg fuel, respectively, indicating the lowest NO_x emission level of the double swirler burner. The mixing of fuel and air is more rapid in the double-swirler burner, which results in a uniform equivalence ratio profile in the combustion region. This was suggested as the reason for the low NO_x emissions.

Novel catalytic radiant burners have been suggested to provide an alternative low emission approach for future applications. Emonts [33] has developed a catalytic burner that can be used for natural gas with hydrogen admixture in a heat recovery boiler for heat production and for methanol with hydrogen admixture in a reformer producing process heat to be used in a fuel cell system. Experimental data show a NO_x emission of less than 0.4 mg/kWh and CO emissions from 0 and 13 mg/kWh. In a more recent study using methane as fuel [167], the burner of a boiler was replaced by a metal honeycomb partially coated with a catalyst and operating as a radiant burner. It was shown that the NO_x and CO emissions with the catalytically stabilized burner were 5.0 and 0.0 ppm, respectively. A catalytic burner with noble metal catalysts Pd/NiO, supported on alumina wash-coated honeycomb has been used to burn natural gas for industrial purposes [168]. Although, the stable catalytic combustion region depended on the catalyst thickness, the authors [168] suggested that catalytic combustion has some special features, as the combustion efficiency was over 99.5 % without blow off or flashback.

More recently, the Canadian Gas Research Institute (CGRI) has developed a multi-jet, nominally non-premixed gas fired burner, intended to give low- NO_x performance at high air preheat [36]. Fuel (natural gas) and air undergo separately extensive mixing with recirculating furnace gases (products of combustion) and arrive at the reaction zone diluted by furnace gases, thus, lowering the temperature of the reaction and reducing NO_x emissions. The burner has NO_x emission levels from 2 to 40 ppm at 3 % O_2 and visually flameless oxidation process. The author stated that the mathematical model of the burner using commercial Computing Fluid Dynamics (CFD) software was capable of adequately

1 predicting jet trajectories and primary flow structures in the furnace. However, the
2 predicted temperature and species (O_2 , CH_4) concentrations depart from measured values,
3 thus raising a question of how to effectively model three-feed processes under severe
4 non-adiabatic conditions.

5
6 A lean premixed-prevaporization combustor (PPL-1) for a 100 kW automotive
7 ceramic gas turbine has been developed to meet the Japanese emission standards for
8 passenger cars without using after treatment [169]. To study the evaporation
9 characteristics, which are indispensable for improvement of a fuel atomizer, the authors
10 built a fuel-air preparation tube that consists of prevaporization-premixing tube (PP-tube)
11 and swirl chamber. The evaporation of fuel spray in the tube with a small diameter of 34
12 mm is controlled by the droplet diameter and the distribution of fuel spray near the wall.
13 Under the operating conditions, the non-evaporated mass fraction of fuel spray is largely
14 influenced by the drop size distribution and dispersion of the fuel spray. Sauter mean
15 diameter (SMD) of the fuel droplets and the non-evaporated mass fraction (NMF) passing
16 through the tube, decrease as the swirl number increases. The SMD of the fuel droplets
17 and the non-evaporated mass fraction (NMF) have an influence on the NO_x emission
18 indices. NO_x and CO emission indices, for the same combustion inefficiency for
19 kerosene, are lower than those for gas oil, because the SMD and NMF for kerosene spray
20 are lower than those for gas oil spray. It should be pointed out that NO_x reduction
21 techniques involve a trade-off between NO_x reduction and an increase in formation of
22 other pollutants, e.g., CO, unburned hydrocarbons and soot. A drop in temperature, which
23 is the basis of many NO_x reduction solutions, decreases the oxidation of CO and volatile

hydrocarbons [162]. These authors's tests showed that the predominant generation of NO_x in a single burner was due to the Fenimore prompt mechanism. Further, they emphasise that a large reduction of NO_x , including prompt and fuel NO , while maintaining zero levels of CO and soot was not observed in their novel 800 kW burner. It is plausible that reburning is responsible for lowering NO_x in this novel burner, whose concept consists in recirculating flue gas with concomitant reduction in flame temperature.

Among hazardous compounds originating from diesel engines, soot and NO_x have attracted most attention. In addition to the selective catalytic reduction (SCR) of NO_x into N_2 and H_2 in the presence of ammonia, the use of synthetic aluminosilicates (zeolites), generally ZSM-5, as catalysts for selective reduction of NO_x in stationary diesel exhaust gas seems promising. It was shown that in the presence of Ce-ZSM-5 catalysts, NO_x conversion could reach 70 % at 773 K in simulated diesel exhaust gas. Deactivation of the catalyst in real diesel exhaust gas occurs mainly in the first 60 h of operation [165]. Thereafter, the catalyst stabilizes and provides up to 40 % NO_x conversion at 723 K. The authors [165] suggested that preparation of Ce-ZSM-5 via solid-state ion exchange results in a remarkably active catalyst. It is noteworthy that blending petroleum diesel with biodiesel can possibly reduce particulate matter emission from engines with a slight reduction in NO_x emissions [170].

5.2. Impact of soot formation on burner technology

Beside the gaseous pollutants, whose level of emission is subject to legislation [163,166], engine and burner technology is concerned with the formation of particulate matter and soot, which are also considered as major pollutants of the atmosphere. The formation of soot during the oxidation and combustion of hydrocarbons is thought to take place via a number of elemental steps: pyrolysis, nucleation, surface growth and coagulation, aggregation and oxidation [163,171]. Some of the polyaromatic hydrocarbons (PAHs) formed during surface growth and remaining adsorbed on the soot surface are carcinogenic [163,172] and have harmful effects on health of the biota.

In an attempt to understand soot formation mechanisms, the effect of temperature and to predict soot yields in practical combustion systems, experiments were conducted by Sato et al. [173] in a toluene/air turbulent premixed flame in a jet stirred combustor. A global soot model was utilized to analyze rates of particle nucleation, coagulation and specific surface growth. Soot mass concentration measurements showed strong dependence of soot production on stoichiometry, residence time and flame temperature. Soot particle nucleation, growth and structure were also modeled [171] with a computer code describing the general steps of PAH growth via the H-abstraction/acetylene-addition reaction sequence and the coagulation of aromatic species containing numerous fused rings up to coronene (polycyclic benzenoid compound with 6 fused benzene rings). The computational results also showed that the surface growth rate is proportional to the acetylene (C_2H_2) concentration and independent of hydrogen at high H concentrations, but it declines at lower H atom concentrations [174].

Using a modified version of the KIVA-2 code, three-dimensional computations of combustion and soot formation were performed during the burning of two reference fuels (*n*-heptane and tetradecane) [175]. Assuming acetylene as the crucial pyrolytic species, the model takes into account the fuel-to-acetylene pyrolysis, acetylene oxidation, soot nucleation, surface growth and soot oxidation. Advances in modeling soot formation and burnout in combustion systems have been surveyed by Kennedy [176]. The models were grouped into three categories: i) purely empirical correlations, ii) semi-empirical approaches that solve rate equations for soot formation with some input from experimental data and iii) detailed models that seek to solve the rate equations for elementary reactions leading to soot. Ambrogio et al. [177] achieved satisfying abatement (> 80%) of diesel soot by coupling ceramic-foam filters with carbon combustion catalysts. A conical fluidized bed of glass was used to disperse the soot produced by an acetylene burner, into the gas flow to assess the pressure drop and the filtration efficiency of the foam traps as a function of the soot particle size, load on the filter and the specific velocity. The best performance was reached by using the catalyst $\text{Cs}_4\text{V}_2\text{O}_7$. The mathematical model of the reactor was validated using experimental data obtained with catalytic and non-catalytic traps. In implementing a new soot model applied to an aeroengine combustor, Balthasar et al. [178] showed that good agreement between experimental and simulation was achieved for laboratory flames, whereas soot is overpredicted for the aeroengine combustor configuration by one or two orders of magnitude. The authors suggested that the agreement between model and experiment would become better, if the surface reactions are calculated to be dependent on the soot surface instead of the soot volume.

Oxidation (gasification) of soot is of great significance for pollution control in industrial flames, auto engines and burners and can be achieved using different oxidants, including oxygen (O_2), carbon dioxide (CO_2), water vapor (H_2O) or nitrogen dioxide (NO_2) [179]. The authors described the use of catalytic regenerative traps at high temperature (> 1073 K) where the combustion takes place inherently in the flames after formation of the soot at low temperature (573-973 K). The four-reactant gases O_2 , CO_2 , H_2O and NO_2 all oxidize and gasify soot. NO_2 appears to be the most reactive at low temperature in the presence of cerium and noble metals, which were revealed to be effective catalysts. Some attention has been paid to fuel additives acting as soot oxidation catalysts, including organometallic compounds, which can be dissolved in diesel fuel [163].

6. Conclusions and prospects for future research

We have reviewed the most recent investigations on the preparation, auto-oxidation and reforming of fuel oils. Bridging the gaps between these three entangled processes would lead to advances required to achieve higher energy production and efficient conversion of fuels coupled with better control of pollution. This will boost human welfare and preserve the environment and the ecosystem health.

In the last two decades, the abundant work on the oxidation of fuels was confined primarily to single component reference fuels, especially, *n*-heptane and *iso*-octane as surrogate for the real fuels, such as diesel and gasoline, which are composed of a

1 multitude of complex hydrocarbon components including alkanes, naphthenes and
2 aromatics. The investigations reported in this study show that the different steps of fuel
3 preparation, including atomization and vaporization, influence the partial oxidation,
4 which is a paramount step in the burner systems, engine combustion and reforming
5 processes. The preparation of fuels is linked to the development of burner technology and
6 the targeting to achieve higher efficiency of fuel conversion coupled with lower emission
7 of pollutants.

8
9 The atomization and vaporization procedures have an important role in conditioning
10 the oxidation of fuels especially at low temperatures around the cool flame and the
11 negative temperature coefficient regions, two phenomena still not well understood. The
12 reaction products resulting from the partial oxidation at low temperatures where the cool
13 flame regime persists are suggested to play an important role in the reforming of fuels
14 into hydrogen-rich gas. The recent investigations on cool flames are promising to pave
15 the way for several beneficial industrial applications including generation of hydrogen for
16 fuel cell systems. Furthermore, the cool flame can be integrated as a preliminary stage to
17 burner combustion. But to date, sufficient data are not available to develop this premise.
18 Thus, further studies are needed to shed more light on the type of reaction products
19 formed during the partial oxidation of fuels at cool flame conditions and the conversion
20 of these reaction products into hydrogen-rich gas upon reforming process. Therefore, a
21 thorough examination of the role of cool flame in the oxidation and reforming of fuels
22 merit ample consideration. Processing of these complex fuels via cool flames leads to
23 reaction products composed of short molecules, such as lower molecular weight alkenes

1 and oxygenate compounds, including aldehydes, ketones and alcohols. Like methanol
2 and acetic acid, oxygenates are partially oxidized, and thus could be more easily
3 reformed to hydrogen-rich gas than the parent fuel oils. Also, it is worth mentioning that
4 biofuels, which contain a significant proportion of oxygenates, could be good candidates
5 for reforming.

6
7 A better understanding of the fuel oxidation chemistry is linked to the progress made
8 in kinetic modeling, which has proven to be a powerful tool in the analysis of many
9 oxidation and combustion systems. In the modeling of oxidation mechanisms, the
10 application of automatic generation techniques seems attractive where the extension of a
11 core-kinetic mechanism to higher hydrocarbons is involved. Apparently, the proposed
12 low and high temperature mechanisms for the oxidation process could be organized into a
13 comprehensive kinetic scheme able to simulate the oxidation of natural gas, gasoline,
14 diesel and biofuels. Nevertheless, despite the development in the computing techniques,
15 more experimental, and theoretical studies on the kinetics of oxidation of real fuels are
16 needed. Even, the kinetic modeling of the oxidation of a hydrocarbon mixture containing
17 alkane, naphthene and aromatic compounds with properties similar to real fuels, are still
18 scanty. Although there is a significant progress in modeling the kinetic mechanisms
19 related to the reaction products formed, ignition delay time and engine knocking
20 tendencies, the literature still remains limited primarily to the reference fuels cited (*n*-
21 heptane, *iso*-octane and to a lesser extent cetane). Investigations should be extended to
22 the complex real fuels, namely, gasoline, diesel, Jet-fuels and biodiesel, which in addition
23 to methanol, ethanol and natural gas, are considered as potential source for reforming

1 processes (catalytic oxidation) leading to the generation of hydrogen for fuel cell
2 systems.

3
4 An in-depth understanding of the preparation and auto-oxidation of fuel oils,
5 especially, using the promising cool flame procedure described in this review, will help
6 to develop more efficient fuel reforming processes with acceptable yields of hydrogen.
7 The proven techniques used in the fuel reforming processes are the partial oxidation,
8 steam reforming and autothermal reforming (combination of both). Partial oxidation and
9 autothermal reforming, apparently, give higher reforming efficiency in practical
10 applications, and thus, are more attractive. Although methanol seems a leading candidate,
11 the presence of infrastructure for gasoline and diesel fuels, which have high energy
12 density and can be carried safely, represents an advantage for these two petroleum
13 distillates to be converted into hydrogen-rich gas via onboard fuel processors. To date,
14 little is known on the auto-oxidation and reforming of biofuels or a blend of diesels and
15 biofuels, and thus, their investigation is recommended.

16
17 Intensive research is needed to improve catalytic processes and uncover new
18 generation of catalysts with higher activity, more resistance to sulfur and CO poisoning
19 and higher ability to reform gasoline and diesel fuels at lower temperatures. In this light,
20 development of nanocatalysts (ultra fine particles of metals, metal oxides and
21 composites), which are supposed to have higher surface area than conventional catalysts,
22 and thereby higher activity, will lead to cost effective reforming processes. This
23 technology is still at the laboratory level, but it seems promising in the future.

Whether for the preparation, oxidation, combustion, reforming or burning processes, the techniques developed have the same concerns about environmental pollution. Therefore, measures are undertaken to identify and reduce pollutants, such as sulfur, nitrogen oxides, mono- and dioxides of carbon, as well as soot emanating from these processes. This effort will help to meet the regulations, and thereby, preserve the ecosystem health. While sulfur can be removed from the fuel by hydrodesulfurization, NO_x emissions can be reduced by selective catalytic reduction with ammonia. However, the latter technique is controversial, and likely, advanced low NO_x burners either for gaseous or liquid fuels are required. The effects of the fuel nitrogen on NO_x emission are still not well known. Apparently, the approach of spiking domestic fuel with nitrogen-containing molecules, such as pyridine, may not be conclusive, and thus, studies should be carried out directly on crude oils and petroleum distillates. Burning of fuels also leads to the undesirable soot formation, which can be inhibited by using catalytic burners, catalytic traps and adequate reactors with inert surfaces. Based on the data of soot formation under different experimental conditions, the validation of the proposed mathematical models will help in better understanding the mechanisms of soot formation, and thus, figuring out new remediation processes. Advancement of the techniques in burner and reactor designs is a dual challenge in decreasing pollutant emissions, and increasing the conversion of fuels in the oxidation reactions.

Since the mechanism of Zeldovich NO is limited to high temperature oxidations, it is of interest to examine the significance of Fenimore NO mechanism at low temperature

under cool flame conditions. Occurring at low temperatures, the process of the cool flame may play a major role in the inhibition of NO_x formation. On the other hand, little is known on soot formation during the cool flame regime. Apparently, at such low temperature, there is little chance for pyrolysis. The reaction products are dominated by oxygenates, and further, the presence of acetylene, which is a soot precursor, was not shown. It is likely that, soot formation will be very limited under cool flame conditions. Studies on soot formation during the oxidation of fuels at cool flame deserve special attention.

Acknowledgements

This work was partially supported through the Laboratory Directed Research and Development (LDRD) funds provided by the Department of Energy under contract No. DE-AC 02-98CH 10886.

1 Appendix

2	A	pre-exponential collision factor (M s^{-1})
3	B_{Mh}	mass transfer number (-)
4	B_{Th}	thermal transfer number (-)
5	C_i	concentration of the specie i (mol m^{-3})
6	c_l	specific heat ($\text{J K}^{-1} \text{kg}^{-1}$)
7	$c_{p,g}$	heat capacity of the gas phase (J K^{-1})
8	d	droplet diameter (m)
9	dm/dt	mass transfer rate (kg s^{-1})
10	E_a	activation energy (J mol^{-1})
11	$h_{f,g}$	enthalpy of formation of the gas phase (J)
12	h_{∞}	convection coefficient (J K^{-1})
13	Δh_{com}	specific enthalpy of combustion (J)
14	k	reaction constant rate (-)
15	L	length of the flow reactor (m)
16	L_v	latent heat of vaporization (J)
17	LHV	lower heating values (J)
18	n_i	number of moles
19	p	pressure (Pa)
20	r	droplet radius (m)
21	R	universal gas constant ($\text{J mol}^{-1} \text{K}^{-1}$)
22	S_{ij}	sensitivity coefficient (-)
23	t	time (s)

- 1 T droplet temperature (K)
- 2 T_{s0} temperature of the droplet surface (K)
- 3 T_s temperature of the stream around the droplet (K)
- 4 T_∞ temperature of the gas phase far away from the droplet (K)
- 5 V average mixture velocity (flow rate) (m s^{-1})
- 6
- 7 $\partial d^2/\partial t$ first derivative of d^2 relative to time ($\text{m}^2 \text{s}^{-1}$)
- 8 $\partial m/\partial t$ first derivative of mass relative to time = mass transfer rate (kg s^{-1})
- 9 λ air to fuel ratio $(\text{O}_2/\text{Fuel})/(\text{O}_2/\text{Fuel})_{\text{stoich}}$ (-)
- 10 λ_g thermal conductivity of the gas phase ($\text{W m}^{-1} \text{K}^{-1}$)
- 11 ϕ Fuel to air ratio = $1/\lambda$ (-)
- 12 v specific mass ratio of the oxidizer to the fuel (-)
- 13 η_{ref} efficiency of the reformer (-)
- 14 ρ_l density of the liquid (kg m^{-3})
- 15 τ residence time (s)
- 16 τ_i ignition delay time (s)

References

- [1] Bowman CT. Control of combustion-generated nitrogen oxide emissions: Technology driven by regulation. Proc. 24th Int Symp Combust 1992. p. 859-878.
- [2] Raine RR, Stone CR, Gould J. Modeling of nitric oxide formation in spark ignition engines with multizone burned gas. Combust Flame 1995;102:241-255.
- [3] Dagaut P, Lecomte F, Chevalier S, Cathonnet M. Experimental and kinetic modeling of nitric oxide reduction by acetylene in an atmospheric pressure jet-stirred reactor. Fuel 1999;78:1245-1252.
- [4] Larmini J, Dicks A. Fuel cell systems explained. New York: Wiley & Sons, 2000
- [5] Thomas CE, James BD, Lomax FD, Kuhn IF Jr. Fuel options for fuel cell vehicle: Hydrogen, methanol or gasoline. Int J Hydrogen Energy 2000;25:551-567.
- [6] Ahmed S, Krumpelt M. Hydrogen from hydrocarbon fuels for fuel cells. Int J Hydrogen Energy 2001;26:291-301.
- [7] Köhne H, Rudolphi I, Gitzinger H-P., Hartman L. Method (procedure) for utilizing fuel by using exothermic pre-reaction in the form of a cold flame. International Patent, No. WO 00/06948, 1999.
- [8] Schrag J-C, Yäger FK, Köhne H, Küchen C. Fuel Oil Burner using cool flame. VDI-Berichte 2002;1643:47-54.
- [9] Dagaut P, Reuillon M, Cathonnet M. High pressure oxidation of liquid fuels from low to high temperature. 1. *n*-heptane and *iso*-octane. Combust Sci Tech 1994a;95:233-260.
- [10] Dagaut P, Reuillon M, Cathonnet M. High pressure oxidation of liquid fuels from low to high temperature. 2. Mixtures of *n*-heptane and *iso*-octane. Combust Sci Tech 1994b;103:315-336.

- 1 [11] Dagaut P, Reuillon M, Boettner J-C, Cathonnet M. Kerosene combustion at
2 pressures up to 40 atm: Experimental study and detailed chemical kinetic modeling. Proc.
3 25th Int Symp Combust 1994c. p. 919-926.
- 4 [12] Ranzi E, Faravelli T, Gaffuri P, Sogaro A. Low-temperature combustion: Automatic
5 generation of primary oxidation reactions and Lumping procedures. Combust Flame
6 1995a;102:179-192.
- 7 [13] Ranzi E, Faravelli T, Gaffuri P, Sogaro A, D'Anna A, Ciajolo A. A wide-range
8 modeling study of *iso*-octane oxidation. Combust Flame 1997;108:24-42.
- 9 [14] Ranzi E, Dente M, Goldaniga A, Bozzano G, Faravelli T. Lumped procedures in
10 detailed kinetic modeling of gasification, pyrolysis, partial oxidation and combustion of
11 hydrocarbon mixtures. Prog Energy Combust Sci 2001;27:99-139.
- 12 [15] Blaine S, Savage PE. Reaction pathways in lubricant degradation. 3. Reaction model
13 for *n*-hexadecane autoxidation. Indust Eng Chem Res 1992;31:69-75.
- 14 [16] Astarita M., Corcione FE, Vaglieco BM. Fuel composition effects on particulate
15 formation in divided chamber diesel system. Experim Therm Fluid Sci 2000;21, 142-149.
- 16 [17] Edwards T. "Real" kerosene aviation and rocket fuels: Composition and surrogates.
17 In: Chemical and Physical processes in Combustion. Conference Eastern States, Section
18 of the Combustion Institute, Hilton Head, SC, 2001. p. 276-279.
- 19 [18] Glassman I. Combustion. New York: Academic press, 1977.
- 20 [19] Sirignano WA. Fuel droplet vaporization and spray combustion theory. Prog Energy
21 Comb Sci 1983;9:291-322.

- 1 [20] Warnatz J, Maas U, Dibble RE. Combustion: Physical and chemical fundamentals,
2 modeling and simulation, experiments, pollutant formation. Berlin: Springer-Verlag,
3 1999.
- 4 [21] Bertoli C, Migliaccio M. A finite conductivity model for diesel spray evaporation
5 computations. *Int J Heat Fluid Flow* 1999;20:552-561.
- 6 [22] Morin C, Chuaveau C, Gokalp I. Droplet vaporization characteristics of vegetable
7 oil derived biofuels at high temperatures. *Experim Therm Fluid Sci* 2000;21:41-50.
- 8 [23] Lozinski D., Matalon M. Vaporization of a spinning fuel droplet. *Proc. 24th Int Symp*
9 *Combust*, 1992. p. 1483-1491.
- 10 [24] Tamim J, Hallett WLH. A continuous thermodynamics model for multicomponent
11 droplet vaporization. *Chem Eng Sci* 1995;50:2933-2942.
- 12 [25] Yule AJ, Shrimpton JS, Watkins AP, Balachandran W, Hu D. Electrostatically
13 atomized hydrocarbon sprays. *Fuel* 1995;74:1094-1103.
- 14 [26] Dombrovsky LA, Sazhin SS, Sazhina EM, Feng G, Heikal MR, Bardsley MEA,
15 Mikhalevsky SV. Heating and evaporation of semi-transparent diesel fuel droplets in the
16 presence of thermal radiation. *Fuel* 2001;80:1535-1544.
- 17 [27] Gradinger TB, Inauen A, Bombach R, Kappeli B, Hubshmid W, Boulouchos K.
18 Liquid-fuel/air premixing in gas turbine combustors: Experimental and numerical
19 simulation. *Combust Flame* 2001;124:422-443.
- 20 [28] Krishna CR, Celebi Y, Butcher TB, Long J, Waldee T, McDonald RJ. Research in
21 future oil burner concepts. *Proc. 4th National Oil Heat Research Alliance Technology*
22 *Conference*, Upton, NY, 1989. p. 37-66.

- 1 [29] Butcher T, Celebi Y, Wei G, Kamath B. Small oil burner concepts based on low-
2 pressure air atomization. Brookhaven National Laboratory Report No. 67227, Upton,
3 NY, 2000.
- 4 [30] Krishna CR, Curtis M. Variable firing rate oil burner using pulse flow control. Proc
5 14th National Oil Heat Research Alliance Technology Conference. Upton, NY, 2001. p.
6 95-100.
- 7 [31] Butcher T, Celebi Y, Wei G. (2001) High flow fan atomization burner (HFAB)
8 development and field trials. Proc. 14th National Oil Heat Research Alliance Technology
9 Conf., Upton, NY, 2001. p. 9-16.
- 10 [32] Kamath BR. Progression and improvements in the design of blue flame oil burners.
11 Proc. 14th National Oil Heat Research Alliance Technology Conf., Upton, NY, 2001. p.
12 133-138.
- 13 [33] Emonts B. Catalytic radiant burner for stationary and mobile applications. Catalysis
14 Today 1999;47:407-414.
- 15 [34] Seo Y-S, Kang S-K, Han M-H, Baek Y-S. Development of a catalytic burner with
16 Pd/NiO catalysts. Catalysis Today 1999;47:421-427.
- 17 [35] Terasaki T, Hayashi S. The effect of fuel-air mixing on NO_x Formation in non-
18 premixed swirl burners. Proc. 26th Int Symp Combust, 2000. p. 2733-2739.
- 19 [36] Fleck BA, Sobiesiak A, Becker HA. Experimental and numerical investigation on
20 the novel low NO_x CGRI. Combust Sci Tech, 2000;161:89-112.
- 21 [37] Steibach N, Dotsch C, Lucka K, Köhne H. Using ignition delay to separate the
22 vaporization from the flame zone in oil fired burner for stirling engines. 2nd European
23 Conference on Small Burner Technology. Vol. 1, Stuttgart, 2000. p. 71-80.

- 1 [38] Gueret C, Cathonnet M, Boettner J-C, Gaillard F. Experimental study and modeling
2 of kerosene oxidation in a jet-stirred flow reactor. Proc. 23rd Int Symp Combust, 1990, p.
3 211-216.
- 4 [39] Pearlman H, Chapek RM. Cool flames and autoignition: Thermal-ignition theory of
5 combustion experimentally validated in microgravity. 1999. [http://www.](http://www.grc.nasa.gov/www/RT1999/6000/6711wu.html)
6 [grc.nasa.gov/www/RT1999/6000/6711wu.html](http://www.grc.nasa.gov/www/RT1999/6000/6711wu.html).
- 7 [40] Affens WA, Sheinson RS. Autoignition: Importance of the cool flame in the two-
8 stage process. Loss Prevention 1980;13:83-88.
- 9 [41] Caprio V, Insola A, Lignola PG. Isobutane cool flames in a CSTR: The behavior
10 dependence on temperature and residence time. Combust Flame 1981;43:23-33.
- 11 [42] Pollard RT. Hydrocarbons. In: Bamford CH, Tipper CFH, editors. Comprehensive
12 chemical kinetics, Gas phase combustion, Vol 17, New York: Elsevier, 1977. p. 249-367.
- 13 [43] Shtern VY. The gas phase oxidation of hydrocarbons, London: Pergamon, 1964.
- 14 [44] Barat P, Cullis CF, Pollard RT. The cool-flame oxidation of 3-methylpentane. Proc
15 Roy Soc London 1972;A329:433-452.
- 16 [45] Luck CJ, Burgess AR, Desty DH, Whitehead DM, Prateley GA. study of the
17 combustion of *n*-heptane in an engine using a novel high-speed sampling technique.
18 Proc 14th Int Symp Combust 1973. p. 501-512.
- 19 [46] Gray BF, Felton PG. Low-temperature oxidation in a stirred-flow reactor-I. Propane.
20 Combust Flame 1974;23:295-304.
- 21 [47] Krishna CR, Berlad AL. Stability of combustible systems. Combust Flame
22 1976;26:133-135.

- 1 [48] Caprio V, Insola A. and Lignola PG. Isobutane cool flames investigation in
2 continuous stirred tank reactor. Proc 16th Int Symp Combust 1977. p. 1155-1163.
- 3 [49] Burgess AR, Laughlin RGW. The role of hydroperoxides as chain branching agents
4 in the cool-flame oxidation of *n*-heptane. Chem Comm Roy Soc London 1967;769-770.
- 5 [50] Barat P, Cullis CF, Pollard RT. Studies of the combustion of branched-chain
6 hydrocarbons. Proc 13th Int Symp Combust 1971. p. 171-192.
- 7 [51] Atherton JG, Brown AJ, Lucketti GA, Pollard RT. Heterogeneity and mechanism in
8 hydrocarbon oxidation. Proc 14th Int Symp Combust 1973. p. 513-522.
- 9 [52] Gaffuri P, Faravelli T, Ranzi E, Cernansky NP, Miller D, D'Anna A, Ciajolo A.
10 Comprehensive kinetic model for the low-temperature oxidation of hydrocarbons. Am
11 Inst Chem Eng J 1997;43:1278-1286.
- 12 [53] Gitzinger H-P. Nutzung kalter flammen für die gemischbildung zur realisierung
13 eines strahlungsbrenners für flussige brennstoffe [Use of cool flames for the air/fuel
14 mixture for the realization of a burner for liquid fuels]. Ph.D. Thesis, RWTH, Aachen,
15 Germany, 1999.
- 16 [54] Pearlman H. Low-temperature oxidation reactions and cool flames at earth and
17 reduced gravity. Combust Flame 2000;121:390-393.
- 18 [55] Chen JS, Lintzinger TA, Curran HJ. The lean oxidation of iso-octane in the low
19 temperature regime. In: Chemical and Physical processes in Combustion. Meeting
20 Eastern States Section of the Combustion Institute, Hilton Head, SC, 2001. p. 268-271.
- 21 [56] Mantashyan AA. Cool flames and oscillations in hydrocarbon oxidation. Proc 25th
22 Int Symp Combust 1994. p. 927-932.

- 1 [57] Chevalier C, Pitz WJ, Warnatz J, Westbrook CK., Melenk H. Hydrocarbon ignition:
2 Automatic generation of reaction mechanisms and applications to modeling of engine
3 knock. Proc 24th Int Symp Combust 1992, p. 93-101.
- 4 [58] Dagaut P, Reuillon M, Cathonnet M. Experiment study of the oxidation of *n*-heptane
5 in a jet stirred reactor from low to high temperature and pressures up to 40 Atm. Combust
6 Flame 1995;101:132-140.
- 7 [59] Ciajolo A, D'Anna A. Controlling steps in the low-temperature oxidation of *n*-
8 heptane and *iso*-octane. Combust Flame 1998;112:617-622.
- 9 [60] Battin-Leclerc F, Glaude PA, Warth V, Fournet R, Scacchi G, Côme GM. Computer
10 tools for modeling the chemical phenomena related to combustion. Chem Eng Sci
11 2000;55:2883-2893.
- 12 [61] Warth V, Stef N, Glaude PA, Battin-Leclerc F, Scacchi G, Côme GM. Computer
13 based generation of reaction mechanisms for gas-phase oxidation. Computers Chem.
14 1998;114:81-102.
- 15 [62] Luka K, Hartmann L, Rudolphi I, Köhne H. Homogene gemischbildung von
16 flüssigen brennstoffen durch nutzung kalter flammen. VDI Berichte 1999;1492: 249-254.
- 17 [63] Sahetchian K, Champoussin JC, Brun N, Levy N, Blin-Simiand N, Aligrot C, Jorand
18 F, Socoliuc M, Heiss A, Guerassi N. Experimental study on modeling of dodecane
19 ignition in a diesel engine. Combust Flame 1995;103:207-220.
- 20 [64] Cooke D. F., Williams A. Shock tube studies of methane and ethane oxidation.
21 Combust. Flame 1975;24:245-256.
- 22 [65] Spadaccini LJ, TeVelde JA. autoignition characteristics of aircraft-type fuels.
23 Combust Flame 1982;46:283-300.

- 1 [66] Cavaliere A, Ciajolo A, D'Anna A, Mercogliano R, Ragucci R. Autoignition of *n*-
2 heptane and *n*-tetradecane in engine-like conditions. Combust Flame 1993;93:279-286.
- 3 [67] Schreiber M, Sakak AS, Lingens A, Griffiths JF. A reduced thermokinetic model for
4 the autoignition of fuels with variable octane ratings, 25th Int Symp Combust 1994. p.
5 933-940.
- 6 [68] Ranzi E, Gaffuri P, Faravelli T, Dagaut P. A wide range modeling study of *n*-
7 heptane oxidation. Combust Flame 1995b;103: 91-106.
- 8 [69] Pfahl U, Fieweger K, Adomeit G. Self-ignition of diesel-relevant hydrocarbon-air
9 mixtures under engine conditions. Proc 26th Int Symp Combust 1996. p. 781-789.
- 10 [70] Dagaut P, Cathonnet M, Rouan JP, Foulatier R, Quilgars, Boettner JC, Gaillard F,
11 James H. A jet-stirrer reactor for kinetic studies of homogeneous gas-phase reactions at
12 pressures up to ten atmospheres (~ 1 MPa). J Phys Sci Instrum 1986;19:207-209.
- 13 [71] Westbrook CK, Dryer FL. Chemical kinetic modeling of hydrocarbon combustion.
14 Prog Energy Combust Sci 1984;10:1-57.
- 15 [72] Axelsson EI, Brezinski K, Dryer FL, Pitz WJ, Westbrook CK. Chemical kinetic
16 modeling of the oxidation of large alkane fuels: *n*-octane and *iso*-octane. Proc 21st Int
17 Symp Combust 1986. p. 783-793.
- 18 [73] Westbrook CK, Dryer FL. Chemical kinetics and modeling of combustion processes.
19 Proc 18th Int Symp Combust 1981. p. 749-766.
- 20 [74] Baulch DL, Cobos CJ, Cox RA, Frank P, Hayman G, Just T, Kerr JA, Murrells T,
21 Pilling M, Troe J, Walker RW, Warnatz J. Summary table of evaluated kinetic data for
22 combustion modeling: Supplement 1. Combust Flame 1994;98:59-79.

- 1 [75] Westbrook CK, Warnaz J, Pitz WJ. A detailed chemical kinetic reaction mechanism
2 for the oxidation of *iso*-octane and *n*-heptane over an extended temperature range and its
3 application to analysis of engine knock. Proc 22nd Int Symp Combust 1988. p. 893-901.
- 4 [76] Chakir A, Bellimam M, Boettner JC, Cathonnet M. Kinetic study of *n*-heptane
5 oxidation. Int J Chem Kin 1992;24:385-410.
- 6 [77] Benson SW. The kinetics and thermochemistry of chemical oxidation with
7 application to combustion and flames. Prog Energy Combust Sci 1981;7:125-134.
- 8 [78] Côme GM, Warth V, Glaude PA, Fournet F, Battin-Leclerc F, Scacchi G. Computer-
9 aided design of gas-phase oxidation mechanism-application to the modeling of *n*-heptane
10 and *iso*-octane oxidation. Proc 26th Int Symp Combust, 1996. p. 755-762.
- 11 [79] Callahan CV, Held TJ, Dryer FL, Minetti R, Ribaucour M, Sauchet LR, Faravelli T,
12 Gaffuri P, Ranzi E. Experimental data and kinetic modeling of primary reference fuel
13 mixtures. Proc 25th Int Symp Combust 1996. p. 730-746.
- 14 [80] Curran HJ, Gaffuri P, Pitz WJ, Westbrook CK. A comprehensive modeling study of
15 *n*-heptane oxidation. Combust Flame 1998;114:149-177.
- 16 [81] Glaude PA, Battin-Leclerc F, Fournet R, Warth V, Côme GM, Scacchi G.
17 Construction and simplification of a model for the oxidation of alkanes. Combust Flame
18 2000;122:451-462.
- 19 [82] Azuelta MU, Glarborg P, Dam-Johansen K. Experimental and kinetic modeling
20 study of the oxidation of benzene. Int J Chem Kinet 2000;32:498- 522.
- 21 [83] Dagaut P, Ristori A, El Bakali A, Cathonnet M. Experimental and kinetic modeling
22 study of the oxidation of *n*-propylbenzene. Fuel 2002;81:173-184.

- 1 [84] Fournet R, Battin-Lecler F, Glaude PA, Judenherc B, Warth V, Côme GM, Scacchi
2 G, Ristori A, Pengloan G, Dagaut P, Cathonnet M. Gas Phase oxidation of *n*-hexadecane.
3 Int J Chem Kinet 2001;33:574-586.
- 4 [85] Ristori A, Dagaut P, Cathonnet M. The oxidation of *n*-hexane: Experimental and
5 detailed kinetic modeling. Combust Flame 2001;125: 1128-1137.
- 6 [86] Weast RC. Handbook of Chemistry and Physics, Boca Raton, Florida: CRC press,
7 1985. p. C295.
- 8 [87] Heneghan SP, Schulz WD. Static tests of Jet fuel thermal and oxidative stability. J
9 Propulsion Power 1993;9:5-9.
- 10 [88] Cookson DJ, Iliopoulos P, Smith E. Composition-property relations for jet and diesel
11 fuels of variable boiling range. Fuel 1995;74:70-78.
- 12 [89] Ervin JS, Zabarnick S. Numerical simulations of jet fuel oxidation and fluid
13 dynamics. 6th International Conference on Stability and Handling of Liquid Fuels. 1997.
14 p. 385-402.
- 15 [90] Breiter MW. Electrochemical processes in fuel cells. New York: Springer-Verlag,
16 1969.
- 17 [91] Blomen LJM, Mugerwa MN. Fuel Cell Systems. New York: Plenum press, 1993.
- 18 [92] Srinivasan S, Dave BB, Murugesamoorthi KA, Parthasarathy A, Appleby AJ.
19 Overview of fuel cell technology. In: Blomen LJM, Mugerwa MN, editors. Fuel Cell
20 systems. New York: Plenum press, 1993. p. 37-72.
- 21 [93] Pietrogrande P, Bezzeccheri M. Fuel processing. In: Blomen LJM., Mugerwa MN,
22 editors. Fuel Cell systems. New York: Plenum press, 1993. p. 121-156.
- 23 [94] Kordesch K, Simader G. Fuel Cells and Their Applications. New York: VCH, 1996.

- 1 [95] Myaki Y, Nakanishi N, Nakajima T, Itoh Y, Saitoh T, Saiai A, Yanaru H. A study of
2 heat and material balances in an internal-reforming molten carbonate fuel cell. *J Power*
3 *Sources* 1995;56:11-17.
- 4 [96] Basio B, Costamagna C, Parodi F. Modeling and experimentation of molten
5 carbonate fuel cell reactors in a scale-up process. *Chem Eng Sci* 1999;54:2907-2916.
- 6 [97] Fang B, Chen H. A new candidate material for molten carbonate fuel cell cathodes. *J*
7 *Eleetroanalyt Chem* 2001;501:28-131.
- 8 [98] Freni S. Rh based catalysts for indirect internal reforming ethanol applications in
9 molten carbonate fuel systems. *J Power Source* 2001;94:14-19.
- 10 [99] Finnerty CM, Tompsett GA, Kendall K, Ormerold RM. SOFC system with
11 integrated catalytic fuel processing. *J Power Sources*, 2000;86:459-463.
- 12 [100] Huijsmans JPP. Ceramics in solid oxide fuel cells. *Curr Opinion Solid State*
13 *Marerials Sci* 2001;5:317323.
- 14 [101] Ivers-Tiffée E, Weber A, Herbstritt D. Materials and technologies for SOFC-
15 components. *J Eur Ceramic Soc* 2001;21:1805-1811.
- 16 [102] Zhu B. Advantages of intermediates temperature solid oxide fuel cells for
17 tractionary applications. *J Power Sources* 2001;93:82-86.
- 18 [103] Sridhar P, Perumal R, Rajalakshmi N, Raja M, Dhathathreyan KS. Humidification
19 studies on polymer electrolyte membrane fuel cell. *J Power Sources* 2001;101:72-78.
- 20 [104] Guo Q, Pintauro PN, Tang H, O'Connor S. Sulfonated and crosslinked
21 polyphosphazene-based proton-exchange membranes. *J Membrane Sci* 1999;154:175-
22 181.

- 1 [105] Pettersson LJ, Westerholm R. State of the art multi-fuel reformers for fuel cell
2 vehicles: problem identification and research needs. *Int J Hydrogen Energy* 2001;26:243-
3 264.
- 4 [106] Brown LF. A survey of processes for producing hydrogen fuel from different
5 sources for automotive-propulsion fuel cells. DOE Report # LA-13112-MS. 1996.
- 6 [107] Bromberg L, Cohn DR, Rabinovich A, O'Brien C, Hochgreb S. Plasma reforming
7 of methane. *Energy Fuels* 1998;12:11-18.
- 8 [108] Marquevich M, Czernik S, Chornet E, Montané D. Hydrogen from biomass: Steam
9 reforming of model compounds of fast-pyrolysis oil. *Energy Fuels* 1999;13: 1160-1168.
- 10 [109] Bebelis S, Zeritis A, Tiropani C, Neophytides SG. Intrinsic kinetics of the internal
11 steam reforming of CH₄ over a Ni-YSZ-Cermet catalyst-electrode. *Ind Eng Chem Res*
12 2000;39:4920-4927.
- 13 [110] Antonucci V, antonucci PL, Aricò AS, Giordano N. Partial oxidation of methane in
14 solid oxide fuel cells: An experimental evaluation. *J Power Sources* 1996;62:95-99.
- 15 [111] Cavallaro S, Freni S. Syngas and electricity production by an integrated
16 autothermal reforming/molten carbonate fuel cell system. *J Power sources* 1998;76:190-
17 196.
- 18 [112] Recupero V, Pino L, Di Leonardo R, Lagana M, Maggio G. Hydrogen generator,
19 via catalytic partial oxidation of methane for fuel cells. *J Power sources* 1998;71: 208-
20 214.
- 21 [113] Freni S, Cavallaro S. Catalytic partial oxidation of methane in a molten carbonate
22 fuel cell. *Int J Hydrogen Energy* 1999;24:75-82.

- [114] Hu YH, Ruckenstein E. Isotopic GCMS of mechanism of methane partial oxidation to synthesis gas. *J Phys Chem A* 1998;102:10568-10571.
- [115] Marschall KJ, Mleczko L. Short-contact-time reactor for catalytic partial oxidation of methane. *Ind Eng Chem Res* 1999;38:1813-1821.
- [116] Ishihara T, Yamada T, Akbay T, Takita Y. Partial oxidation of methane over fuel cell type reactor for simultaneous generation of synthesis gas and electric power. *Chem Eng Sci* 1999;54:1535-1540.
- [117] Amphlett JC, Mann RF, Peppley BA, Roberge PR, Rodrigues A. A practical PEM Cell model for simulating vehicle power sources. 10th Proceeding Battery Conference on Applied and Advanced Technology 1995. p. 221-226.
- [118] Otsuka K, Mito A, Takenaka S, Yamanaka I. Production of hydrogen from methane without CO₂-emission mediated by indium oxide and iron oxide. *Int J Hydrogen Energy* 2001;26:191-194.
- [119] Amendola SC, Sharp-Goldman SL, Janjua MS, Spencer NC, Kelly MT, Petillo PJ, Binder M. A safe, portable, hydrogen gas generator using aqueous borohydride solution and Ru catalyst. *Int J Hydrogen Energy* 2000;25:969-975.
- [120] Dicks AL. Hydrogen generation from natural gas for the fuel cell systems of tomorrow. *J Power Sources* 1996;61:113-124.
- [121] Chan SH, Wang HM. Thermodynamic analysis of natural-gas fuel processing for fuel cell applications. *Int J Hydrogen Energy* 2000;25:441-449.
- [122] Abdel-Aal HK, Shalabi MA. Noncatalytic partial oxidation of sour natural gas versus catalytic steam reforming of sweet natural gas. *Ind Eng Chem Res* 1996; 35:1785-1787.

- 1 [123] Abdel-Aal HK, Shalabi MA, Al-Harbi DK, Hakeem T. Simulation of the direct
2 production of synthesis gas from sour natural gas by noncatalytic partial oxidation
3 (NCPO): Thermodynamics and stoichiometry. *Ind Eng Chem Res* 1999;38:1069-1074.
- 4 [124] Nauman ST, Myrèn C. Fuel processing of biogas for small fuel cell power plants. *J*
5 *Power sources* 1995;56:45-49.
- 6 [125] Borgwardt RH. Biomass and natural gas as co-feedstocks for production of fuel for
7 fuel-cell vehicles. *Biomass Bioeng* 1997;12:333-345.
- 8 [126] Wang D, Czernik S, Chornet E. Production of hydrogen from biomass by catalytic
9 steam reforming of fast pyrolysis oils. *Energy Fuels* 1998;12:19-24.
- 10 [127] Wang D, Czernik S, Montané D, Mann M, Chornet E. Biomass to hydrogen via fast
11 pyrolysis and catalytic steam reforming of the pyrolysis oil or its fractions. *Ind Eng Chem*
12 *Res* 1997;36:1507-1518.
- 13 [128] Thomas CE, Kuhn IFJr, James BD, Lomax FD, Baum GN. Affordable hydrogen
14 supply pathways for fuel cell vehicles. *Int J Hydrogen Energy* 1998;23:507-516.
- 15 [129] Kumar R, Ahmed S, Krumpelt M. The low-temperature partial-oxidation reforming
16 of fuels for transportation fuel cell systems. DOE Report # ANL/CMT/CP-896669. 1996.
- 17 [130] Peppley BA, Amphlett JC, Kearns LM, Mann RF, Roberge PR. Hydrogen
18 generation to fuel-cell power systems by high-pressure catalytic methanol-steam
19 reforming. *Proc 32nd Int Energy Conversion Engineering Conference*, 1997. p. 831-836.
- 20 [131] Ahmed S, Kumar R, Krumpelt M. Methanol partial oxidation reformer. US Patent
21 No. 5,939,025. 1999a.

- [132] Ramaswamy S, Sundaresan M, Eggert A, Moore RM. System dynamics and efficiency of the fuel processor for an indirect methanol fuel cell vehicle. Proc 35th Int Energy Conversion Engineering Conference, 2000. p. 1372-1377.
- [133] Sundaresan M, Ramaswamy S, Moore R. Steam reformer/Burner integration and analysis for an indirect methanol fuel cell vehicle. Proc 35th Int Energy Conversion Engineering Conference, 2000. p. 1367-1371.
- [134] Avci AK, Onsan ZI, Trimm DL. On-board fuel conversion for hydrogen fuel cells: comparison of different fuels by computer simulations. Appl Catal A 2000;216:243-256.
- [135] Scott K. Direct methanol fuel cells for transformation. Proc 35th Int Energy Conversion Engineering Conference, 2000. p.1-3.
- [136] Mahajan D, Krisdhasima V, Sproull RD. Kinetic modeling of homogeneous methanol synthesis catalyzed by base-promoted nickel complexes. Can J Chem 2001;79:845-853.
- [137] Mahajan D. A Method for Low Temperature Catalytic Production of Hydrogen. US Patent application, 2001.
- [138] Mahajan D, Wegrzyn JE. Atom-Economical Pathways to Methanol Fuel Cell from Biomass. Symposium on "Chemistry of Renewable Fuels and Chemicals", Divisions of Fuel Chemistry and Cellulose, Paper, and Textile, Spring ACS National Meeting, Anaheim, CA. March 21-25, 1999.
- [139] Ahmed S, Kumar R, Krumpelt M. Fuel processing for fuel cell power systems. Fuel Cell Bull 1999b;12:4-7.
- [140] Docter A, Lamm A. Gasoline fuel cell system. J Power Sources 1999;84:194-200.
- [141] Borup R, Inbody M, Morton B, Brown L. Fuel Processing for fuel cells: Effects on catalysts durability and carbon formation. Los Alamos National Laboratory Report No. LA-UR-01-2289, Los Alamos, New Mexico. 2001.

- 1 [142] Kopasz J P, Wilkenhoener R, Ahmed S, Carter J D, Krumpelt M. Fuel-flexible
2 partial oxidation reforming of hydrocarbons for automotive applications. Department of
3 Energy Report No. ANL/CMT/CP-98970. 1999.
- 4 [143] Ahmed S, Krumpelt M, Kumar R, Lee SHD, Carter JD, Wilkenhoener R., Marshall
5 C. Catalytic partial oxidation reforming of hydrogen fuels. Fuel Cell Seminar, Palm
6 Springs, CA. Argonne National Laboratory Report No. ANL/CMT/CP-96059. 1998.
- 7 [144] Pereira C, Baes J-M, Ahmed S, Krumplet M. Liquid fuel reformer
8 development: Autothermal reforming of diesel fuel. Department of Energy Report No.
9 ANL/CMT/CP-102382. 1999.
- 10 [145] Pereira C, Wilkenhoener R, Ahmed S, Krumplet M. Liquid fuel reformer
11 development. Department of Energy Report No. ANL/CMT/CP-99684. 2000a.
- 12 [146] Pereira C, Wilkenhoener R, Ahmed S, Krumplet M. Catalytic reforming of gasoline
13 and diesel fuel. Department of Energy Report No. ANL/CMT/CP-100320. 2000b.
- 14 [147] Anumakonda A, Yamanis J, Ferrall J. Catalytic partial oxidation of hydrocarbon
15 fuels to hydrogen and carbon monoxide. US Patent No. 6,221, 280. 2001.
- 16 [148] Yanhhui W, Diyong W. The experimental research for production of hydrogen
17 from *n*-otane through partially oxidizing and steam reforming method. Int J Hydrogen
18 Energy 2001;26:795-800.
- 19 [149] Amphlett JC, Mann RF, Peppley BA, Roberge PR. Simulation of a 250 kW diesel
20 fuel processor/PEM fuel cell system. J Power Source 1998;71:179-184.
- 21 [150] Hartmann L, Lucka K, Mengel C, Kôhne H. Design and test of a partial oxidation
22 (POX) Process for fuel cell applications using liquid fuels. 1st European Conference on
23 Small Burner Technology, p. 411-417. 1998.

- 1 [151] Moon DJ, Sreekumar K, Lee SD, Lee BG, Kim S. Studies on gasoline fuel
2 processor system for fuel-cell powdered vehicules application. Appl Catal A
3 2001;215:1-9.
- 4 [152] Ogden JM, Steinbugler MM, Kreutz G. A comparison of hydrogen, methanol and
5 gasoline as fuels for fuel cell vehicles: Implications for vehicle design and infrastructure
6 development. J Power Sources 1999;79:143-168.
- 7 [153] Moshida I, Sakanish K, Ma X, Nagano S, Isoda T. Deep hydrodesulfurization of
8 diesel fuel: Design of reaction process and catalysts. Catalysis Today 1996;29:185-189.
- 9 [154] Shafi R, Hutchings J. Hydrodesulfurization of hindered dibenzothiophenes: An
10 overview. Catalysis Today 2000;59:423-442.
- 11 [155] Trimm DL. Catalysis for the control of coking during steam reforming. Catalysis
12 Today 1999;49:3-10.
- 13 [156] Wang X, Gorte RJ. A study of reforming of hydrocarbon fuels on Pd/ceria. Appl
14 Catal A 2002;224:209-218.
- 15 [157] Suzuki T, Iwanami H-I, Yoshinari T. Steam reforming of kerosene on Ru/Al₂O₃
16 catalyst yield hydrogen. Int J Hydrogen Energy 2000;25:119-126.
- 17 [158] Zhou C Q, Neal LG, Bolli R, Haslbeck J, Chang A. Control of NO_x emissions by
18 NO_x recycle approach. Proc 26th Int symp Combust 1996. p. 2091-2097.
- 19 [159] Haase F, Köhne H. Design of scrubbers for condensing boilers. Prog Energ
20 Combust Sci 1999;25:305-337.
- 21 [160] Nizami AA, Cernansky NP. NO_x formation in monodisperse fuel spray
22 combustion. Proc 17th Int Sym Combust 1979. p. 475-483.

- 1 [161] Fenimore CP. Formation of nitric oxide in premixed hydrocarbon flames. Proc 13th
2 Int Symp Combust 1971. p. 373-380.
- 3 [162] Delabroy O, Haile E, Lacas F, Candel S, Pollard A, Sobiesiak A. Passive and active
4 controle of NO_x in industrial burners. Experim Therm Fluid Sci 1998;16:64-75.
- 5 [163] Neeft JPA, Makkee M, Moulijn JA. Diesel particulate emission control. Fuel
6 Processing Technol 1996;47:1-69.
- 7 [164] Krishnan AT, Boehman AL. Selective catalytic reduction of nitric oxide with
8 ammonia at low temperatures. Appl Catal B 1998;18:189-198.
- 9 [165] Van Kooten WEJ. Ce-ZSM-5 catalysis for the selective catalytic reduction of NO_x
10 in stationary diesel exhaust gas. Appl Catal B 1999;21:203-213.
- 11 [166] Muzio LG, Quartucy GC. Implementing NO_x control: Research to application. Prog
12 Energy Combust Sci 1997;23:233-266.
- 13 [167] Vaillant SR, Gastec AS. Catalytic combustion in a domestic natural gas burner.
14 Catalysis Today 1999;47:415-420.
- 15 [168] Seo Y-S, Kang S-K, Han M-H, Baek Y-S. Development of a catalytic burner with
16 Pd/NiO catalysts. Catalysis Today 1999;47:421-427.
- 17 [169] Ohkubo Y, Idota Y, Nomura Y. Evaporation characteristics of fuel spray and low
18 emissions in a lean premixed-prevaporization combustor for a 100 kW automotive
19 ceramic gas turbine. Energy Convers Mgmt 1997;38:1297-1309.
- 20 [170] Graboski M S, McCormick RL. Combustion of fat and vegetable oil derived fuels
21 in diesel engines. Prog Energy Combust Sci 1998;24:125-164.
- 22 [171] Frenklach M, Wang H. Detailed modeling on soot particle nucleation and growth.
23 Proc 23rd Int symp Combust. 1990. p. 1559-1566.

- 1 [172] Hall-Roberts VJ, Hayhursts AN, Knight DE, Taylor SG. The origin of soot in
2 flames: Is the nucleus an ion? *Combust Flame* 2000;120:578-584.
- 3 [173] Sato H, Tree DR, Hodges JT, Foster D. A study on the effect of temperature on
4 soot formation in a jet stirred combustor. *Proc 23rd Int Symp Combust* 1990. p. 1469-
5 1475.
- 6 [174] Frenklach M. On surface growth mechanism of soot particles. *Proc 26th Int Symp*
7 *Combust* 1996. p. 2285-93.
- 8 [175] Belardini P, Bertoli C, D'Anna A, Del Giacomo N. Application of reduced kinetic
9 model for soot formation and burnout in three-dimensional diesel combustion
10 computations. *Proc 26th Int Symp Combust* 1996. p. 2517-2524.
- 11 [176] Kennedy IM. Models of soot formation and oxidation. *Prog Energy Combust Sci*
12 1997;23:95-132.
- 13 [177] Ambrogio M, Saracco G, Specchia V. Combining filtration and catalytic
14 combustion in particulate traps for diesel exhaust treatment. *Chem Eng Sci*
15 2001;56:1613-1621.
- 16 [178] Balthasar M, Maus F, Pfitzner M, Mack A. Implementation and validation of a new
17 soot model and application to aeroengine combustors. *J Eng Gas Turbines Power*
18 2002;124:66-74.
- 19 [179] Stanmore BR., Brilhac JF, Gilot P. The oxidation of soot: A review of experiments,
20 mechanisms and models. *Carbon* 2001;39:2247-2268.
- 21 [180] Philips 66 Company, A subsidiary of Philips Petroleum Company. Specialty
22 Chemicals. P.O. Box 968, Borger, TX 79008, USA.

Legend to Figures

Fig. 1. Proposed major steps involved in fuel preparation for combustion and fuel cell systems

Fig. 2. Illustration of a high flow air-atomizer (HFAB) burner head [29]

Fig. 3. Reaction scheme of *n*-heptane oxidation mechanism, showing the main possible reaction products [45]

Fig. 4. Effect of temperature on the reaction selectivity during the oxidation of *n*-heptane [14]

Fig. 5. Conversion of *n*-heptane as a function of temperature. Oxidation of 0.1 % of fuel at 1 MPa and a residence time of 1s, experimental: Plain line and predicted: Dashed [68]

Fig. 6. Relationship between initial and final gas temperatures during atomization of fuel in a hot air flow ($\lambda = 1$, $p = 1$ bar) [7]

Fig. 7. Cool flame temperature rise as a function of the fuel type [7]

Fig. 8. Conversion of hydrocarbons as a function of temperature and residence time, estimated from equation 27. The kinetic parameters are given in Table 1

Fig. 9. Distillation curve of D-2 Diesel control fuel, Lot K-848 [177] and a pure single component fuel (*n*-heptane)

Fig. 10. Schematic representation of the oxidation and reforming paths of different classes of conventional and alternative fuels for fuel cell systems, adapted from Thomas et al. [5]

Table 1. Major intermediate products of 3-ethylpentane (C_7H_{16}) formed during cool flame oxidation (523-683 K) at $p = 22$ kPa. 3-ethylpentane consumed = 2.5×10^{-4} moles [50]

Product	Yield* %	Conversion† %
Ethylene (major), ethane	17.5	28.0
Methanol (major), <i>n</i> -butanal + 2methyl-2-propene-1-al	10.3	16.6
Pent-2-ene (cis and trans)	7.4	12.0
Acetaldehyde	7.0	11.2
2-Methyl-3-ethyltetrahydrofuran	4.8	7.7
Pentane-3-one	3.2	5.1
Propanal	2.63	4.2
3-Ethylpent-2-ene (<i>cis</i> and <i>trans</i>)	2.13	3.4
2,4-dimethyl-3-ethyl oxetan (anti)	1.78	2.88
2,4-dimethyl-3-ethyl oxetan (sym) + 2,2-diethyl-3-methyl oxiran (cis) major	1.58	2.52
Oxiran	1.56	2.50
2-Ethylut-1-ene	1.13	1.80
But-2-en-1-al	1.13	1.80
Pent-1-en-3-one	1.00	1.60
2,2-methyl propene	1.00	1.60
2,2-Diethyloxetan	0.90	1.44
3-Ethylpent-1-ene	0.75	1.20
Butan-2-one	0.75	1.20
Propenal	0.63	1.00
Butane,2-methylpropene, pent-1-ene,1,3-butadiene (major)	0.60	0.96
But-1-en-3-one	0.53	0.85
3-Ethylpentane-2-one	0.50	0.80
3-Methylpent-2-ene (<i>cis</i>)	0.50	0.80
Ethanol	0.38	0.60
4-Methylhexan-3-one	0.33	0.52
2-Ethyl-3-methyloxiran	0.30	0.48
Propylene	0.25	0.40
Hexan-3-one	0.25	0.40
Pentane-2-one	0.24	0.40
But-2-ene (<i>cis</i> and <i>trans</i>)	0.22	0.35
Propane-2-one (major) + 2-methylpropanal	0.17	0.23
Heptan-3-one	0.16	0.26
Heptanol	0.06	0.10

* % Yield = moles product formed/moles of fuel introduced

† % Conversion = moles product formed/moles Fuel consumed

Table 2. Major intermediate reaction products of *n*-heptane formed in different systems:
 (A) cool flame "static system", $p = 13$ kPa, $T = 523$ K, $O_2/F = 1$; (B) fired engine
 "end gas", $p > 3.5$ MPa, $T > 723$ K, $O_2/F = 9$; (C) cool flame flow system, $p =$
 0.1 MPa, $T = 538-723$ K, $O_2/F = 4$ [45]. (a) Values of Luck et al. [45] and (b) our
 approximate calculation* in %

Product	(A)		(B)		(C)	
	(a)	(b)	(a)	(b)	(a)	(b)
Heptane	11.0	-	450	-	6.3	-
butadiene	0.27	2.1	0.36	3.1	< 0.01	0.13
1-butene	0.63	4.9	0.90	7.8	0.03	0.42
1-Pentene	0.50	3.9	2.28	19.9	0.19	2.6
1-hexene	3.70	29.0	1.16	10.1	0.09	3.4
(1 and 2)-heptene	2.10	16.5	2.0	17.4	1.02	13.9
2-methyl tetrahydrofuran	1.61	12.6	1.22	10.6	1.05	14.4
benzene	0.43	3.4	0.06	0.5	0.09	1.2
<i>n</i> -propyl benzene	0.03	0.2	-	-	0.07	0.95
<i>Trans</i> -2-methyl-5-ethyl-tetrahydrofurane	0.59	4.6	0.51	4.4	0.73	10.0
* <i>Cis</i> -2-methyl-5-ethyl-tetrahydrofurane	1.00	7.8	1.00	8.7	1.00	13.7
2-Propyltetrahydrofuran	0.30	2.3	0.53	4.6	0.49	6.7
2- <i>n</i> -butyl oxiran	0.31	2.4	0.23	2.0	0.40	5.4
2-ethyl-3-propyl oxiran	0.07	5.5	0.07	0.6	0.12	1.6
<i>Trans</i> -2-methy-4-propyl-oxetan	0.15	1.1	0.16	1.4	0.20	2.7
<i>Cis</i> -2-methy-4-propyl-oxetan	0.68	5.3	0.73	6.3	0.55	7.5
2- <i>n</i> -pentyloxiran	0.01	0.08	0.04	0.35	0.12	1.6
4-heptanone	0.10	0.8	0.16	1.4	0.10	1.3
3-heptanone	0.03	0.2	-	-	0.16	2.2
2-heptanone	0.09	0.7	0.04	0.35	0.53	7.2
styrene	0.07	0.55	-	-	0.17	2.3
4-heptanol	0.03	0.2	-	-	0.07	0.96
3-heptanol	0.02	0.15	-	-	0.06	0.82
2-heptanol	0.01	0.08	-	-	0.05	0.70

*Assuming that the same initial amount of *n*-heptane was introduced in the different systems and compared to the reference compound formed. The amount of *n*-heptane non-transformed is 11x higher than the reference in (A), 450x higher than the reference in (B) and 6.3x higher than the reference in (C).

Table 3. Effect of the pressure on the conversion (%) of initial products during the slow oxidation of *n*-pentane at 523 K, Fuel/O₂ = 0.75 [51]

Product	9.3	14.7	p (kPa) 18.9	22.4	26.3
Ethylene	2.5	2.3	2.1	1.7	2.0
Propylene	0.4	0.3	0.2	0.2	0.2
Pent-2-ene	10.8	8.9	7.0	6.0	5.1
Acetaldehyde	26.4	24.5	25.9	28.4	24.5
Propionaldehyde	9.4	10.3	11.1	12.7	14.8
Acetone	23.2	28.0	31.8	30.9	32.7
Butanone	10.5	11.1	10.5	10.9	11.8
C5 Ketones	1.1	0.9	1.3	1.4	1.7
Methyl vinyl ketone	1.6	1.2	0.8	0.9	1.2
Pent-2-en-4-one	1.3	1.1	0.9	0.7	0.6
2-Methyltetrahydrofuran	4.0	2.9	2.0	1.9	1.7
2-methyl-3-ethylorixan	1.0	0.7	0.8	0.6	0.6
2-methyloxiran	2.2	2.2	2.0	2.5	1.2
Ethanol	0.8	0.5	0.7	0.5	1.0
Pentan-3-ol	0.4	0.4	0.4	0.4	0.7
Pentan-2-ol	0.2	0.1	0.1	0.1	0.2

Table 4. Conversion of hydrocarbons from experimental (a) and calculated data (b), using kinetic modeling. λ : Equivalence ratio, τ : Residence time

Fuel	λ	τ (s)	p (MPa)	T (K)	Fuel Conversion (%)		References
					(a)	(b)	
<i>n</i> -heptane	1	1	1	575	20	17	[71]
				625	59	48	
				650	65	47	
				750	9	38	
				825	80	77	
				930	100	95	
<i>n</i> -heptane	1	0.2	0.7	575	5	-	[59]
				620	42	-	
				640	38	-	
				683	27	-	
<i>n</i> -heptane	0.5	1	1	600	55	40	[60]
				625	67	50	
				650	74	52	
				673	72	55	
				683	59	52	
<i>iso</i> -octane	1	0.4	0.7	590	5	-	[59]
				610	36	-	
				675	26	-	
				983	20	-	
<i>iso</i> -octane	2	1	1	625	19	7	[13]
				675	15	6	
				750	20	6	
				800	50	3	
				825	72	73	
				940	92	100	
<i>iso</i> -octane	0.5	1	1	600	0	0	[13]
				625	8	12	
				650	8	12	
				673	8	8	
				683	5	0	

Table 5. Temperature dependence of reaction products formed from *n*-heptane. Experimental data (a) from reference [10] and calculated values (b) from reference [78]. λ : Equivalence ratio, τ : residence time

Fuel	λ	τ (s)	p (MPa)	T (K)	Compound	mole fraction	
						(a)	(b)
<i>n</i> -heptane*	1	0.2	0.1	627	C ₂ H ₄	0	0
					C ₃ H ₆	0	0
					C ₄ H ₆	0	0
					C ₅ H ₁₀	0	0
					CH ₄	0	0
					CO	0	0
	1	0.2	0.1	712	C ₂ H ₄	0.80x10 ⁻³	0.6x10 ⁻³
					C ₃ H ₆	0.26x10 ⁻³	50.0x10 ⁻⁶
					C ₄ H ₆	0.12x10 ⁻⁴	0.0
					C ₅ H ₁₀	0.15x10 ⁻⁴	0.0
					CO	0	0.0
	1	0.2	0.1	777	C ₂ H ₄	2.00x10 ⁻³	1.0 x10 ⁻³
					C ₃ H ₆	0.35x10 ⁻³	0.12 x10 ⁻³
					C ₄ H ₆	0.04x10 ⁻³	0.015 x10 ⁻³
					C ₅ H ₁₀	0	0.0
					CH ₄	0.40x10 ⁻³	0.0
					CO	2.50x10 ⁻³	0.05x10 ⁻³

* Initial concentration of *n*-heptane: $C_0 = 0.15$ % V/V (1.5×10^{-3} moles)

Table 6. Kinetic parameters of the oxidation reaction of kerosene and a ternary mixture of hydrocarbons [38,71]

Fuel	a	b	A	E _a (kcal)
Kerosene	1	0.8	2.8×10^{15}	45
Equivalent mixture				
<i>n</i> -undecane	1	0.8	5×10^{15}	45
<i>n</i> -propylcyclohexane	1	0.5	5×10^{12}	40
Trimeylbenzene	1	1	7×10^{16}	50
n- heptane	0.25	1.5	4.3×10^{11}	30

Table 7. Composition and physicochemical properties of selective fuels

Properties	<i>n</i> -heptane ^a	Cetane ^b	Diesel # 2 ^{c,d}	JP-8 ^f
Formula	C ₇ H ₁₆	C ₁₆ H ₃₄	C _n H _{1.8n}	C ₁₁ K ₂₁
Octane number	0	-	-	-
Cetane number	53.6	100	47.4 ^c	-
Density (kg/m ³)	0.68x10 ³	-	0.85x10 ³	0.81x10 ³
Gravity, API	-	51.2	35.6 ^c	-
Boiling point (K)	371.4	560	460 ^c	330-510
Dist. Temp. (K) T ₁₀	371.4	560	492	-
T ₅₀	371.4	560	531	-
T ₉₀	371.4	560	572	-
LHV ^g (Btu/lb)	-	20400	~18600 ^d	18,550
Sulfur %	-	0	0.26 ^c	0.05
Carbon	84	84.95	-	132
Hydrogen	16	15.05	-	21
Parafins (% v/v)	100	100	54.8 ^d	60.0
Olefins	0	0	2.41	2.0
Aromatic	0	0	27.5	18.0
Nephtenes	0	0	15.3	20.0

^a[16]; ^b[65]; ^cD-2 diesel control fuel lot K-848 [180]; ^d[65]; ^fAverage values from [17],

^gLower heating value.

Table 8. Conversion of conventional and alternative fuels by catalytic partial oxidation
[139]

Fuel	T (K)	complete conversion, dry N ₂ free (%)		
		H ₂	CO ₂	CO
Methanol	723	60	20	18
Ethanol	853	60	18	15
<i>iso</i> -Octane	903	60	20	16
Hexadecane	-*	-	-	-
Toluene	928	50	39	8
2-Pentene	943	60	22	18
Gasoline	1033	58	20	18
Diesel # 2	1128	50	20	20

* Not given

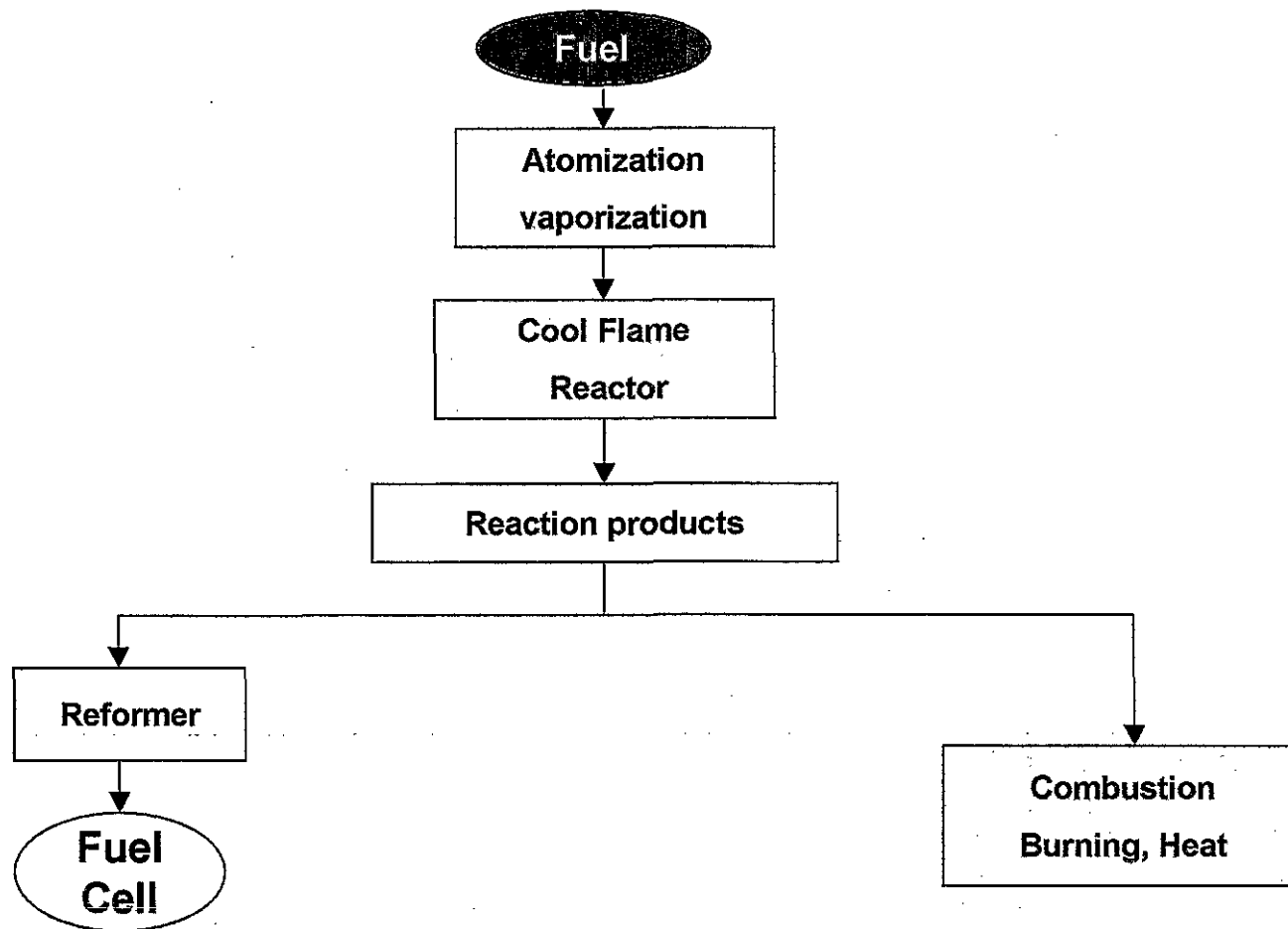


Fig. 1

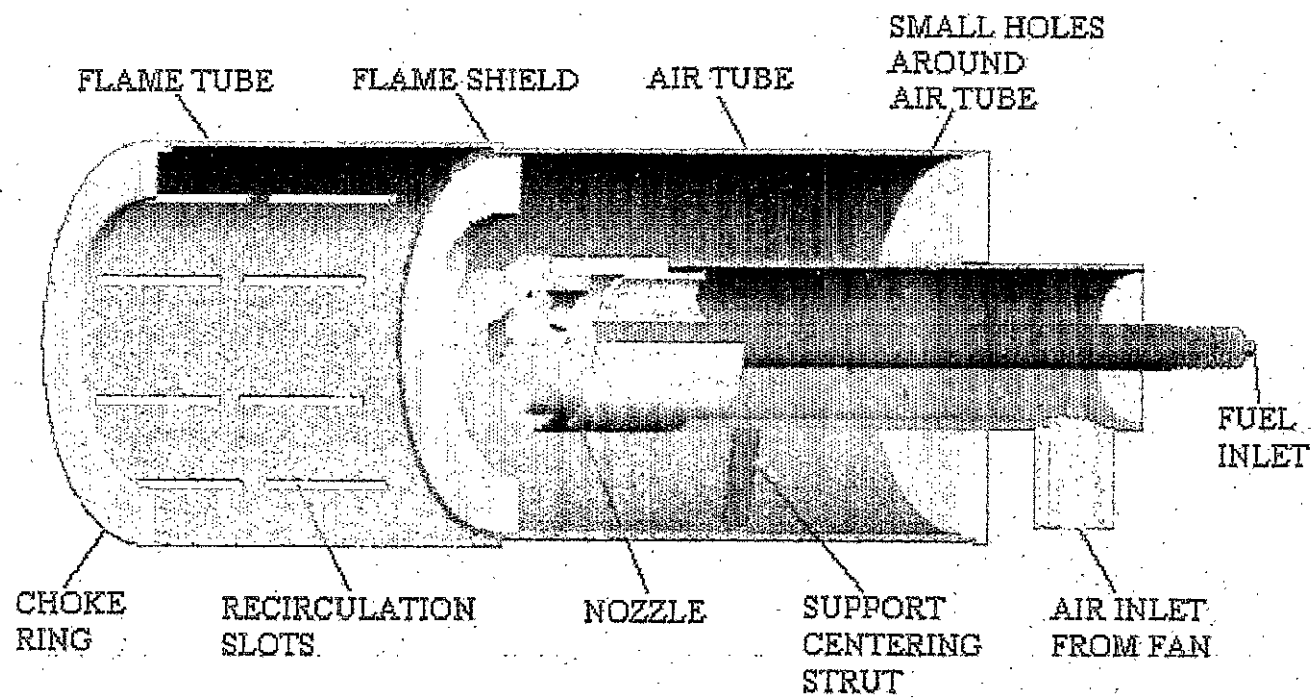


Fig. 2

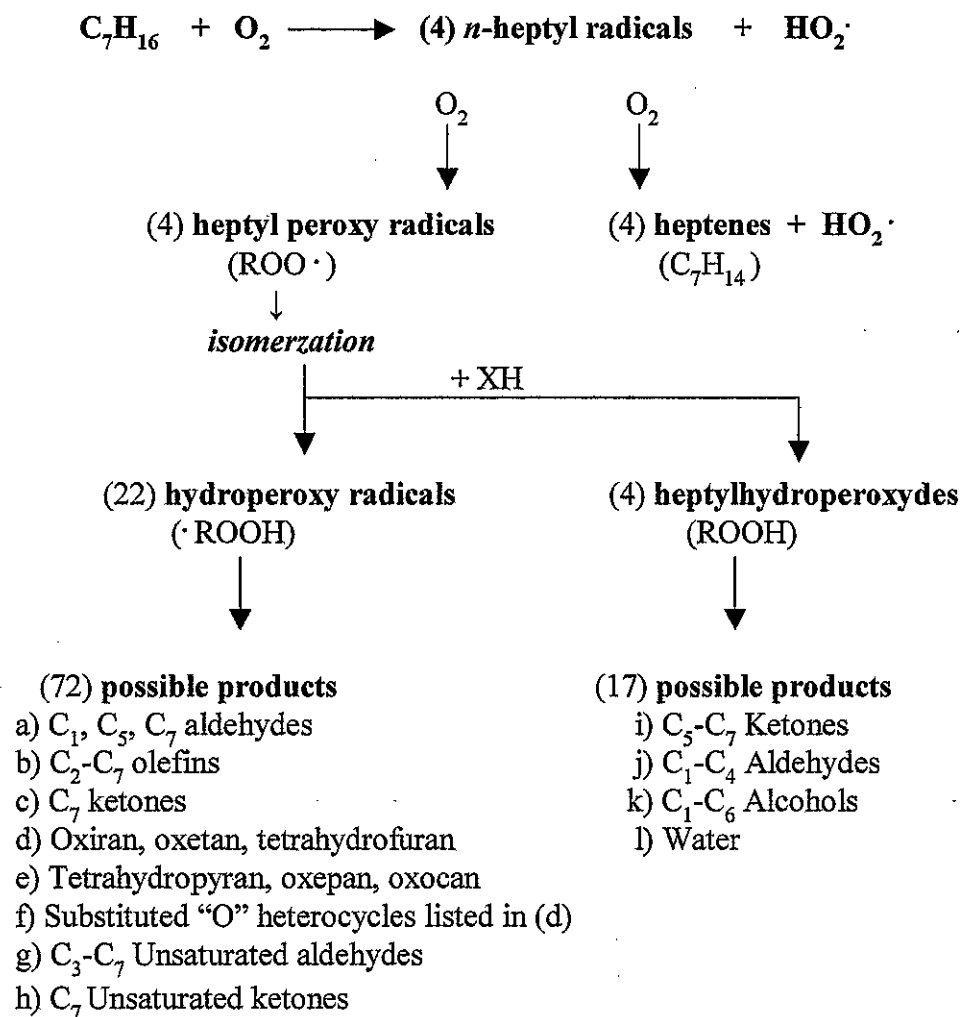
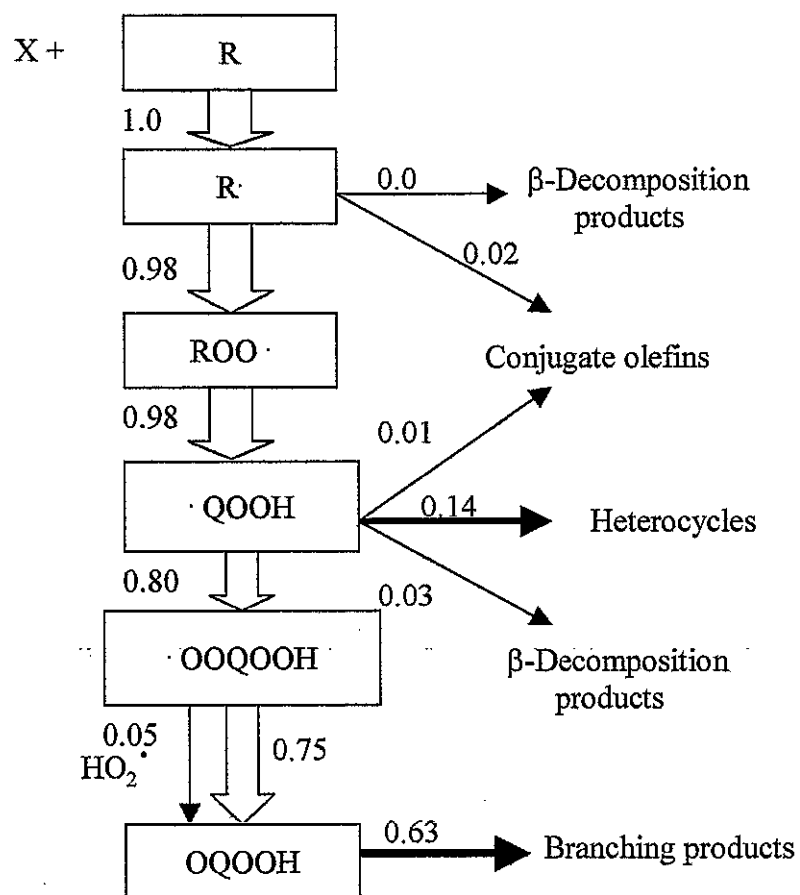


Fig. 3

T = 620 K
Conversion 54.5 %



T = 820 K
Conversion 77.6 %

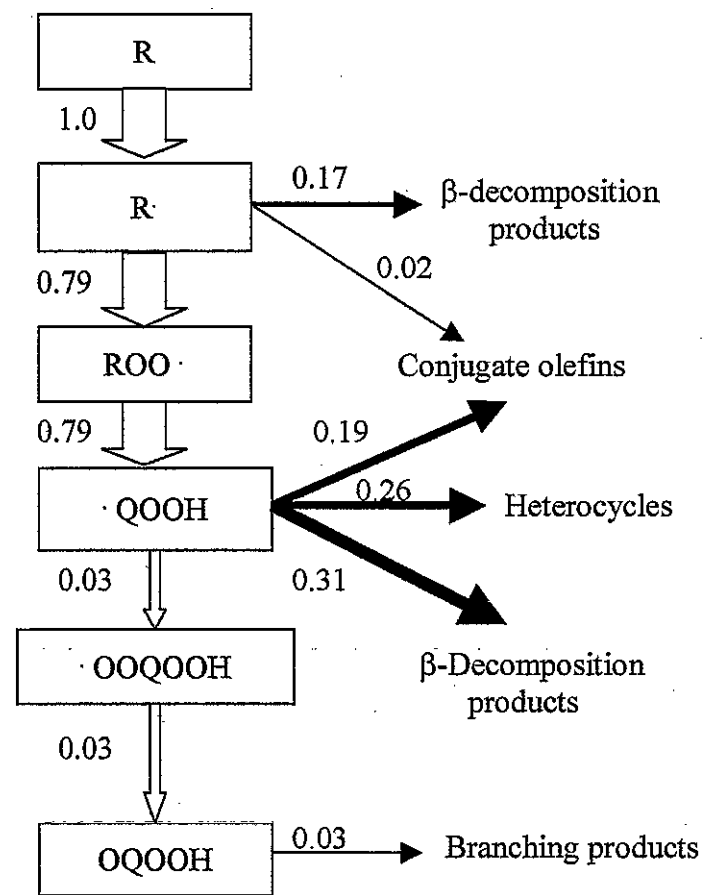


Fig. 4

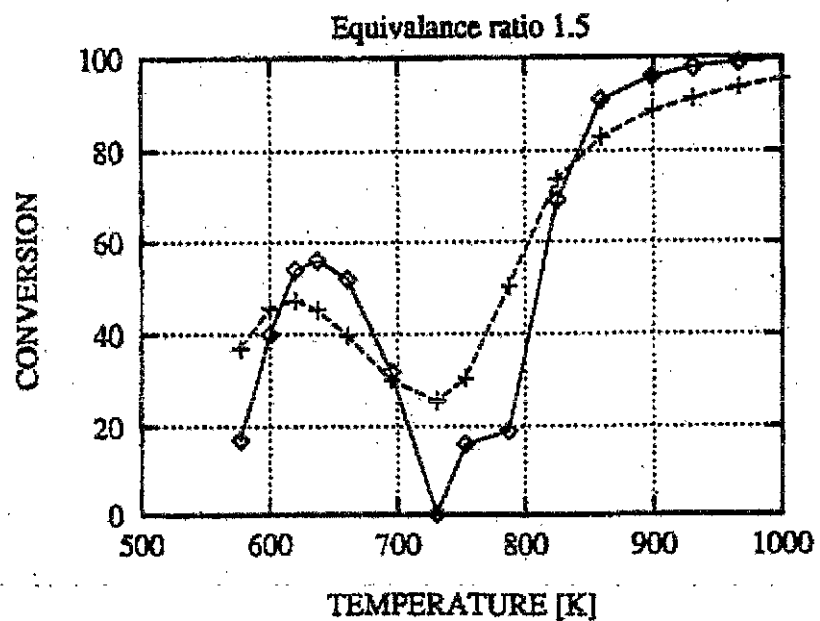
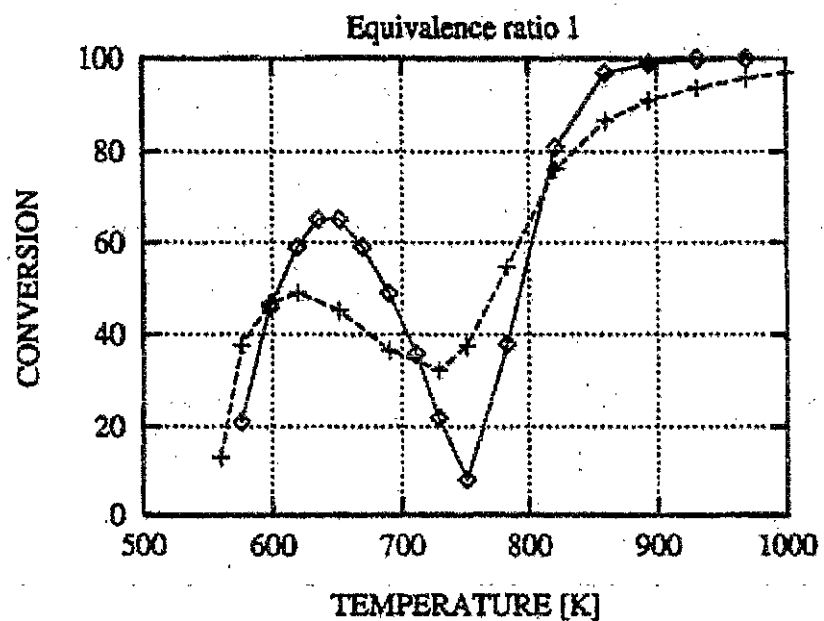
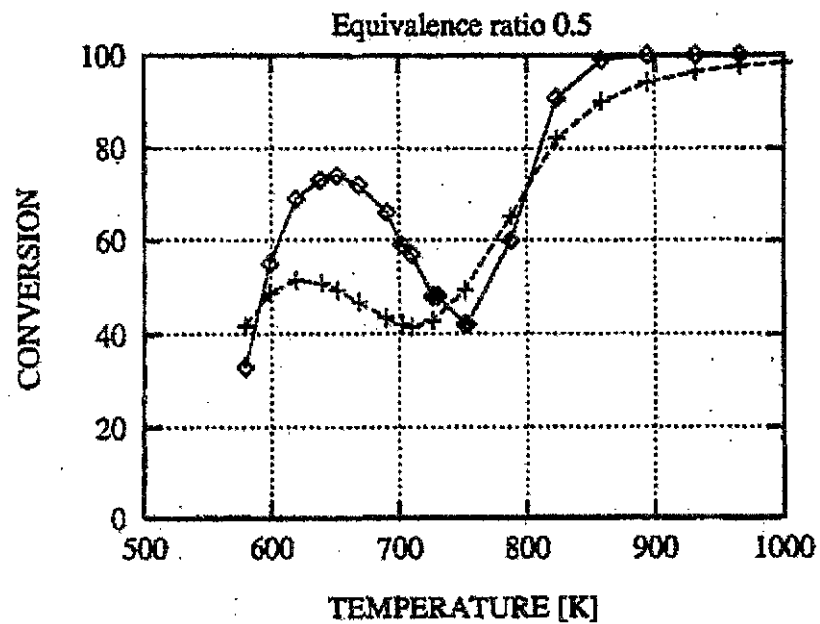
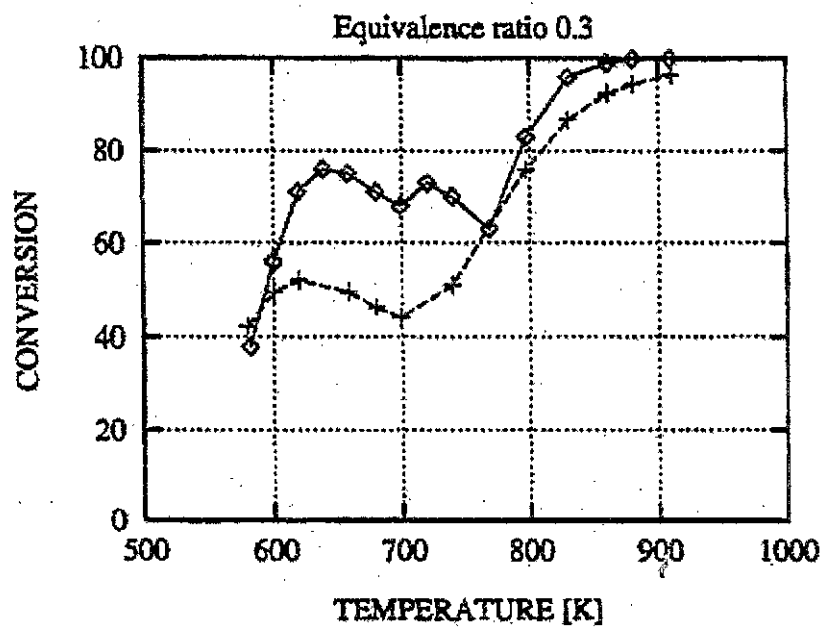


Fig. 5

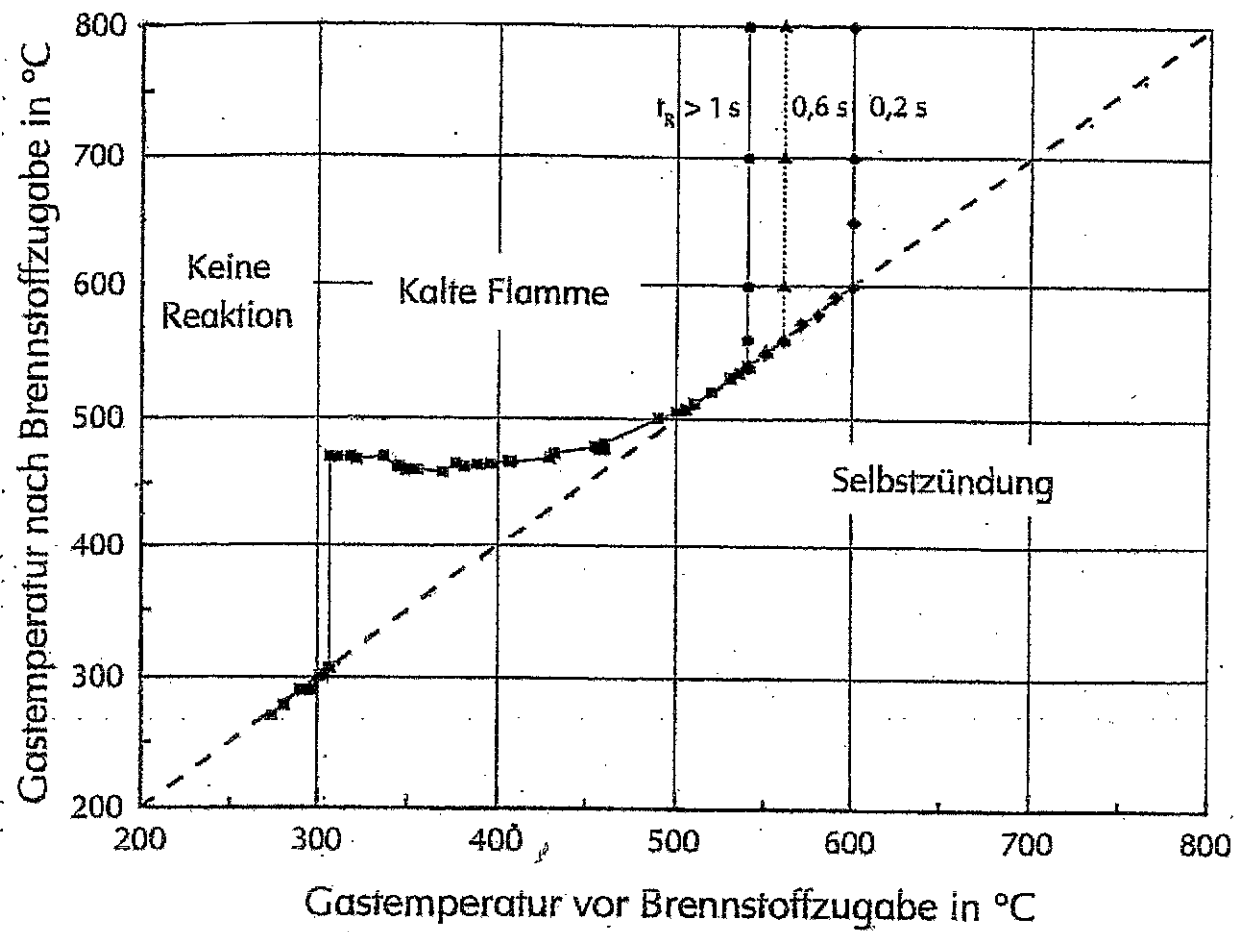


Fig. 6

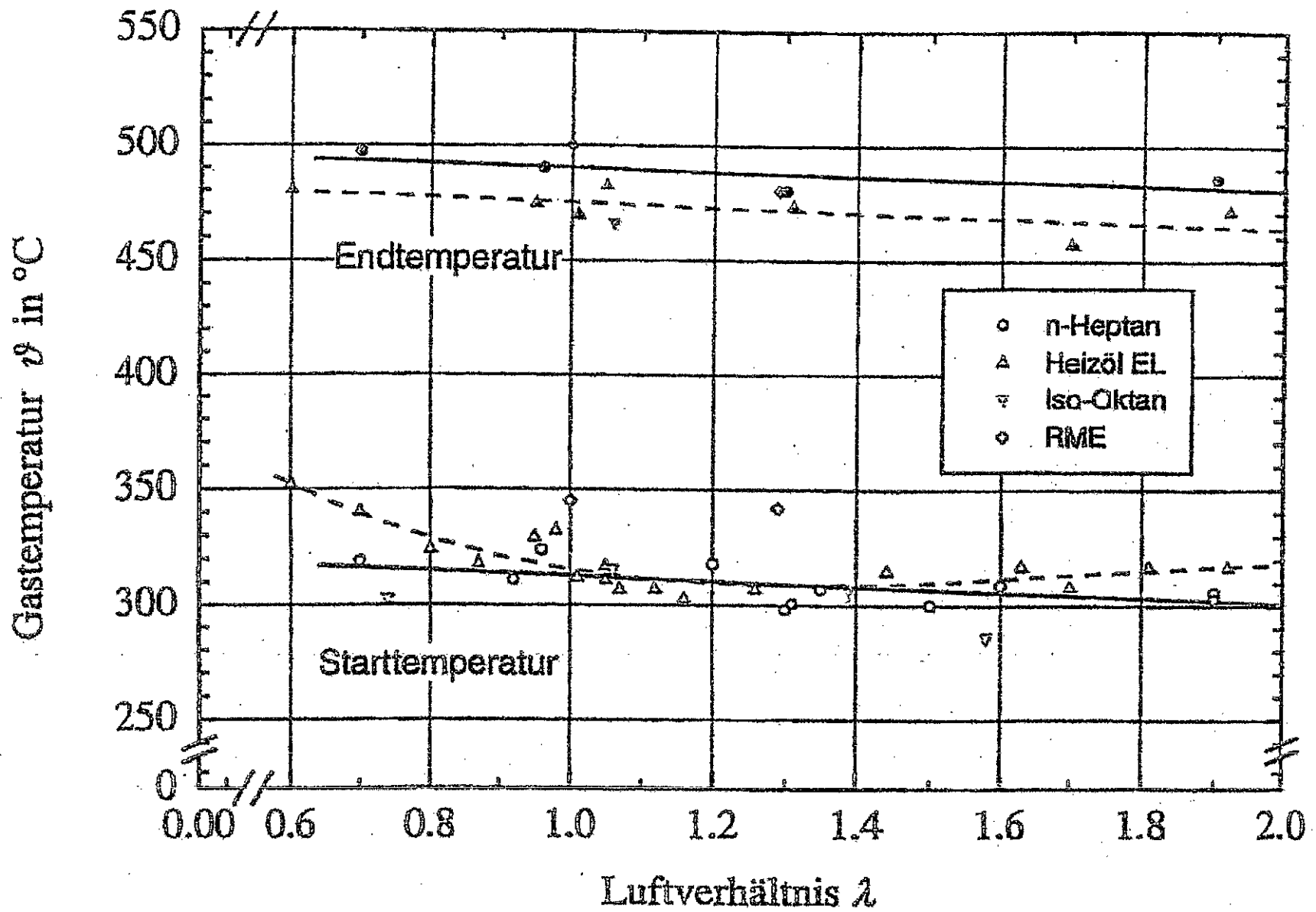


Fig. 7

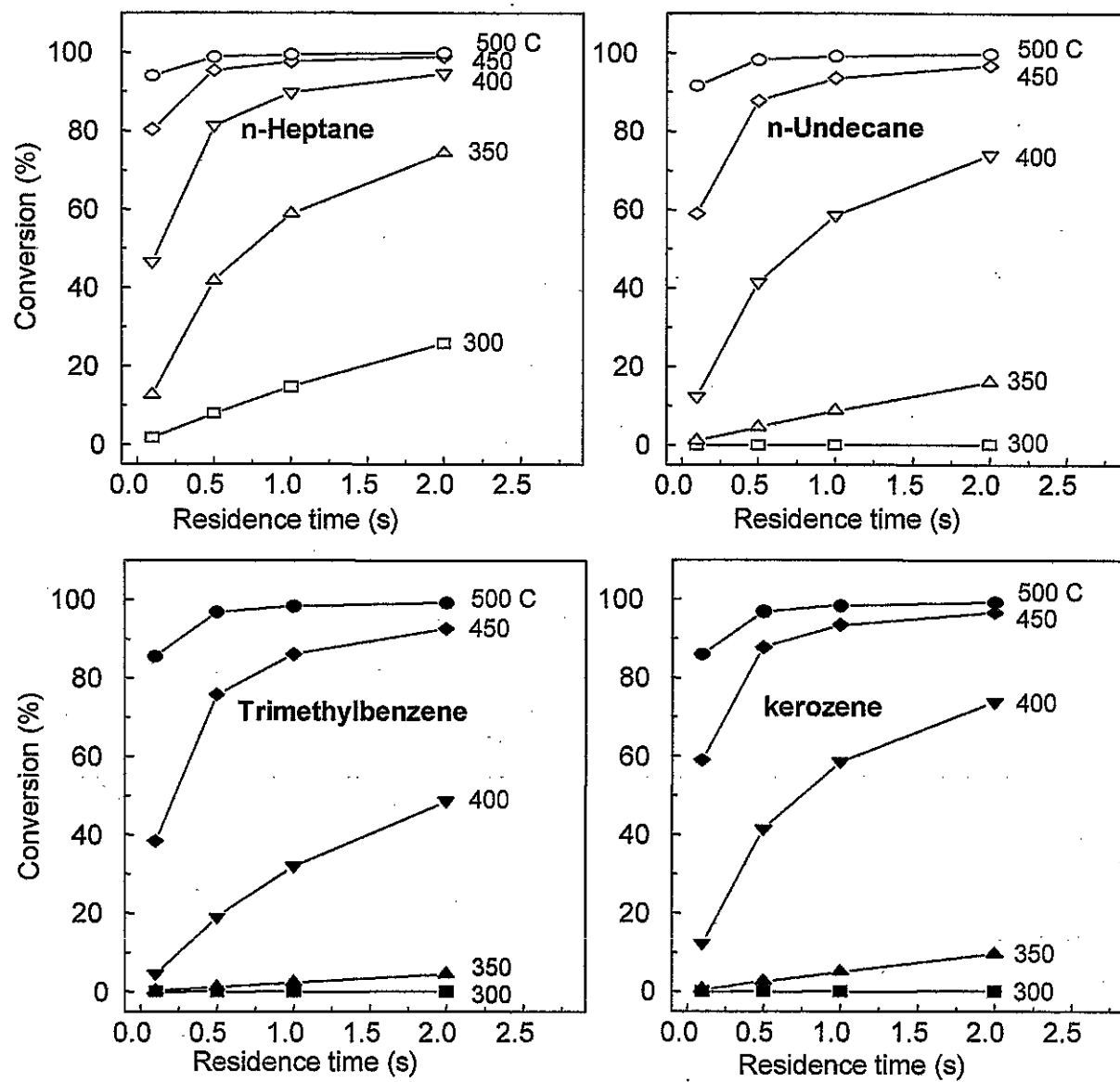


Fig. 8

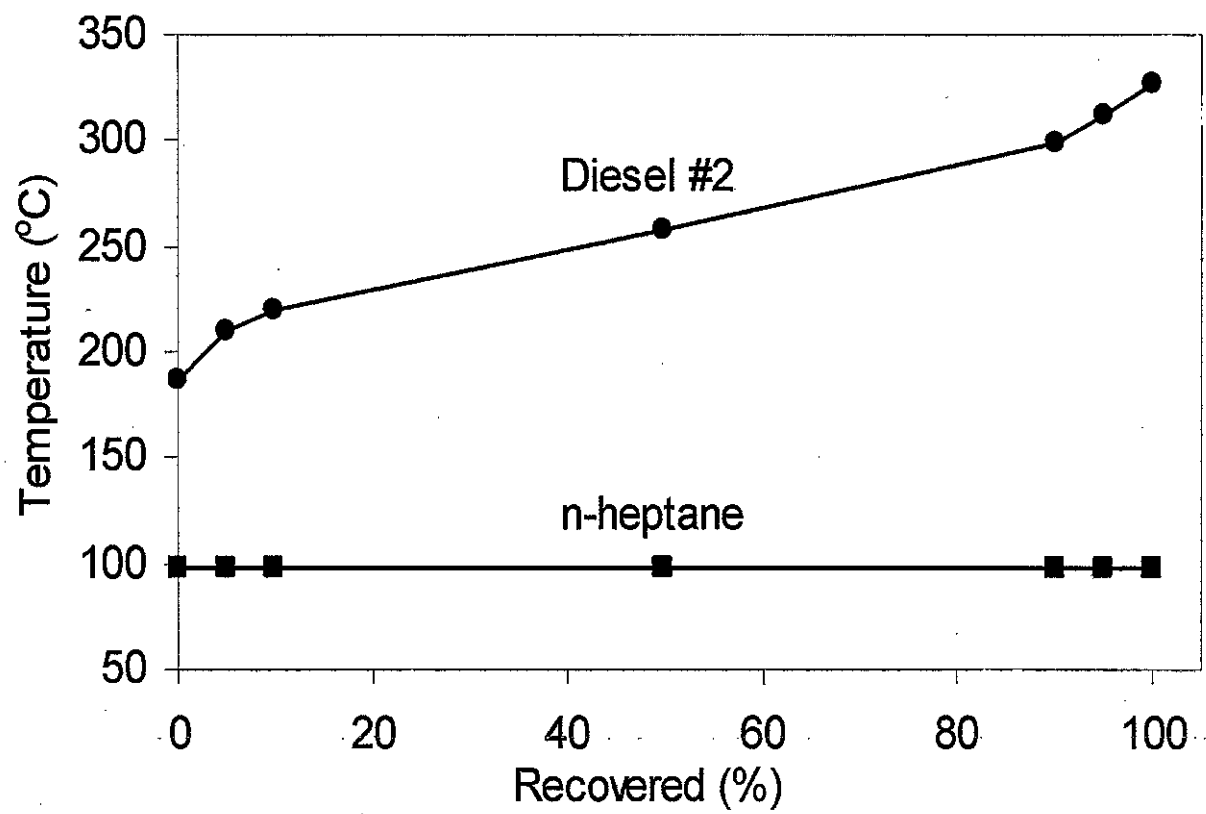


Fig. 9

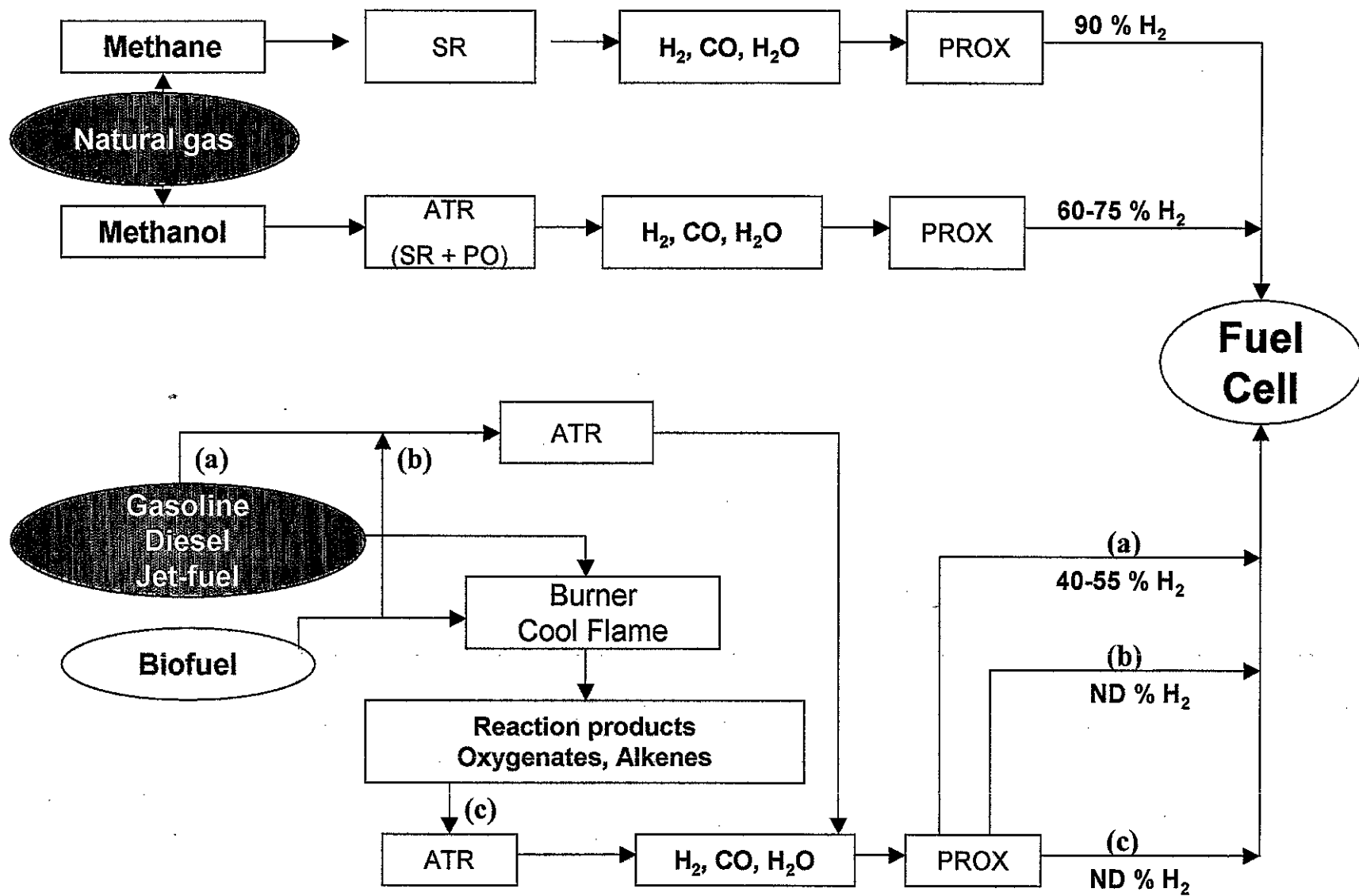


Fig. 10